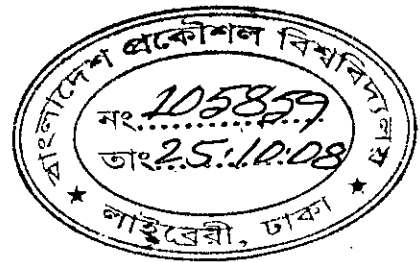
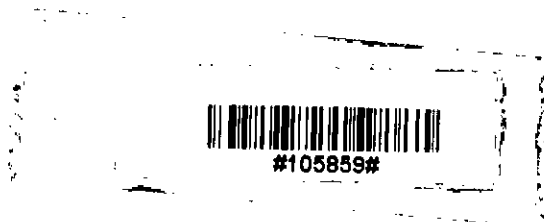


# BEHAVIOR OF LARGE DIAMETER BURIED FLEXIBLE PIPES UNDER SURFACE LIVE LOADS

By  
SUJAN DUTTA



A Thesis submitted to the Department of Civil Engineering of Bangladesh University of Engineering and Technology, Dhaka, in partial fulfillment of the requirement for the degree of  
**MASTERS OF SCIENCE IN CIVIL ENGINEERING (GEOTECHNICAL)**



DEPARTMENT OF CIVIL ENGINEERING  
BANGLADESH UNIVERSITY OF ENGINEERING AND TECHNOLOGY  
DHAKA, BANGLADESH.

August, 2008.

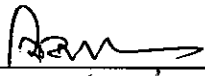
The thesis title "Behavior of Large Diameter Buried Flexible Pipes under Surface Live Loads" submitted by Sujan Dutta, Roll: 100604223F, Session:October'06 has been accepted as satisfactory in partial fulfillment of the requirement for the degree of Master of Science in Civil Engineering (Geotechnical) on 16<sup>th</sup> August, 2008.

### Board of Examiners



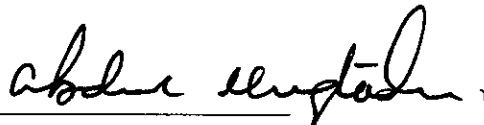
Dr. Ashutosh Sutra Dhar  
Associate Professor  
Department of Civil Engineering  
BUET, Dhaka.

Chairman  
(Supervisor)



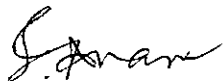
Dr. Muhammad Zakaria  
Professor and Head  
Department of Civil Engineering  
BUET, Dhaka.

Member  
(Ex-officio)



Dr. Abdul Muqtadir  
Professor  
Department of Civil Engineering  
BUET, Dhaka.

Member



Dr. Iftekhar Anam  
Associate Professor  
Department of Civil Engineering  
The University of Asia Pacific, Dhaka.

Member  
(External)

## CANDIDATE'S DECLARATION

I hereby declare that the research work reported in this thesis has been performed by me and that this work has not been submitted elsewhere for any other purpose, except for publication.

*Sujan Dutta.*  
(Sujan Dutta)

**To My**

**Parents**

## ACKNOWLEDGEMENT

First all thanks go to Almighty GOD, for giving me the opportunity to complete this thesis successfully.

The research work was carried out under the supervision of Dr. Ashutosh Sutra Dhar, Associate professor, Department of Civil Engineering, Bangladesh University of Engineering and Technology (BUET), Dhaka. I want to express my gratitude to him from the very core of my heart for his keen supervision, invaluable suggestion, and affectionate encouragement throughout the work.

I want to express my special thanks to Dr. Mahbuba Begum, Assistant professor, Department of Civil Engineering, Bangladesh University of Engineering and Technology (BUET) for her friendly co-operation. I also thank to Dr. Mahmud Ashraf, Assistant professor, Department of Civil Engineering, Bangladesh University of Engineering and Technology (BUET) for his assistance and guidance in the research work.

Thanks are also extend to every staff in the Department of Civil Engineering, BUET especially Md. Abdul Malek, Section officer, for his friendly association in different ways that also made it possible to work in the computer Lab during holiday and vacation.

## ABSTRACT

Surface load due to vehicular traffic influences the performance of shallow buried pipes. This thesis presents an investigation of the behavior of buried flexible pipes due to surface load. Two-dimensional finite element analysis was performed through idealization of the concentrated surface load as an equivalent line load. A general purpose finite element program ABAQUS was used for modeling of the pipe-soil interaction under surface loads. Finite element model was developed and evaluated using full scale test data of buried flexible pipe from the literature, where responses of buried flexible pipe were measured under surface live loads. Through a comprehensive study on different parameters of buried structure under different burial depth, it was observed for large diameter flexible pipe that influences of surface loads are localized within a zone around the pipe crown for shallow buried pipes ( $<0.5D$ ) and for pipes with low material modulus. However, the influence extends downward covering the full pipe circumference for deeper pipes and pipes with high material modulus. For a particular pipe, the effects of the surface load reduced rapidly with the depths of soil cover up to a depth of half of the pipe diameter, beyond which the effect reduced steadily. The concentrated surface load induces compressive wall thrust and negative bending moment (outward concave bending) at the shoulder, and positive bending moment (outward concave bending) at the crown and invert.

The study revealed that the effects of the concentrated surface load depend on the burial depth, pipe material, and geometry of the pipe wall. Although sectional area of pipe wall do not affect largely, moment of inertia of pipe wall affect the thrust and moments that develop around the pipe. The effects are very significant on the development of bending moment. Material modulus of pipe also affects the thrust and moment developing around the pipe circumference. However, the influence is small on the thrusts, while the bending moment is significantly affected. The maximum moment induced due to surface load can be expressed as a function of the relative bending stiffness of the pipe-soil system. The mechanism of the stress development around the pipe was found different for shallow and deep burial

conditions for High-Density polyethylene (HDPE) pipe. Boussinesq solution always over-predicted the crown level stress for HDPE pipe. However for the stiffer (steel) pipe, Boussinesq equation under predicted the stress. These are due to development of arching from soil-pipe interaction that is not captured in Boussinesq's equation. AASHTO, ASCE code yielded conservative values of the average soil stresses for pipes with greater burial depths.

# CONTENTS

	Page
DECLARATION	iv
ACKNOWLEDGEMENT	vi
ABSTRACT	vii
CONTENTS	ix
LIST OF FIGURES	xii
LIST OF TABLES	xvi
LIST OF SYMBOLS	xvii
<b>CHAPTER 1: Introduction</b>	<b>1</b>
1.1 GENERAL	1
1.2 BACKGROUND AND PRESENT STATE OF THE PROBLEM	3
1.3 INSTALLATION PRACTICES	4
1.4. OBJECTIVES	6
1.5 METHODOLOGY AND SCOPE	6
1.6 THESIS ORGANIZATION	7



<b>CHAPTER 2: Literature Review</b>	<b>8</b>
2.1 INTRODUCTION	8
2.2 PIPE ANALYSIS METHODS	8
2.2.1 Analysis for Dead Load	9
2.2.2 Effect of Wheel Load	9
2.3 LIVE LOADS IN DESIGN CODES	14
2.4 RESEARCHES WITH LIVE LOAD STUDY	27
2.5 FINITE ELEMENT ANALYSES	30
2.5.1 SPIDA Code	30
2.5.2 SOILCON Code	30
2.5.3 CANDE Code	31
2.5.4 Other Finite Element Analysis for Buried Pipe Analysis	33
<b>CHAPTER 3: Development of Finite Element Model</b>	<b>34</b>
3.1 INTRODUCTION	34
3.2 PROBLEM STATEMENT AND IDEALIZATION	35
3.3 ASPECTS OF ABAQUS	40
3.4 FINITE ELEMENT MODEL FORMULATION	41
3.5 MATERIALS USED IN FE ANALYSIS	45
3.6 VERIFICATION OF FINITE ELEMENT MODEL	45

<b>CHAPTER 4: Investigation of Pipes under Live Load</b>	<b>51</b>
4.1 INTRODUCTION	51
4.2 EFFECT OF SECTIONAL AREA OF PIPE WALL	52
4.3 EFFECT OF MOMENT OF INERTIA OF PIPE WALL	60
4.4 EFFECT OF MODULUS OF ELASTICITY OF PIPE MATERIAL	67
4.5 EFFECT OF RELATIVE STIFFNESS	76
4.6 EFFECT OF BURIAL DEPTH	82
4.7 COMPARISON WITH DESIGN CODES	93
<b>CHAPTER 5: Conclusions and Recommendations</b>	<b>96</b>
5.1 INTRODUCTION	96
5.2 FINDINGS FROM THE STUDY	97
5.3 RECOMMENDATIONS FOR FUTURE STUDY	99
<b>REFERENCES</b>	<b>101</b>
<b>APPENDIX</b>	<b>A-i</b>

## LIST OF FIGURES

	Page	
Figure 1.1	Types of Pipe Profiles (After Sargand and Madsada, 2007, McGrath et al. 2002)	2
Figure 1.2	Trench Cross Section Showing Terminologies	5
Figure 2.1	Uniform and non-uniform deformation of buried pipe (Moore, 2000)	12
Figure 2.2	Vertical Stresses in the Soil Mass Due to Concentrated Surface Load	15
Figure 2.3	Distribution of surface live loads versus loads on a plane at depths of Pipe Crown (After Moser, 2001)	17
Figure 2.4	Soil stress models for minimum cover as truncated pyramid and cone (Moser, 2001)	18
Figure 2.5	Effective Supporting Length (after ASCE, 1993)	21
Figure 2.6	Effective Area of the Live Load (After ASCE, 1993)	22
Figure 2.7	AASHTO Wheel Load Surface Contact Area (Foot Print)	22
Figure 2.8	AASHTO Wheel Loads and Wheel Spacings	24
Figure 2.9	Spread Load Area-Single Dual Wheel	25
Figure 2.10	Spread Load Area-Two Single Dual Wheels of Trucks in Passing Mode	25
Figure 2.11	Spread Load Area-Two Single Dual Wheels of Two Alternate Loads in Passing Mode	26
Figure 3.1	Buried Pipe soil system under Surface Concentrated Load	37
Figure 3.2	Plain Strain Idealization of Surface load	38
Figure 3.3	Two Dimensional Idealizations	38

Figure 3.4	Different Soil Zones in Finite Element Mesh	43
Figure 3.5	Effect of Boundary Position on Crown Moment	44
Figure 3.6	Axle load from 80 kN axle Truck	46
Figure 3.7	One of the Profile of Pipe Wall Used by McGrath et al., (2002)	46
Figure 3.8	Pipe Deflections under Concentrated Load	48
Figure 3.9	Comparison of Vertical Stress	49
Figure 4.1	Vertical Stress along Vertical Line above Crown for 300 mm Pipe Burial Depth with Various areas of Cross Section.	54
Figure 4.2	Vertical Stress along Vertical Line above Crown for 600 mm Pipe Burial Depth with Various areas of Cross Section	55
Figure 4.3	Variation of Vertical Stress at 75 mm above the Pipe Crown for Different Sectional Area of Pipe Wall	55
Figure 4.4	Maximum Pipe Deflection with Cross sectional Area for Different Depths	56
Figure 4.5	Variation of Thrust around the Pipe with Sectional Area for 300 mm Buried Depth of Pipe	57
Figure 4.6	Variation of Moment around the Pipe with Sectional Area for 300 mm Buried Depth of Pipe	58
Figure 4.7	Deflected Shape under Concentrated live Load	58
Figure 4.8	Variation of Thrust around the Pipe with Sectional Area for 600 mm Buried Depth of Pipe.	59
Figure 4.9	Variation of Moment around the Pipe with Sectional Area for 600 mm Buried Depth of Pipe	59
Figure 4.10	Vertical Stresses along Vertical Line above Crown for 300 mm Pipe Burial Depth with Various Moments Of Inertias	61
Figure 4.11	Vertical Stresses along Vertical Line above Crown for 600 mm Pipe Burial Depth with Various Moments Of Inertia	62
Figure 4.12	Variation of Vertical Stress at 75 mm above the Pipe Crown for Different Moment of Inertia	62

Figure 4.13	Maximum Pipe Deflections with Moment of Inertia for Different Depths	63
Figure 4.14	Variation of Thrust around the Pipe with Moment of Inertia for 300 mm Buried Depth of Pipe	65
Figure 4.15	Variation of Bending Moment around the Pipe with Moment of Inertia for 300 mm Buried Depth of Pipe	65
Figure 4.16	Variation of Thrust around the Pipe with Moment of Inertia for 600 mm Buried Depth of Pipe	66
Figure 4.17	Variation of Bending Moment around the Pipe with Moment of Inertia for 600 mm Buried Depth of Pipe	66
Figure 4.18	Vertical Stresses along Vertical Line above Crown for 300 mm Pipe Burial Depth with Various Pipe Material Modulus	68
Figure 4.19	Vertical Stresses along Vertical Line above Crown for 600 mm Pipe Burial Depth with Various Pipe Material Modulus	68
Figure 4.20	Variation of Vertical Stress at 75 mm above the Pipe Crown for Different Pipe Material Modulus	69
Figure 4.21	Maximum Deflection of Pipe at Different Depths for variation of Pipe Material Modulus	69
Figure 4.22	Variation of Thrust around the Pipe with Pipe Material Modulus for 300 mm Pipe Buried Depth	72
Figure 4.23	Variation of Bending Moment around the Pipe with Pipe Material Modulus for 300 mm Pipe Buried Depth	73
Figure 4.24	Variation of Thrust around the Pipe with Pipe Material Modulus for 600 mm Pipe Buried Depth	74
Figure 4.25	Variation of Thrust around the Pipe with Pipe Material Modulus for 600 mm Pipe Buried Depth	75
Figure 4.26	Variation of Maximum Moment with $\frac{E_p I_p}{E_s R^3}$	77
Figure 4.27	Variation of Bending Moment with Relative bending Stiffness around the Pipe for 300 mm Pipe Burial Depth	78

Figure 4.28	Variation of Bending Moment with Relative bending Stiffness around the Pipe for 600 mm Pipe Burial Depth	78
Figure 4.29	Variation of Maximum Thrust with $\frac{E_p A_p}{E_s R}$	80
Figure 4.30	Variation of Thrust around the Pipe with Relative Hoop Stiffness for 300 mm Buried Depth of Pipe	81
Figure 4.31	Variation of Thrust around the Pipe with Relative Hoop Stiffness for 600 mm Buried Depth of Pipe	81
Figure 4.32	Finite Element Mesh Used for the Study with Various Burial Depths	82
Figure 4.33	Variation of Vertical Stress above Crown for Different Burial Depth	83
Figure 4.34	Variation of Vertical Stress with Boussinesq's Stress above Crown for Different Burial Depth	84
Figure 4.35	Variation of Vertical Stress with Boussinesq's Stress at 600 mm Buried Depth for pipe with $E_p = 760$ MPa	85
Figure 4.36	Variation of Vertical Stress with Boussinesq's Stress at 600 mm Buried Depth for pipe with $E_p = 210000$ MPa	86
Figure 4.37	Variation of Vertical Stress with Boussinesq's Stress at 300 mm Buried Depth for pipe with $E_p = 760$ MPa	88
Figure 4.38	Variation of Vertical Stress with Boussinesq's Stress at 300 mm Buried Depth for pipe with $E_p = 210000$ MPa	89
Figure 4.39	Variation of Vertical Stress at 75 mm above Crown for Different Burial Depths	90
Figure 4.40	Variation of Vertical Stress at 75 mm below invert for Different Burial Depths	91
Figure 4.41	Variation of Horizontal Stress at 75 mm from Springline for Different Burial Depth	92
Figure 4.42	Comparison of Soil Stress for Pipe with 300 mm Burial Depth	94
Figure 4.43	Comparison of Soil Stress for Pipe with 600 mm Burial Depth	95

## LIST OF TABLES

Table 2.1	Impact Factor $F'$ versus Height of cover (Moser, 2001)	17
Table 2.2	Values of load co-efficient $C_s$ for concentrated superimposed loads vertically centered over conduit (Moser, 2001)	18
Table 2.3	Distributed Live Load Area (ASCE, 1993)	20
Table 2.4	Impact Factor	20
Table 2.5	AASHTO LRFD Load Spreading Rate	26
Table 2.6	LRFD Critical Wheel Loads and Spread Dimensions at the Top of the Pipe for select Granular Soil Fill	26
Table 2.7	LRFD Critical Wheel Loads and Spread Dimensions at the Top of the Pipe for Other Soil Fill	27
Table 3.1	Co-ordinates of Control Nodes	44
Table 3.2	Comparison of Field Quantities with FE Model	49
Table 4.1	Parameter Considered for the Effects of Section Area	53
Table 4.2	Maximum Bending Moments for Variation of $I_p$	64
Table 4.3	Comparison of Stresses 75 mm above Pipe Crown for HDPE Pipe (Burial Depth = 600 mm)	85
Table 4.4	Comparison of Stresses 75 mm above Pipe Crown for Steel Pipe (Burial Depth = 600 mm)	87
Table 4.5	Comparison of Stresses 75 mm above Pipe Crown for HDPE Pipe (Burial Depth = 300 mm)	88
Table 4.6	Comparison of Stresses 75 mm above Pipe Crown for Steel Pipe (Burial Depth = 300 mm)	89

## LIST OF SYMBOLS

Symbols	Meanings
$A_m$	: Arching Factor
$A_{d\sigma}$	: Arching Factor
$A_{d\tau}$	: Arching Factor
$A_{l,l}$	: Distributed Live Load Area
$W_c$	: Soil Weight per unit length transmitted to the pipe
$B_c$	: Diameter of pipe
$B_d$	: Trench Width for Trench Installation
$C_d$	: Load Coefficient
$C_s$	: Load co-efficient which is a function of
$D_l$	: Deflection lag factor
$\Delta D_v$	: Vertical deflection or change in diameter
$\Delta D_H$	: Horizontal deflection or change in diameter
$\Delta D$	: Change in diameter
$d_s$	: Offset distance of ground point from line of application of surface load
$E_s$	: Horizontal modulus of soil reaction as defined by the Iowa equation (MPa)
$F_v$	: Vertical arching factor
$F'$	: Impact Factor
$I_f$	: Impact Factor,
$K$	: Ratio of Active Lateral Unit pressure to Vertical Unit Pressure
$L_e$	: Effective supporting length of pipe
$M_{cr}$	: Moment at Pipe Crown
$M_{sp}$	: Moment at Pipe Springline
$N_{cr}$	: Thrust at Pipe Crown
$N_{sp}$	: Thrust at Pipe Springline



$q_0$	: Pressure at crown level without a pipe
$S_r$	: Stiffness ratio
$S_L$	: Outside horizontal span of pipe or width of $A_{LL}$ transverse to longitudinal axis of pipe, whichever is less
$w_o$	: External stresses due to the isotropic loading
$w_d$	: External stresses due to the deviatoric loading
$w_o$	: components of the external stresses
$W_{sc}$	: Load on pipe per unit length
$W_T$	: Total live load on pipe per unit length
$\sigma_h$	: Lateral Earth Pressure
$\sigma_v$	: Vertical Earth Pressure
$\sigma_m$	: Uniform Component of Pressures in 2D Load System
$\sigma_d$	: Non-uniform Component of Pressures in 2D Load System
$\sigma_L$	: Average pressure intensity
$\sigma_L$	: The average pressure intensity
$\gamma_s$	: Average Unit Weight of Soil

# CHAPTER 1

## INTRODUCTION



### 1.1 GENERAL

Buried pipes have been used to improve the standard of living for city dwellers through transporting portable and waste water since the beginning of modern civilization. Many different pipe products have been developed for these applications, and work is still continued to improve the economy and performances of buried pipe structures.

Use of flexible pipe for underground application started in the early twentieth century, when pipes were installed without engineering design. Soon after introduction, the use of the flexible pipe increased steadily. Design of the flexible pipe was started in the mid-1900 when Sprangler developed the deflection equation for corrugated steel pipe (Sprangler, 1941). Flexible pipes with different materials such as steel, High Density Polythene (HDPE), Polyvinyl Chloride (PVC) etc. were developed with a variety of wall profile geometry over the last several decades. Figure 1.1 shows some of the wall profiles of flexible pipe. Design of those pipes considers several limit states under the earth overburden load. The effects of vehicle loads are generally accounted as an additional uniform pressure over the pipe crown (ASCE, AASHTO) which is added to the overburden pressure. However, the behavior of the pipe under concentrated surface load can be more complex, particularly for shallow buried pipe. The concentrated load is a three dimensional load effect of which may be localized within a zone depending upon the ground condition. Presence of the pipe within the ground may also influence the effects of the load. The issues of buried flexible pipes under concentrated surface loads are investigated in this research.

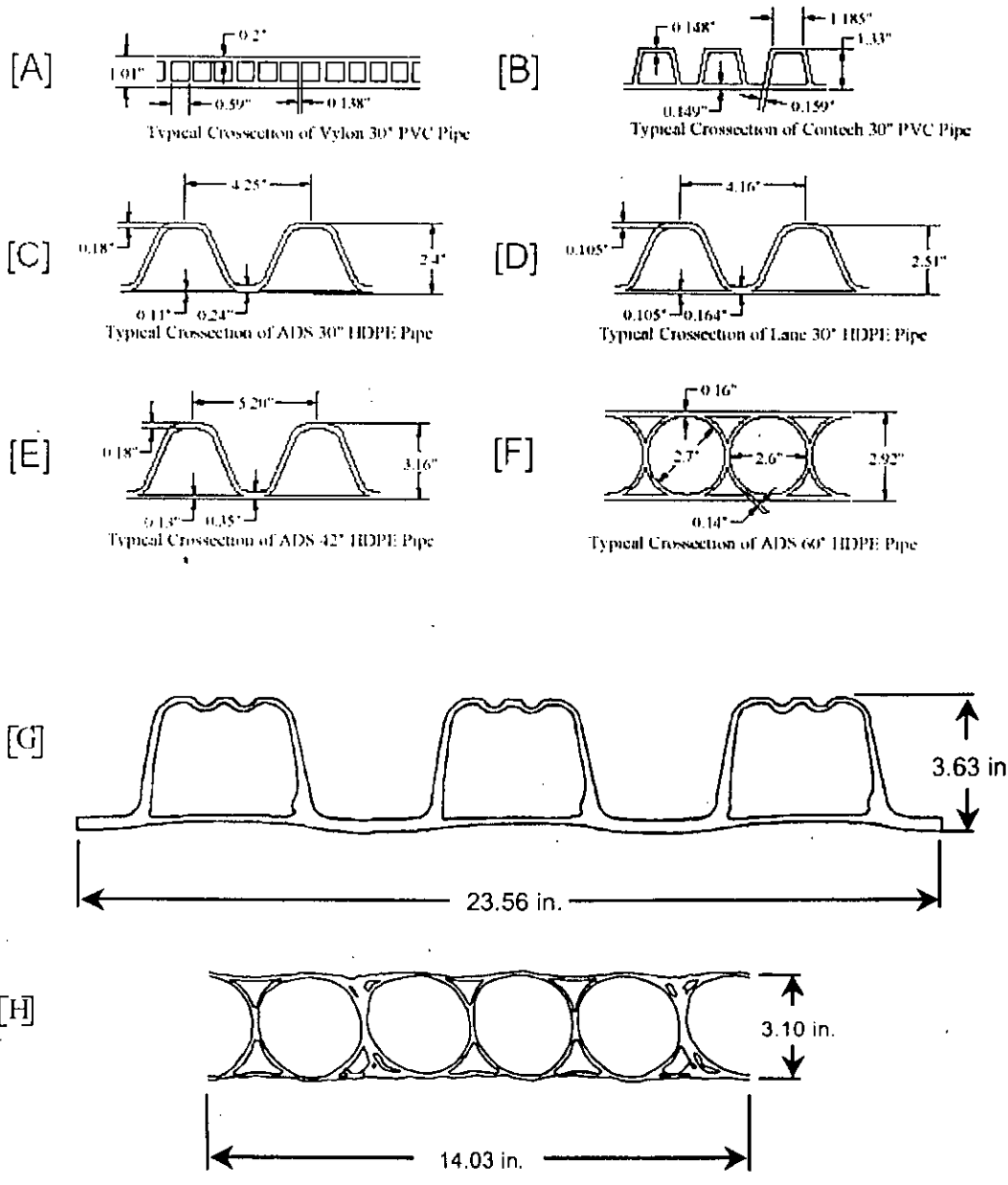


Figure 1.1 Types of Pipe Profiles (After Sargand and Masada, 2007, McGrath et al., 2002)

## 1.2 BACKGROUND AND PRESENT STATE OF THE PROBLEM

The use of flexible pipes, such as corrugated high density polyethylene (HDPE) pipes, polyvinyl chloride (PVC) pipes, and metal pipes have been increasing recently in many countries around the world. The principal applications of the polymer pipes (HDPE and PVC) are in agriculture, construction industry, and highway and roads. Polymer pipes are also used for airport runway drainage and telephone and power line transmission. The wide acceptance of polymer pipes in these various applications is due primarily to their (a) ease of installation, (b) light weight, (c) resistance to corrosion, (d) unique structural properties, (e) resistance to abrasion and, above all, (f) low cost. In Bangladesh, flexible pipes are used sometimes as buried culverts for drainage of water across roads and embankments. However, use of the flexible pipes is increasing for sewer systems and underground telephone, electric, gas, and water distribution systems in the country (Dhar et al., 2004).

Flexible buried pipes should be designed to withstand soil overburden, ground water and surface loads from vehicular traffic. The pipe design and installation are usually based on American Association of State Highway and Transportation Officials (AASHTO) requirements. The AASHTO designs of buried thermoplastic and metal pipes are generally based on the factored thrust and pipe wall resistance. The pipe wall resistance must be, greater than the factored thrust to ensure safety against structural failure. Vertical pressure at pipe crown level and the pipe outside diameter are the two important factors used for determination of the factored thrust. When flexible pipes are buried under shallow depths, the vertical crown pressure is mainly influenced by the surface live loads. Soil backfill quality, pipe geometry, and material properties, pipe installation condition, and loading configuration are the other important factors that govern the soil pressure distribution over buried flexible pipes under surface live load. Design codes assume that the traffic loadings add a uniform pressure at the crown level of the pipe, (ASCE, 1993; AASHTO, 1996 & 1998) and the wheel pressures are taken into account in forms of a calculated average pressure. Also the soil is taken as homogeneous and elastic. AASHTO standard specifications for Highway Bridges consider a wheel load as a point load on the ground surface that spread through the fill at a rate of 1.75 times the depth, AASHTO (1996). However, the AASHTO LRFD specification made a significant change in the procedure of

calculating live load distribution through inclusion of the area of the tire footprint on the ground surface, AASHTO (1998). The LRFD specification also restricted the rate of spread from 1.15 to 1.0 times the depth, depending on the type of backfill. In the case of overlapping, the total load is distributed over the combined effective area. An influence factor was introduced to increase the stress for shallow burial (burial depth < 0.9m). AASHTO LRFD specification increased the maximum impact factor from 30% to 33% and increased the maximum depth at which impact was considered from 0.9m (3 ft) to 2.4m (8 ft). The basis for these changes and their impact on pipe design has been the subject of much discussion. Literature review, conducted on buried flexible pipes subjected to live load, indicates that a minimum soil cover over the pipe crown appears to be the most important parameter on pipe-soil system responses, Arockiasamy et al. (2004). However, there is very limited information on the pipe-soil system behavior with a variation of soil cover particularly for large diameter pipes (i.e.  $d > 600\text{mm}$ ) under live load. Limited research was conducted through measurement of soil stresses and pipe deflections under live load of flexible pipes. McGrath et al. (2001) initiated a project to investigate the performance of large diameter corrugated PE pipe installed under roadways with shallow depth of fill. Dhar et al. (2004) conducted full scale test of buried PVC pipes under surface line load. Arockiasamy et al. (2006) conducted field test to investigate the behavior of buried thermoplastic and metal flexible pipes under the application of static concentrated wheel loads. However, a better understanding about the behavior of the pipes under the live load is required for developing a rational design method of the pipes.

### 1.3 INSTALLATION PRACTICES

Construction of a pipeline depends on many controlling factors including pipe materials, soil conditions, topography, operation conditions etc. Pipes are sometime placed on a prepared ground surface under an embankment which was the covered with embankment material. This type of installation is called "embankment installation". Usually, pipes are installed in a trench that is excavated in the natural ground (also called "native soil"). The pipe is then backfilled using suitable materials. Granular free-draining materials are generally chosen as the backfill material to provide sufficient structural strength and support to the pipe. Figure 1.2 shows a

typical installation condition of buried pipe in a trench. Different terminologies such as crown, springline, invert, shoulder and haunch are generally used to identify a location around the pipe circumference as shown in Figure 1.2. Crown means the vertex or top of an arch, applied to about one third of the curve, but in a pointed arch to the apex only. In case of pipe, crown indicates the top most point of a pipe as shown in the Figure 1.2. Pipe springline means the point which is 90 degree apart from the crown in both sides i.e. vertically mid-level of the pipe. Pipe invert is the bottom point of pipe, vertically below the crown. The nearby zones of pipe invert are known as haunch. The pipe periphery from pipe springline to crown is known as shoulder.

The trench is an excavation made during a pipe installation for the purpose laying the pipe, which is then covered. Sometimes foundations are required for pipe installation depending on the pipe, ground and operation conditions. Backfill indicates the soil which is used to cover the pipe after being installed in the trench.

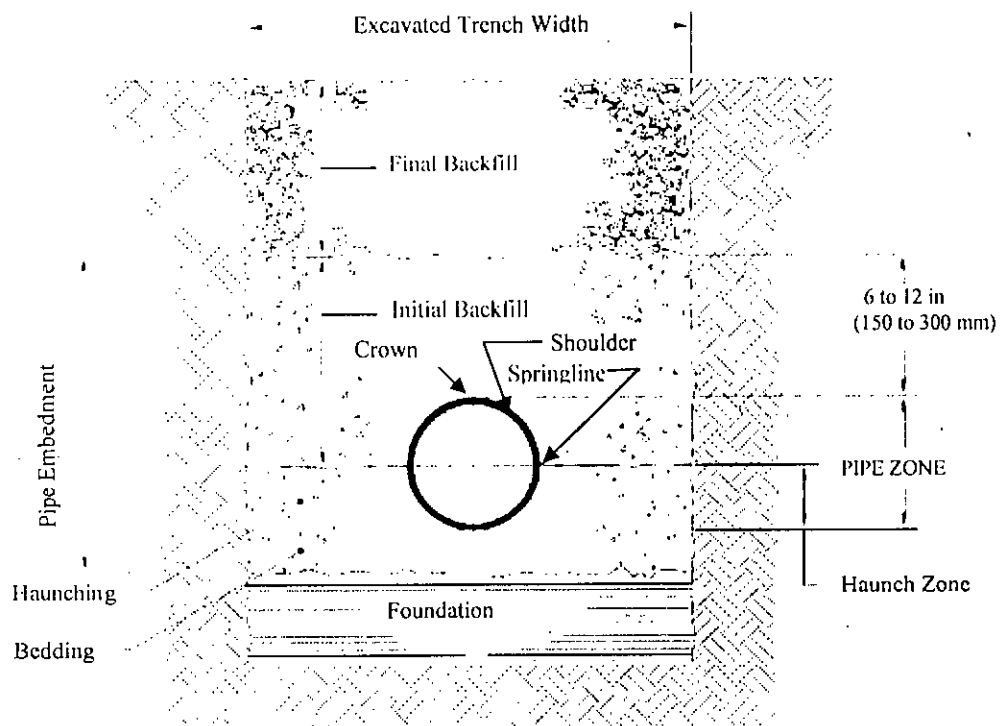


**Figure 1.2 Trench Cross Section Showing Terminologies**

## 1.4 OBJECTIVES

The research mainly attempts to study the parameters that influence the design and performance of buried flexible pipe under surface live load and to evaluate the current design methods for incorporating live load in pipe design. The specific objectives of the research are summarized as follows:

1. Development of a model for numerical analysis of buried flexible pipes under live load.
2. Evaluation of developed model with existing field observation data.
3. Parametric study to identify the parameters contributing on live load distribution around the pipe.
4. Evaluation of the current design method for live load analysis for flexible pipe.

## 1.5. METHODOLOGY AND SCOPE

A general purpose finite element program ABAQUS was used to model pipe-soil interaction for analysis of the pipe under the surface loads. Different finite element meshes were developed to represent variation of burial depth, pipes sectional properties, and parameters of pipe's material. Variations of the parameters of backfill and pipe materials were used to investigate the effect of geometric and material parameters on the live load distribution around the pipe.

Two dimensional finite element analyses were used through idealization of the three-dimensional concentrated load into an equivalent line load. Four burial depths i.e. 300 mm, 600 mm, 1500 mm and 3000 mm were considered for investigation of the effect of the burial depths. For each burial depth sectional parameters of pipe walls were varied along with material modulus. Sectional areas of 20 mm<sup>2</sup>/ mm, 30 mm<sup>2</sup>/ mm and 60 mm<sup>2</sup>/ mm and moments of inertia of 300 mm<sup>4</sup>/ mm, 7000mm<sup>4</sup> / mm15700 mm<sup>4</sup>/mm were considered based on available geometries of wall profile (Dhar and Noor, 2007). Material modulus of pipe was varied from long term modulus of HDPE (200 MPa) to steel (210000 MPa). Finite element results were compared with the stresses calculated according to ASCE and AASHTO design codes for evaluation.

## 1.6 THESIS ORGANIZATION

This thesis was organized to reveal the outcome of this research work in a systematic way in five chapters. First chapter demonstrates introduction and objectives along with the present state of the problem. Scope of this research work and methodology is also describes in this chapter.

Chapter 2 describes the recent research works that have performed in the analysis of buried flexible pipe under surface load. Moreover, different finite element code that had been used for analysis of buried pipe world wide was described briefly. Different design codes and incorporation of live loads in those codes are also outlined.

Finite element modeling, simulation and problem idealizations are discussed in Chapter 3. Finite element model was evaluated using existing full-scale test data on buried pipe under concentrated surface load.

In Chapter 4, a detailed parametric study is demonstrated and their effects are described elaborately. Finally in Chapter 5 conclusions and recommendations of this research work are described.



## CHAPTER 2

### LITERATURE REVIEW

#### 2.1 INTRODUCTION

Flexible pipes have been used for buried applications since the early days of corrugated metal pipe in the 1870's. The early uses of flexible pipe were mainly for storm water drainage and culverts. As the acceptance grew, flexible pipes started being used for sewer application. The early designs of flexible pipe were based on extensions of rigid pipe theory. For direct buried application, deflection control is generally considered as the governing design criteria. Although flexible pipes can be deflected 30% without reverse curvature, generally either 5 or 7.5% deflection is allowed in design. Excessive deflections of the pipe may affect integrity of the joints and cause excessive ground settlements. A semi-empirical deflection equation developed at the Iowa State University has generally been used to calculate pipe deflections. Spangler (1941) developed the equation, known as the "Iowa Formula", using assumptions based on his observations during field-loading experiments on corrugated metal pipe culverts. Spangler (1941) expressed horizontal deflection as a function of the vertical load and the bending resistance provided by the pipe and the surrounding soil. The vertical deflection was generally assumed to be of equal magnitude to the horizontal deflection but with opposite sign. Watkins later performed model studies and examined the Iowa formula, from which some modifications were made to incorporate a soil parameter with dimensions equivalent to modulus (Watkins and Spangler, 1958). The Modified Iowa Formula has been the principal tool for estimating deflection for flexible pipe for the past 50 years. However, it has been recognized that the modified Iowa formula, which only consider the flexural deflection, is not applicable for very flexible pipes like pipes made of thermoplastic materials. Dhar et al. (2002) presented a simplified equation for the deflection of flexible pipe that account for the shortening due to hoop forces in addition to the flexural/bending deflection. The simplified equation has been adopted

in AASHTO for flexible pipe design. Wall stress and wall strain on the buried pipe are calculated based on thrust and bending moment obtained from soil-structure interaction solution (Dhar et al., 2002).

Buried culverts and pipelines under roadways are subjected to earth loads and vehicular loads. The earth load covers the weight of the pavement, soil and bedding above the pipe. The vehicular loads come from cars and trucks traveling on the roadway. Soil-structure interaction solutions have been developed to calculate the pipe deflection, wall thrust and bending moment for buried flexible pipes due to earth load and adopted in the design codes (Moore 1993, McGrath et al., 1998, Dhar et al., 2002). However, the effects of surface traffic load are estimated in the pipe design codes as a uniform load averaged over an assumed surface area. This chapter presents the current design status of buried flexible pipe with particular attention to the incorporation of the effect of surface live load.

## 2.1 PIPE ANALYSIS METHODS

### 2.2.1 Analysis for Dead Load

The amount of load taken by a pipe under dead load depends on the relative stiffness of the pipe to the soil fill at the side of the pipe and the relative movement between the backfill and the natural soil. Marston load theory, as cited by Moser (1990), recognized the amount of load taken by a pipe in a trench due to relative movement between the backfill and the natural soil and developed following formula for the vertical force acting on the rigid pipe:

$$W_d = C_d \gamma B^2 \quad (2.1)$$

Where:

$W_d$  = Load on rigid pipe

$C_d$  = Load coefficient accounting for the frictional resistance due to the relative movement between the backfill and natural soil. It is expressed as a function of trench width, burial depth, soil friction angle and lateral earth pressure.

$\gamma$  = Unit weight of backfill

B = Width of trench

While the Marston theory provides a useful tool for calculating earth load, it does not properly appreciate pipe-soil interaction or arching within the backfill for non-rigid pipes (Cameron, 2006). Molin (1981) derived the vertical soil pressure,  $w$ , above a pipe in an infinitely wide trench (e.g. under embankment fill) considering relative stiffness of pipe-soil system and proposed the average pressure at crown level as:

$$W = Cq_0 \quad (2.2)$$

Where:

$q_0$  = Pressure at crown level without a pipe

C = Load factor (minimum value of 1), and is given by

$$C = \frac{36S_r(20S_r + 1)}{(12S_r + 1)(36S_r + 1)} \quad (2.3)$$

$$\text{And } S_r = \text{Stiffness ratio} = \frac{8S}{E_s}$$

Where:

$$S = \text{Stiffness of pipe} = \frac{EI}{D^3}$$

$E_s$  = Horizontal modulus of soil reaction as defined by the Iowa equation (MPa)

Cameron (2006) reported that Molin's expressions have little influence on flexible pipes as pipe stiffness,  $S$ , of 50 kPa is required to override the minimum C value of unity, assuming a relatively low soil stiffness of 5 MPa. This pipe stiffness value exceeds common flexible pipe stiffnesses.

Pipe stress estimated at the crown level is used to calculate the pipe deflection, wall stress and wall strain for buried flexible pipe. The Iowa Deflection Equation (Sprangler 1941) has been the primary tools for calculation of pipe deflection. The vertical pipe deflection (assumed to be the same as the horizontal deflection) according to the modified Iowa formula as expressed in AASHTO is given by:

$$\frac{\Delta D_v}{D} = \frac{D_l K W_c}{EI/r^3 + 0.061 E_s} \quad (2.4)$$

Where:

$D_l$  = Deflection lag factor

$K$  = Bedding constant

$W_c$  = Load per unit length of pipe

$r$  = Mean radius of pipe

$E$  = modulus of elasticity of pipe material

$I$  = Moment of inertia of pipe wall per unit length

$E_s$  = Modulus of passive resistance of side fill

$\Delta D_v$  = Vertical deflection or change in diameter

$D$  = Diameter of the pipe

However, it has been recognized that the Iowa formula gives the flexural deflection of the pipe and neglect the contribution of circumferential shortening (hoop deflection). Dhar et al. (2002) presented the Iowa equation for flexural pipe deflections and a pipe deflection term accounting for the hoop deflection to be summed up to give the total deflection of the pipe. The hoop component of deflection is given by (McGrath et al., 1998):

$$\frac{\Delta D}{D} = \frac{F_v W_c}{EA/r + 0.57 E_s} \quad (2.5)$$

Where:

$F_v$  = Vertical arching factor

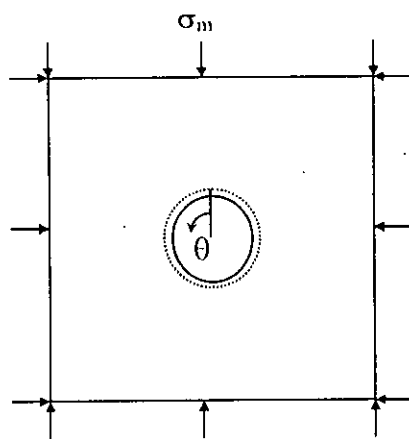
$A$  = Cross sectional area per unit length of pipe

$\Delta D$  = Change in diameter

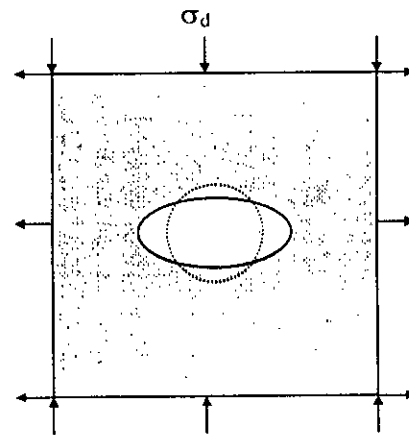
Moore (1993) adopted the continuum solution of Hoeg (1968) for soil-structure interaction solution for pipe analysis. Hoeg (1968) derived the formulation for the more generalized case of  $\sigma_h = K\sigma_v$ , where  $\sigma_v$ ,  $\sigma_h$  are vertical and lateral earth pressure and  $K$  is the coefficient of earth pressure at rest, respectively. However, to simplify

the interpretation, the two-dimensional load system was divided into uniform ( $\sigma_m$ ) and non-uniform components ( $\sigma_d$ ) of pressures as shown in Figure 2.1. For a particular condition (i.e. for a certain K), the uniform ( $\sigma_m$ ) and non-uniform components ( $\sigma_d$ ) of pressures were expressed by Moore (2000) as:

$$\left. \begin{aligned} \sigma_m &= \frac{\sigma_v + \sigma_h}{2} \\ \sigma_d &= \frac{\sigma_v - \sigma_h}{2} \end{aligned} \right\} \quad (2.6)$$



(a) Uniform deformation



(b) Non-uniform deformation

**Figure 2.1 Uniform and non-uniform deformation of buried pipe (Moore, 2000)**

Distributions of interface radial and shear stress on the external boundary of the pipe were then defined as:

$$\begin{aligned} \sigma &= \sigma_o + \sigma_2 \cos 2\theta \\ \tau &= \tau_2 \sin 2\theta \end{aligned} \quad (2.7a)(2.7b)$$

Where  $\theta$  is measured from the vertical axis, and

$$\left. \begin{aligned} \sigma_o &= A_m \sigma_m \\ \sigma_2 &= A_{d\sigma} \sigma_d \\ \tau_2 &= A_{d\tau} \sigma_d \end{aligned} \right\} \quad (2.8a) (2.8b) (2.8c)$$

Factors  $A_m$ ,  $A_{d\sigma}$  and  $A_{d\tau}$  are called arching factors.

Pipe deflection, wall thrust and wall bending moment can be estimated from these interface pressure components  $\sigma_0$ ,  $\sigma_2$  and  $\tau_2$  (Equation 2.8). For harmonic interface stresses defined by Equation 2.8, thrusts at the crown,  $N_{cr}$ , and spring-line,  $N_{sp}$ , are given by:

$$N_{cr} = \sigma_o r - \left( \frac{\sigma_2}{3} - \frac{2\tau_2}{3} \right) r \quad (2.9)$$

$$N_{sp} = \sigma_o r - \left( \frac{\sigma_2}{3} - \frac{2\tau_2}{3} \right) r \quad (2.10)$$

The bending moments at the crown,  $M_{cr}$ , and at the springline,  $M_{sp}$ , are given by:

$$M_{cr} = \left( \frac{\sigma_2}{3} + \frac{\tau_2}{6} \right) r^2 \quad (2.11)$$

$$M_{sp} = - \left( \frac{\sigma_2}{3} + \frac{\tau_2}{6} \right) r^2 \quad (2.12)$$

Pipe wall stresses based on the axial thrust and the bending moment can be estimated as:

$$\sigma = \frac{N}{A} + \frac{Mc}{I} \quad (2.13)$$

Where:

N = Axial Thrust

M = Bending Moment

A = Sectional Area of Pipe Wall

I = Moment of Inertia of Pipe Wall

C = Distance from Neutral Axis

Deflections can be determined from the pipe stresses by considering the components of the external stresses,  $w_o$ , due to the isotropic loading and  $w_d$  due to the deviatoric loading as follows:

$$w_o = \frac{\sigma_o r^2}{EA} \quad (2.14)$$

and

$$w_d = \frac{(2\sigma_d - \tau_d)r^4}{18EI} \quad (2.15)$$

The changes in diameter of the pipe in the vertical and horizontal directions,  $\Delta D_V$  and  $\Delta D_H$  respectively, may then be formulated as:

$$\Delta D_V = 2(w_o - w_d) \quad (2.16)$$

$$\Delta D_H = 2(w_o + w_d) \quad (2.17)$$

### 2.2.2 Effects of Wheel Load

Pipes that have been buried at shallow depths will be subjected to the loads imparted by traffic. If high strength pavements designed for heavy traffic, it can reduce the pressure transmitted through a wheel to the sub-grade and consequently to the underlying buried pipe. If roads are intermediate and thin, no general acceptable theories are available so that load distribution can be recognized easily. For such case, roads should be considered as un-surfaced one in the analysis of buried pipe. However, during the construction phase, buried pipe may experience such load which is not uncommon now a day. Traffic must include construction plant since, during construction, the pipe is most susceptible to damage; protection afforded by backfill cover height may be incomplete and overlying pavements may yet to be completed. After construction, pipelines underlying roads, railways or airport runways will experience live loading. Traffic imparts a local loading, which has most impact when the traffic direction is transverse to the longitudinal axis of the pipeline. Pneumatic tires which transmit axle loads have an almost elliptical footprint on a road surface. Pavement engineers approximate the footprint to a uniformly loaded, rectangular patch (Cameron, 2006). Fernando and Carter, (1998) use such type of loading in the buried pipe analysis.

Pipe's performance under vehicular loading depends on the depth of backfill cover, properties of both the backfill and the native soil, the geometry of the trench installation and relative and bending stiffness of the buried pipe. Boussinesq calculated the distribution of stresses for point load applied on the surface in a semi-infinite elastic medium without any consideration of pipe. An elastic, homogenous, isotropic medium was assumed in the process of calculation for distribution of soil

stress. The vertical stress in the soil mass (Figure 2.2) due to a concentrated surface load was expressed as:

$$\sigma_v = \frac{3P}{2\pi H^2 [1 + (d_s/H)^2]^{5/2}} \quad (2.18)$$

Where:

$\sigma_v$  = Pressure transmitted to the soil

$P$  = Concentrated load at surface

$H$  = Depth below the ground surface

$d_s$  = Offset distance of ground point from line of application of surface load

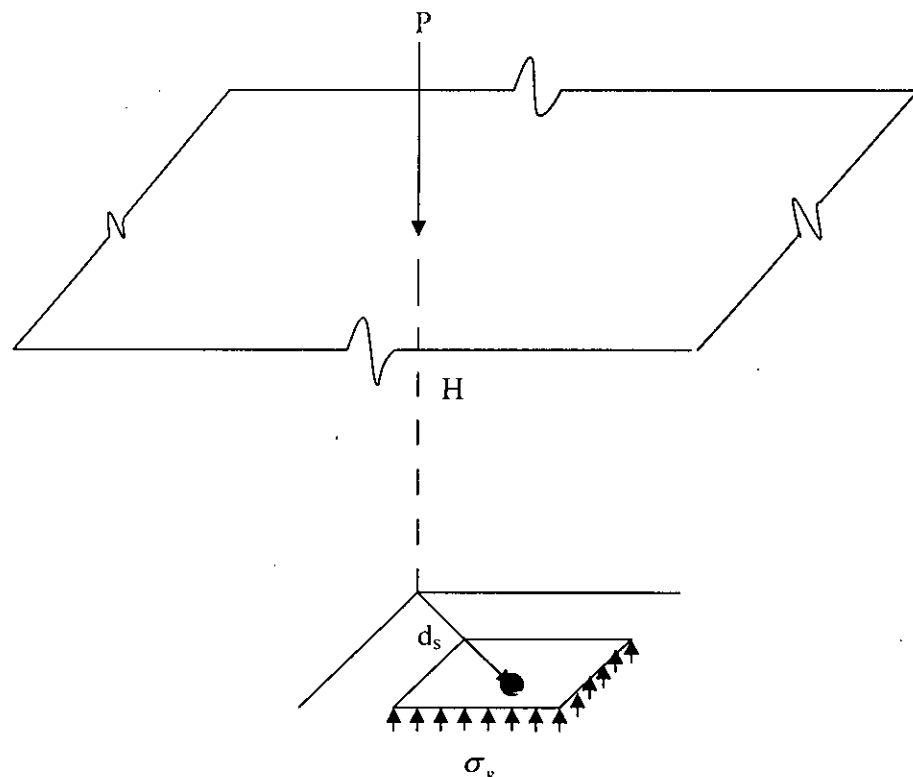


**Figure 2.2 Vertical Stresses in the Soil Mass Due to Concentrated Surface Load**

Moser (2001) interpreted the stress as the pressure felt by the pipe for the concentrated load, considering the depth,  $H$ , as the height of soil cover above the pipe crown. Boussinesq developed the graph as shown in Figure 2.3 for surface live load as



a function of burial depth, which was expressed as a fraction of a surface load transmitted to buried pipe or culvert. Deviations of Boussinesq curve with the field measurements are also showed in Figure 2.3. Hall and Newmark (1977) later worked on Boussinesq solution by integration to obtain load co-efficient. The integration developed by Hall is used for calculating concentrated loads (such as truck wheel load) and given in the following form:

$$W_{sc} = \frac{C_s P F'}{L} \quad (2.19)$$

Where:

$W_{sc}$  = Load on pipe per unit length

P = Concentrated Loads

$F'$  = Impact Factor

L = Effective length of Conduit

$C_s$  = Load co-efficient which is a function of  $B_c/2H$  and  $L/2H$ ,

Where:

H = Height of fill from top of pipe to ground surface

$B_c$  = Diameter of pipe

Surface live load may act either as an impact or static loading case. For impact loading, values of the impact factor  $F'$  can be determined from Table 2.1 and the load co-efficient  $C_s$  from Table 2.2.

When surface live load act, it can create either circular or a truncated cone (Moser, 2001). If the loaded surface area is circular, a truncated cone is punched through. Again, if loaded surface area is a rectangle, a truncated pyramid is also punched through. These cases are shown on Figure 2.4.

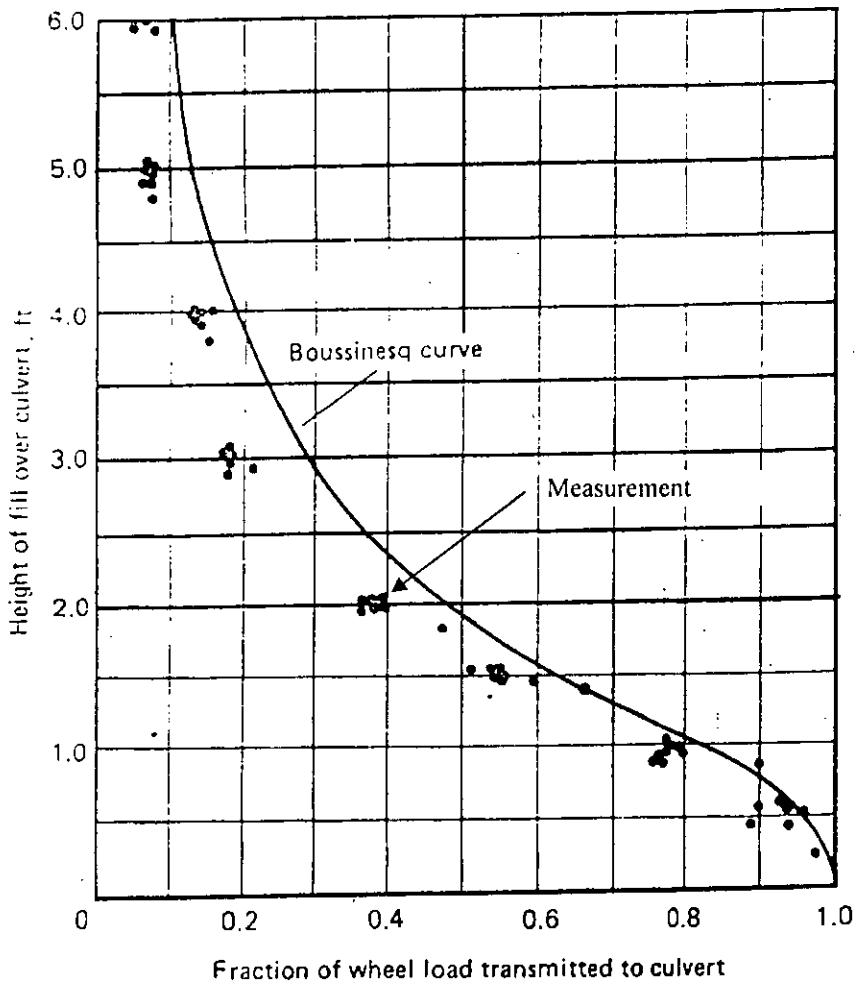


Figure 2.3 Distribution of surface live loads versus loads on a plane at depths of Pipe Crown (After Moser, 2001)

Table 2.1 Impact Factor  $F'$  versus Height of cover (Moser, 2001)

Height of Cover	Installation Surface Condition			
	Highways	Railways	Runways	Taxiways, aprons, hardstands, run-up pads
0 to 1	1.50	1.75	1.00	1.50
1 to 2	1.35	*	1.00	*
2 to 3	1.15	*	1.00	*
Over 3	1.00	*	1.00	*

\* Information could not be collected

**Table 2.2 Values of load co-efficient  $C_c$  for concentrated superimposed loads vertically centered over conduit (Mosser, 2001)**

$B_c/2H$	$L/2H$													
	0.1	0.2	0.3	0.4	0.5	0.6	0.7	0.8	0.9	1	1.2	1.5	2	5.0
0.100	0.019	0.037	0.053	0.067	0.079	0.089	0.097	0.103	0.108	0.112	0.117	0.121	0.124	0.128
0.037		0.072	0.103	0.131	0.155	0.174	0.189	0.202	0.211	0.219	0.229	0.238	0.244	0.248
0.053		0.103	0.149	0.190	0.224	0.252	0.274	0.292	0.306	0.318	0.333	0.345	0.355	0.360
0.400	0.067	0.131	0.190	0.241	0.284	0.320	0.349	0.373	0.391	0.405	0.425	0.440	0.454	0.460
0.500	0.079	0.155	0.224	0.284	0.336	0.379	0.414	0.441	0.463	0.481	0.505	0.525	0.540	0.548
0.600	0.089	0.174	0.252	0.320	0.379	0.428	0.467	0.499	0.524	0.544	0.572	0.596	0.613	0.624
0.700	0.097	0.189	0.274	0.349	0.414	0.467	0.511	0.546	0.584	0.597	0.628	0.650	0.674	0.688
0.800	0.103	0.202	0.292	0.373	0.441	0.499	0.546	0.584	0.615	0.639	0.674	0.703	0.725	0.740
0.900	0.108	0.211	0.306	0.391	0.463	0.524	0.574	0.615	0.647	0.673	0.711	0.742	0.766	0.784
1.000	0.112	0.219	0.318	0.405	0.481	0.544	0.597	0.639	0.673	0.701	0.740	0.774	0.800	0.816
1.200	0.117	0.229	0.333	0.425	0.505	0.572	0.628	0.674	0.711	0.740	0.783	0.820	0.849	0.868
1.500	0.121	0.238	0.345	0.440	0.525	0.596	0.650	0.703	0.742	0.774	0.820	0.861	0.894	0.916
2.000	0.124	0.244	0.355	0.454	0.540	0.613	0.674	0.725	0.766	0.800	0.849	0.894	0.930	0.956

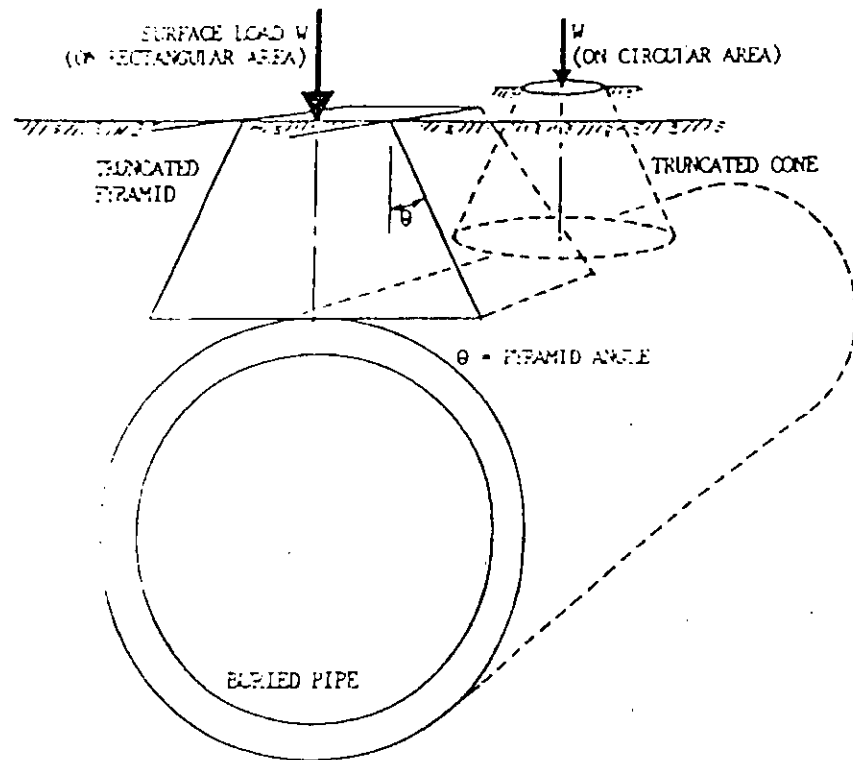


**Figure 2.4 Soil stress models for minimum cover as truncated pyramid and cone (Mosser, 2001)**

Among these two types, pyramids are more realistic because the tire print of dual wheels is nearly rectangular and can easily form pyramid. However, the pyramid concept is imperfect because sharp corners do not form in such a way in reality.

## 2.2 LIVE LOADS IN DESIGN CODES

It is recognized in pipe design that if the pavements are of high strength and thick, it can obviously take heavy truck traffic substantially and can reduce the pressure transmitted through a wheel to the sub-grade. Thus, pressure can be reduced to the underlying pipe in an easy way. The pressure reduction is so great that generally the live load can be neglected. Westergaard (1926) showed the effects of loading conditions, sub-grade support, and boundary conditions on concrete pavements and developed a method to calculate the stresses in concrete slabs. After that, Portland Cement Association, (PCA, 1944), developed a method to determine the vertical pressure on buried pipe due to wheel loads applied to concrete pavements. But if the pavement is flexible or intermediate and thin thickness of asphalt, then no such theory are available to calculate the pressure transmitted from a wheel to sub-grade to any significant degree. Various codes are now available to calculate the live load pressure at the buried pipe crown. The wheel load in ASCE (1993) is assumed as a uniform pressure produced at crown level. Dimension for load spread area is provided, which is about 1.75 times the depth of fill plus foot print dimension. For shallow depth an impact factor was introduced. In the case of overlapping of two or more areas, the total load will be distributed over the combined effective area. The design load of 7273 Kg (16 Kip) is used for an overburden height of less than 0.44 m with corresponding distributed area,  $A_{LL}$ , of  $0.27 + 1.75H$  by  $0.55 + 1.75H$ . The distributed live load area is based on the load due to single dual wheel acting on the ground surface with a contact area of 0.5 m by 0.25 m. The equivalent design loads and corresponding distributed live load areas for overburden height ranging between 0.44m and 1.34m and for overburden heights greater than 1.34 m are listed in Table 2.3.

**Table 2.3 Distributed Live Load Area (ASCE, 1993)**

H (m)	P (Kg)	Aw (m)	A <sub>LL</sub> (m)
H < 0.44	7,473	0.27+1.75H	0.55+1.75H
0.44 < H < 1.34	13,636	0.27+1.75H	1.86+1.75H
H > 1.34	21,818	1.58+1.75H	1.86+1.75H

The average pressure intensity,  $\sigma_l$ , is taken as the soil stress at the elevation of the crown of the pipe crown by:

$$\sigma_l = \frac{P(1 + I_f)}{A_{LL}} \quad (2.20)$$

Where:

P = Total applied surface wheel loads

A<sub>LL</sub> = Distributed Live Load Area

I<sub>f</sub> = Impact Factor, From Table 2.4

**Table 2.4 Impact Factor**

H (m)	I <sub>f</sub>
0-0.3	1.3
0.3-0.6	1.2
0.6-0.9	1.1
>0.9	1.0

The live load, per unit length of the pipe,  $W_l$ , can be expressed in terms of  $W_T$ , the total live load subjected to the surcharge in the following way:

$$W_l = \frac{W_T}{L_c} \quad (2.21)$$

Where:

$W_l$  = Live load per unit length

$W_T$  = Total live load on pipe per unit length

$L_e$  = Effective supporting length of pipe, shown in Figure 2.5.

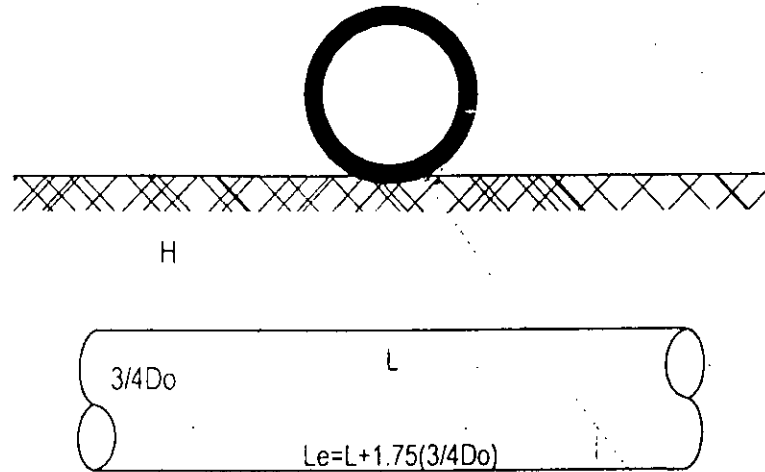


**Figure 2.5 Effective Supporting Length (after ASCE, 1993)**

The total live load,  $W_T$ , is a function of pressure intensity and effective area (Figure 2.6) where effective area depends on the direction of traveling. When direction of traveling is perpendicular to the axis of pipe, then total live load can be expressed in:

$$W_T = \sigma_l L S_l \quad (2.22)$$

Where:

$\sigma_l$  = Average pressure intensity

L = Length of  $A_{ll}$  parallel to longitudinal axis of pipe

$S_l$  = Outside horizontal span of pipe or width of  $A_{ll}$  transverse to longitudinal axis of pipe, whichever is less

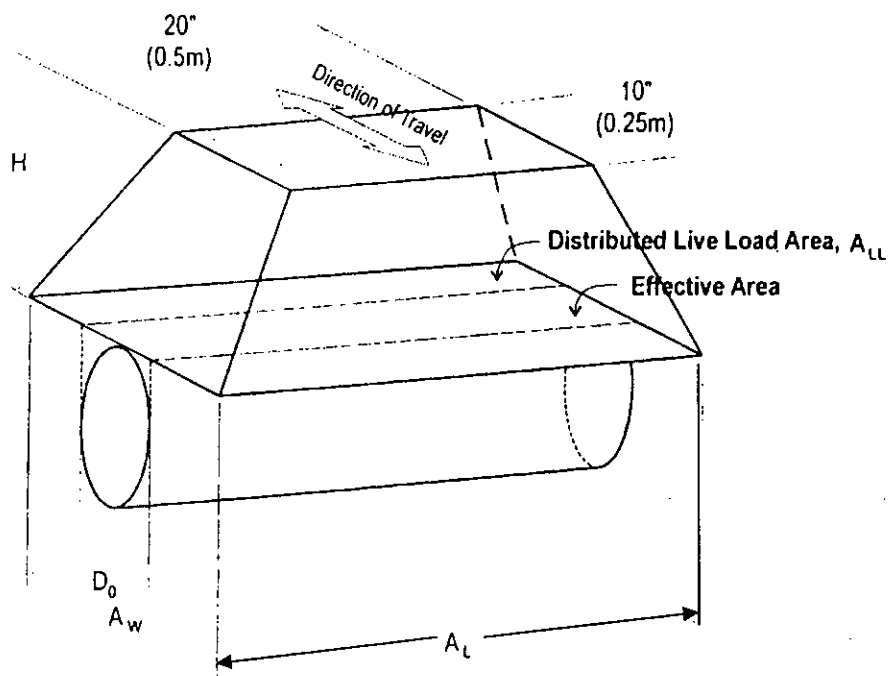


Figure 2.6 Effective Area of the Live Load (After ASCE, 1993)

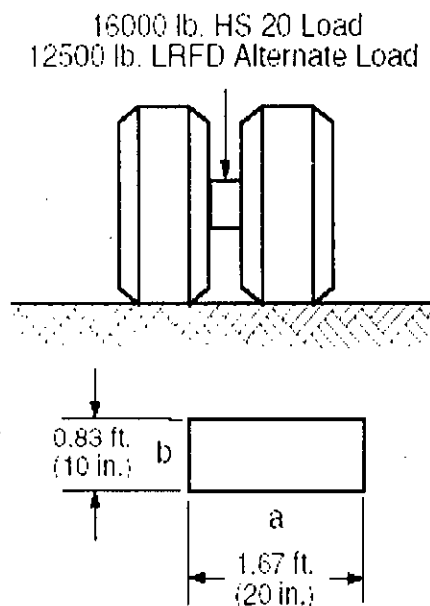


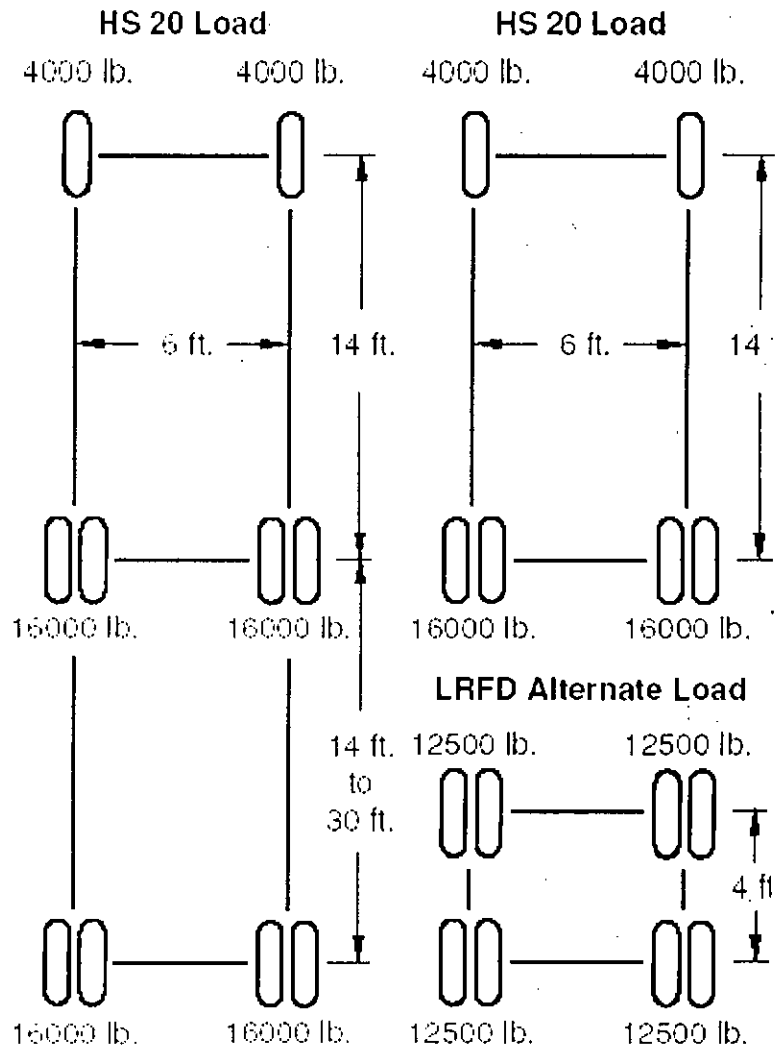
Figure 2.7 AASHTO Wheel Load Surface Contact Area (Foot Print)

In AASHTO design, loads commonly used in the past were HS20 with a 32,000 lb axle load in the normal truck configuration and a 24,000 lb axle load in the alternate load configuration. Almost all trucks possess dual wheels as per AASHTO and wheel foot print is assumed to be rectangular as shown in the Figure 2.7. Figure 2.8 shows AASHTO wheel loads and wheel spacing.

AASHTO also assumes uniform load spreading as in ASCE. Figure 2.9 shows spread load area for a single dual wheel. In case of overlapping of areas, the wheel loads are assumed to be uniformly distributed over the combined area. Figure 2.10 and Figure 2.11 shows load spread was for the cases with overlapping of areas. However, AASHTO LRFD assumed two different load spreading rate for granular and other soil as shown in Table 2.5. Thus the load spreading used in AASHTO LRFD code is lower than other codes (ASCE, CAN/CSA). Canadian Highway Bridge Design Code (CAN/CSA) uses the same load spreading rate (1.75 times the length) as in ASCE (1993).

From Figure 2.10 and Figure 2.11 it is clear that spread load areas from adjacent wheels will overlap as the height of earth cover over the top of the pipe increase. For different backfill type, spread load area is also different. Since the exact geometric relationship of individual or combinations of surface wheel loads cannot be anticipated, the most critical loading configurations along with the axle loads and rectangular spread loads area are presented as in Table 2.6 and Table 2.7.





**HS 20 & LRFD Alternate Loads**

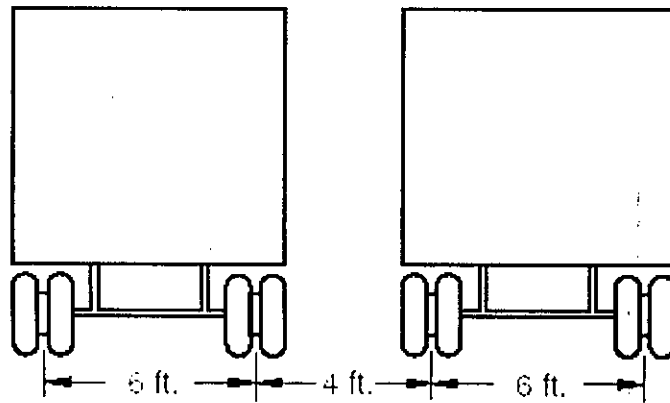


**Figure 2.8 AASHTO Wheel Loads and Wheel Spacings**

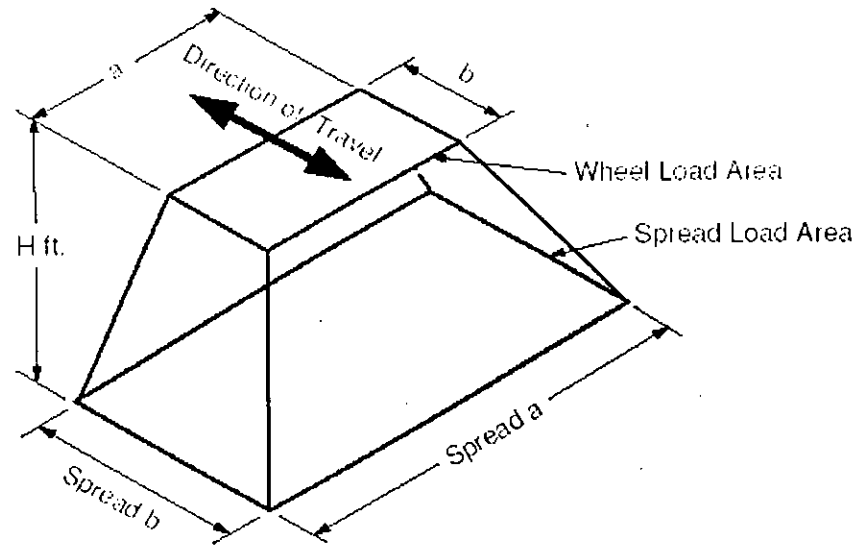


Figure 2.9 Spread Load Area-Single Dual Wheel

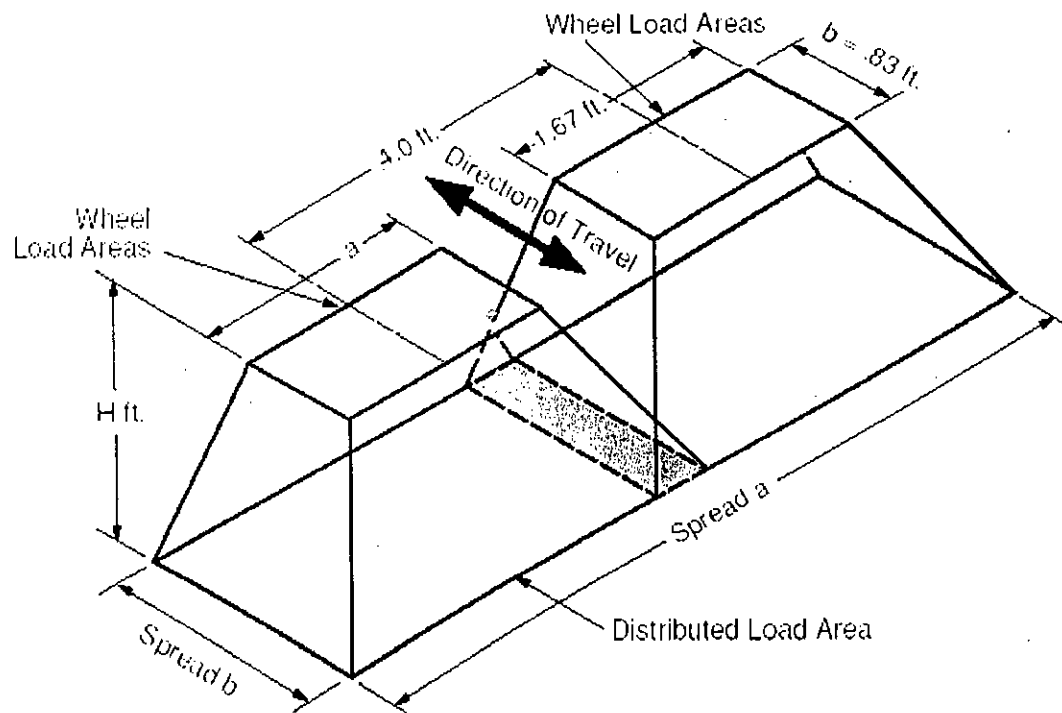
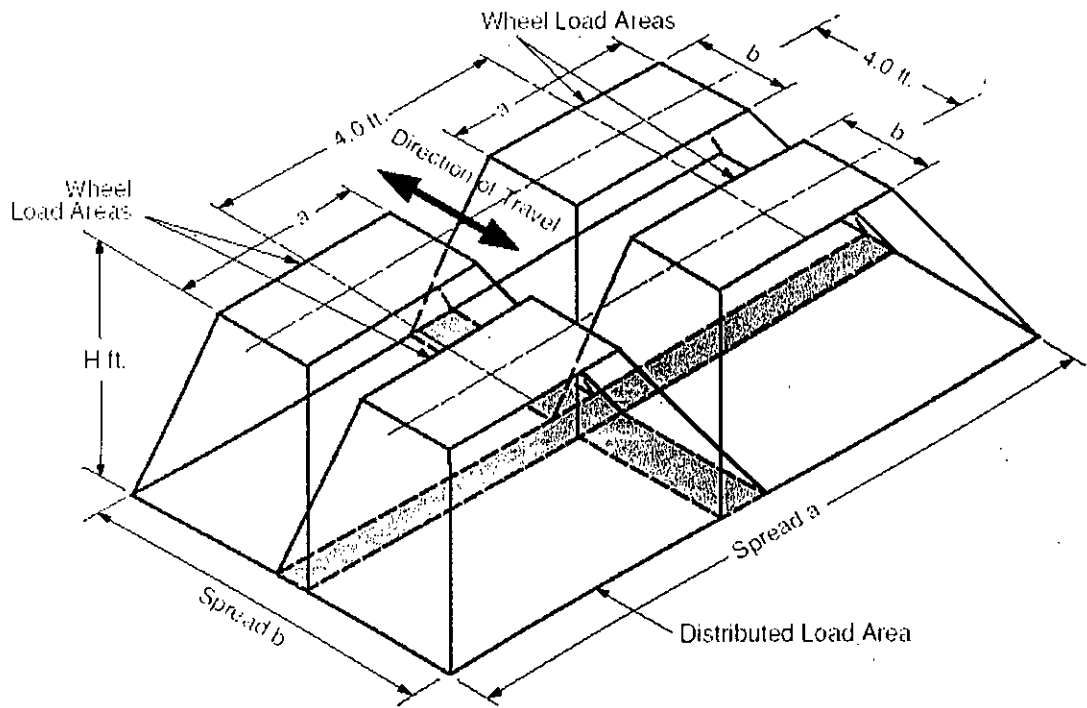


Figure 2.10 Spread Load Area-Two Single Dual Wheels of Trucks in Passing Mode



**Figure 2.11 Spread Load Area-Two Single Dual Wheels of Two Alternate Loads in Passing Mode**

**Table 2.5 AASHTO LRFD Load Spreading Rate**

Soil Type	Dimensional Increase Factor
Granular Soil	1.15H
Other Soil	1.00H

**Table 2.6 LRFD Critical Wheel Loads and Spread Dimensions at the Top of the Pipe for select Granular Soil Fill**

H, ft (m)	P, lbs (Kg)	Spread a	Spread b
$H < 2.03$ (0.619)	16,000 (7257)	$a + 1.15H$	$b + 1.15H$
$2.03$ (0.619) $\leq H \leq 2.76$ (0.841)	32,000 (14,514)	$a + 4 + 1.15H$	$b + 1.15H$
$2.76$ (0.841) $\leq H$	50,000 (22,678)	$a + 4 + 1.15H$	$b + 4 + 1.15H$

**Table 2.7 LRFD Critical Wheel Loads and Spread Dimensions at the Top of the Pipe for Other Soil Fill**

<b>H, ft (m)</b>	<b>P, lbs (Kg)</b>	<b>Spread a</b>	<b>Spread b</b>
H<2.33 (0.710)	16,000 (7,257)	a+1.00H	b+1.00H
2.33 (0.710)≤H≤3.17 (0.966)	32,000 (14,514)	a+4+1.00H	b+1.00H
3.17(0.966)≤H	50,000 (22,678)	a+4+1.00H	b+4+1.00H

AASHTO LRFD standard applies a dynamic load allowance to account for truck load being non-static. The dynamic load allowance, IM, is determined by:

$$IM = \frac{33(1.0 - 0.125H)}{100} \quad (2.23)$$

Where:

H = Height of earth cover over the top of the pipe

#### 2.4 RESEARCHES WITH LIVE LOAD STUDY

Jayawickrama et al. (1998) performed research taking as large as 1200 mm diameter flexible pipe with a project to develop minimum pipe cover for heavy construction wheel load. High density polyethylene pipes of 900 mm, 1050 mm and 1200 mm diameter were used under a larger axle load like 600 kN to develop design charts. Pipes met the requirements for AASHTO M294 Type S and had smooth inner liners and corrugated outer liners. For both pipes a constant moment of inertia was used i.e.  $9000 \text{ mm}^4/\text{mm}$  was used. The cross sectional area of  $9.2 \text{ mm}^2/\text{mm}$  was used for 900mm diameter pipe and  $11.2 \text{ mm}^2/\text{mm}$  was used for 1200 mm diameter pipe. Modulus for in situ soil was used as 3500 KPa indicating a soft to medium stiff clay. Emphasis was given in the development of minimum soil cover to protect the pipes from its installation phase. Full scale load test was performed under two different loading conditions along with eight pilot construction projects. Locally available materials were used as the backfill for the pipes used in this cases that were locally

available. Backfill compaction was achieved using impact rammer. Load was applied using hydraulic cylinder. To measure the deflection deflectometer was used. Back analysis was performed to determine the material stiffness parameters and finite element tools named CANDE were also used to predict pipe performance. Minimum trench width of 2.25 m was provided. It was found that when deflections were expressed as a percentage of the nominal pipe diameter the differences between results obtained for different pipe diameters were small. All subsequent analysis was performed for 1200 mm diameter pipe only. Thus, design charts were developed for minimum soil cover without considering the effect of repetitive load.

Fernando and Carter (1998) performed numerical study with a wide parametric variation to develop a non-dimensionalized graph for incorporating the effects of surface loads. Parametric study was performed to assess the effects of the various geometric and material parameters on the behavior of buried pipe under vehicular live loads approximated as a patch of vertical stresses over a square centrally placed area. Predictions of the maximum circumferential bending moments induced in the buried pipe were presented in a non-dimensionalized design charts. This was developed using ratio between height of cover to pipe diameter as 0.1, 0.25, and 0.5 and ratio of pipe modulus to soil modulus as 100,000, 10,000, and 1,000. A semi-analytical finite element scheme was used based on Fourier transform for three dimensional modeling of patch load. Thus, the analysis was limited to the solid wall pipes with uniform wall thickness. However, the thickness of pipe was varied from 0.05 to 10% of the pipe diameter.

McGrath et al. (2002) used pipe diameter of larger than 1200 mm for full-scale live load tests and worked with different pipe such as Type S PE, Type D PE, steel and concrete pipes of diameter 1500 mm. A burial depth of 300 mm and 600 mm was used. Live loads were applied as the axle loads of 80 kN and 107 kN for full scale field tests. Arrangements were made along with LVDTs, strain gages, soil pressure cells etc. Thermocouples were also used so that temperature effect throughout the year can be recognized easily along with other factors. Trench was made following proper guide line and at a distance of 450 mm from springline and 150 mm below invert. Bedding was compacted using 90% compaction level (Standard Proctor) and backfill was compacted using 85-90% compaction level. Pavement was also placed

over the backfill and 200 mm thick flexible pavement was provided. Axle load was placed at four different locations to see the effect in flexible pipe behavior. Findings from this research indicated that corrugated steel pipes were generally less deflected than the polyvinyl pipe for same condition. Even deflections were below 1% under live load. It had been showed that the load that acts as static creates more deflection than the same load that acts as a dynamic one. No parametric study was performed to see the pipe behavior with variation of different parameters.

Dhar et al. (2004) investigated small diameter pipes under surface line load with a wide variation in burial depth and sectional and geometric properties of pipe. Different burial depth of 600 mm, 900 mm and 1200 mm was used for polyvinyl chloride pipes of diameter 203 to 790 mm under quasi-live load along with clayey backfill in context of Bangladesh. Areas per unit length were used as 13 to 34  $mm^2/mm$  with a moment of inertia of 266 to 7,925  $mm^4/mm$ . Full scale load test was performed with a load of 73.3 kN. Pipes were placed in a trench of 2.4 m X 2.4 m X 2.4 m in such a way that it was equidistant from walls horizontally. Soil bedding below the pipe varied from 350 mm to 1000 mm for 1200 mm burial depth. For 600 mm burial depth 960 to 1620 mm soil bedding was used. Load was applied with the help of a steel plate of width 300 mm and length as same as the trench to simulate plain-strain condition. A load increment rate of 5 kN/m was provided in a faster way to represent live load. Seven different profiled polyvinyl chloride pipes were used for this purpose. To measure the load-deformation data, electronic deformation transducer was used and stored in computer through an ADU-700 data logger. It was revealed from the study that calculations using a load-spreading rate of 1.15 times the depth performed better in calculating the live load deflections. Deflections were underestimated by 30% to 48% for pipes at 600 mm depth and by 25% to 60% for the pipes at 1200mm depth when load spreading rate of 1.75 times the depth was used.

Arockiasamy et al. (2006) performed full scale field tests for flexible pipe using 0.5 D, 1.0 D and 2.0 D (D = nominal pipe diameter) under live load with a minimum trench width of not less than the greater of either 1.5 times the pipes outer diameter plus 305 mm or pipe outside diameter plus 406 mm. A bedding thickness of 152 mm was provided along with 19 mm crushed lime stone overlying the undisturbed natural

soil. Pipe with diameter of 900 mm, 1200 mm were used along with the variation in moment of inertia and sectional area of pipe wall. Variation also occurred for pipe wall thickness, Poisson's ratio and modulus of elasticity of pipe. Arrangements were made for taking readings of deflection, soil pressure and for strain with the equipment of linear variable differential transducers (LVDTs), pressure cell and strain gauge. Both two dimensional and three dimensional finite element packages were used for comparison. For two dimensional analyses CANDE-89 was used while for three dimensional analysis ANSYS was used. From comparison between analytical and field test, it was seen that Iowa formulac gives more deflection than others and field test yields least deflection in the case of installation only. For live load application, ANSYS yields good results than others where other tools overestimated the deflections. In case of soil pressure, finite element analysis at pipe crown and spring-line were generally in the same range with that of field test. This research was limited with the flexible pipe of lower than 1200 mm and effect of bending and hoop stiffness was not addressed. It was showed that 457 mm burial depth was enough for 900 mm diameter pipe for live load of 142 kN axle load. Moreover, effect of repeated load on buried pipe behavior was totally ignored.

## **2.5 FINITE ELEMENT ANALYSES**

Finite element method has been extensively used around the world for soil-structure interaction analysis for buried pipes. Analyses were performed using general purpose finite element programs and specific purpose finite element programs for analysis soil-structure interaction. Codes that commonly used for soil-pipe interaction analysis are SPIDA, SOILCON, CANDE etc. Following is a discussion of the finite element program used for pipe-soil interaction analysis.

### **2.5.1 SPIDA Code**

SPIDA is a finite element package, owned and made available by the American Concrete Pipe Association. But Heger et al. (1985) developed a Soil-Pipe Interaction Analysis (SPIDA) program for analyzing buried concrete pipe. The program provides the stress distribution around pipe, moments and shear forces within pipe-wall, and

area of required reinforcement having a wide variety of embedment soil backfill and natural soil around and over the pipe. This program has versatile capabilities of analysis and design of buried concrete pipe. It uses a predefined finite element mesh of the soil-pipe system and is capable of incorporating construction sequence during analysis. But its use is limited to circular pipe with constant wall thickness. Another limitations of SPIDA is idealized assuming a plane strain condition and symmetric about vertical centerline. Predefined material models based on hyperbolic elasticity can only be used in SPIDA.

### 2.5.2 SOILCON Code

The program SOILCON (SOIL CONduit analysis) models buried conduit installation behavior as well as the behavior under earth load eliminating some extent the uncertainty involved in sub-surface exploration by evaluating known conditions of the site and recommending appropriate methods to continue exploration if required. The system is designed to incorporate subsurface considerations into contract design, thereby reducing contractor contingencies. The output of SOILCON includes a list of recommended investigation procedures ranked by certainty, display of their descriptions and cost estimates for the methods. The system uses backward chaining from knowledge base of the rules encoded in a PROLOG like syntax. It is a developmental ES that does not have the capability to handle quantitative information (Ashley and Wharry, 1985). SOILCON was derived at UMass from NLSSIM which was developed by Duncan and his colleagues at the University of California, Berkeley. Some of the modifications are described by Haggag (1989).

In SOILCON structural stress-strain behavior is assumed to be bilinear. It can calculate stresses, strains and displacements in soil elements, and internal forces, and displacements in structural elements where the structure is modeled with straight beam-column elements. Horizontal and vertical motions, as well as rotation for each of the structural element nodes, are inherent in the model.

SOILCON uses the Young's modulus and Bulk modulus in a hyperbolic formulation as described by Selig (1990). The soil model used is nonlinear and stress state dependent.



Load steps are used in incremental construction modeling that represent placement of a layer of soil, placement of structure, or application of loads after the end of construction. Therefore, each load increment is iterated twice to represent the nonlinear and stress-dependent stress-strain properties of the soil. At the beginning of the load step, the first uses values of Young's modulus and bulk modulus based on the stresses. The second uses Young's modulus and bulk modulus based on the average stresses during the load step. The incremental stresses, strains, and displacements in the soil elements, and the incremental internal forces, moments and displacements in the structural elements during each step are added to the values at the beginning of the step to get the final values for the current load step and the initial values for the next load step.

The program reads initial stresses, strains, and displacements of the preexisting soil elements. Placement of fill on top of the buried pipe is simulated by applying forces to represent the weight of the added layer. Preexisting soil may also be represented by SOILCON. The incremental values at the end of each load step calculated in the program are added to the initial values.

### **2.5.3 CANDE Code**

CANDE (Culvert Analysis and Design) was first introduced in 1976 for the structural analysis and design of buried culverts (Katona et al., 1976). The code was modified twice (Katona et al., 1981; Musser, 1989).

As with SOILCON, CANDE is based on a two-dimensional geometry called plane-strain. Plane-strain implies that there is no deformation in the longitudinal direction, and that every cross section deforms in the same manner.

CANDE has two execution modes; analysis and design. Analysis means that a particular soil-pipe system is completely defined in terms of geometry, material properties, and loading conditions. The problem is then solved and output consists of structural responses (displacements, stresses, strains) and soil responses, as well as an evaluation of culvert performance in terms of safety factors. Design requires the same input definition except that the culvert wall section properties are not specified.

CANDE can design and analyze pipe installations for any one of four pipe types: corrugated aluminum, corrugated steel, reinforced concrete, and plastic pipe. Only analysis can be performed on a fifth type, called BASIC, which allows for the description of non-standard pipe materials or built-up pipe properties.

Three solution levels are available in CANDE. Level 1 uses the exact elasticity solution as described by Burns and Richard (1964). It is restricted to circular pipes deeply buried in a homogeneous soil. Levels 2 and 3 use the finite element methodology. In level 2 the finite element mesh is automatically generated. Level 3 requires data input to define the mesh. This provides the user with a modeling flexibility in case the predefined meshes of level 2 are not applicable.

CANDE can model slippage at the soil-structure interface as well as structural joint slippage. As in SOILCON, incremental construction is modeled using load steps to represent placement of a structure or placement of a soil layer.

The pipe structure is modeled by a sequence of connected straight beam-column elements with nonlinear stress-strain behavior. The soil can be modeled using one of several choices of constitutive models including the hyperbolic model used in SOILCON.

#### **2.5.4 Other Finite Element Models for Buried Pipe Analysis**

Finite element packages are increasing day by day simplifying the procedure for modeling along with solving various limitations update versions are also available. Researchers are using several finite element programs for soil-pipe interaction analysis. Taleb and Moore (1999), Wong et al. (2002) and Dhar and Moor (2004) used a general purpose finite element program AFENA (A Finite Element Numerical Algorithm) for analysis buried pipe structures. Noor and Dhar (2003) used another general purpose finite element program ANSYS for live load analysis of buried pipe. Other FE programs used for analysis of buried pipe-soil interaction include DIANA, ADINA, ABAQUS etc. ABAQUS has been used in this research for analysis of buried pipe under live load.

## CHAPTER 3

### DEVELOPMENT OF FINITE ELEMENT MODEL

#### 3.1 INTRODUCTION

Computer modeling is a powerful technique that can effectively be used soil-structure interaction analysis. Finite element analysis has been used extensively in order to understand the mechanics of complex problems under various loading conditions. Various finite element programs were developed over several decades for these analyses. Some of these finite element packages are general purpose software, which are suitable for analysis of any system, while other programs were developed for specific purpose, suitable for analysis of a specific system. Specific purpose software's, are developed to generate the model addressing the issues specific to the type of problem analyzed easily. The general purpose software, on the other hand, requires special attention so that finite element model can represent the problem in a realistic way. However, there is flexibility for the idealization of the model according to user's need. Use of a general purpose program for an analysis is limited to the availability of material models, facilities to the mesh generations, solution techniques, post-processing features etc. ABAQUS is a versatile general purpose finite element program that has flexibility of using a wide variety of material models. Mesh generation in ABAQUS require special attention since the user require to define node numbers, element numbers and element connectivity. However, a facility to generate the node numbers, element numbers and the element connectivity according to user's requirement is available. The "Frontal Technique" used in ABAQUS in the solution has provided the freedom to choose any number for the nodes and the elements, without any consideration to "band width". A consideration of the "band width" is required in some-other finite element programs to minimize the computational time.

Many specific finite element packages like CANDE (Culvert Analysis and Design), SPIDA (Soil-pipe Interaction Design and Analysis), and PIPE etc were developed for

soil-pipe interaction analysis of buried pipe. Many research works on buried pipe-soil system are performed using general purpose and specific purpose finite element packages. Arockiasamy et al. (2006) showed that general purpose software yields very good results if simulation can be performed effectively. ABAQUS has been proven to be relatively easy to use due to detailed documentations and vastness of its capabilities. Therefore, ABAQUS is used in this research for analysis of buried flexible pipe under live load. The version of ABAQUS that has been used for this research is ABAQUS 6.4.

### 3.2 PROBLEM STATEMENT AND IDEALIZATION

Significant research concerning the soil-structure interaction phenomena has been performed in recent years to develop a better understanding of the performance of the complex soil-pipe system. A large portion of the analytical works focused on the soil-pipe interaction under earth load. The soil stiffness of the backfill and native soil and the pipe stiffness were used as the analysis parameters. Two-dimensional plain-strain analysis was generally sufficient to analyze the pipe behavior under the earth load. However, the surface live loads from vehicle traffic (wheel load) over the pipe make the problem as three dimensional. The wheel loads are idealized as a concentrated load in various design code (i.e. AASHTO 1996), while idealization as a distributed load over the area of tire foot-print is also used (AASHTO, 1998). Analysis is also conducted considering the wheel load as a patch load (Fernando and Carter, 1998). However, because of the finite dimension of the patch load or concentrated load, the wheel loads induce a three-dimensional stress pattern around the pipe. Boussinesq's (1885) developed solution for three-dimensional ground stress in a homogeneous, isotropic and elastic ground under concentrated load and distributed loads. However, the presence of pipe with different stiffness limits the applicability of the Boussinesq's solution for calculation of the soil-stresses around the pipe. The stiffness of pipe material cause redistribution the soil-stresses which may also be affected by soil cover. As a general understanding, a stiffer pipe will be attract load from the surrounding soil, resulting in a greater stress on top of the pipe than those expected from Boussinesq's solution. The phenomenon is called "Negative arching". Positive arching, on the other hand, may develop if a flexible pipe is present, which may result

in less stress over the pipe than those expected from Boussinesq's solution. Differences in stiffness of the backfill and native soil make the problem more complex, where stress shearing also occurs between the backfill and native soil. Dimension of the problems such as pipe size, soil cover, backfill width and native soil may influence the load shearing between different components.

A three-dimensional finite element analysis could be used to analyze the problem of pipe-soil interaction under surface vehicular load. However, a three-dimensional finite element analysis is extremely time consuming and requires a lot of computer memory, particularly when a large soil mass with non-linear stress field is discretized. Besides, visualization of three-dimensional analysis and error detections are not straightforward. Two-dimensional analyses of the problems are generally preferred in finite element analysis. Researchers have analyzed the problems with buried pipes and culverts using two-dimensional idealization of three dimensional loads (Moore and Brachman, 1994; Fernando and Carter, 1998; Moore and Taleb, 1999; Jayawickrama et al., 2002). In some of the analyses, a Fourier integral transform technique was used to represent the three dimensional load while the analysis is performed over a longitudinal section. In other analyses, the Boussinesq solution for a vertical load at the surface of an elastic half-space were used to convert the three-dimensional loading to an equivalent two-dimensional load, which can then be examined using conventional two-dimensional finite element analysis (Moore and Taleb, 1999; Jayawickrama et al., 2002).

The technique with conversion of the three-dimensional load into equivalent two-dimensional load has been used in this research for investigation of the pipe-soil system under surface concentrated load, Figure 3.1 shows a buried pipe-soil system under the concentrated load, which was idealized by an equivalent line load as shown in Figure 3.2.

Concentrated load can be converted to equivalent line load using the formula (Jayawickrama et al., 2002)

$$\left(\frac{P}{b}\right) = r \left(\frac{P}{BL}\right)_{\text{wheelload}} \quad (3.1)$$

Where:

$(P/b)$  = Load per unit length,

$(P/BL)$  = Load per contact area used in the full-scale testing,

$r$  = Reduction factor.

Jayawickrama et al. (2002) used the reduction factor as 0.5335 for wheel load based on Boussinesq's solution. Dhar et al. (2004) also used the same reduction factor successfully for analysis for flexible pipe under surface load. A similar factor was used for idealization of concentrated load as the line load in this study. The problem was thus reduced to a two-dimensional plane-strain problem. Analysis of a cross-section as shown in Figure 3.3 would thus provide information of buried pipe under the surface load. A parametric study was carried out to assess the effects of the various geometric and material parameters on the behavior of pipes under surface load.

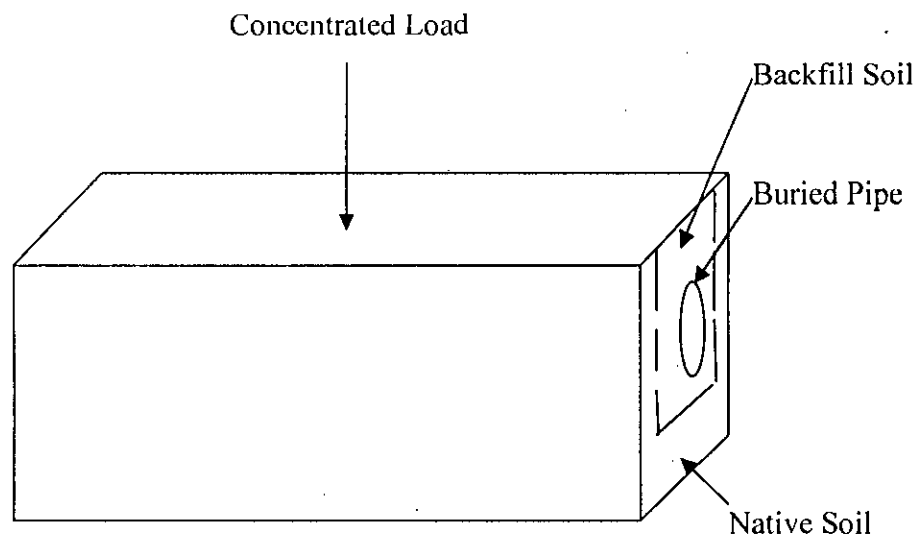


**Figure 3.1 Buried Pipe-Soil System under Surface Concentrated Load**

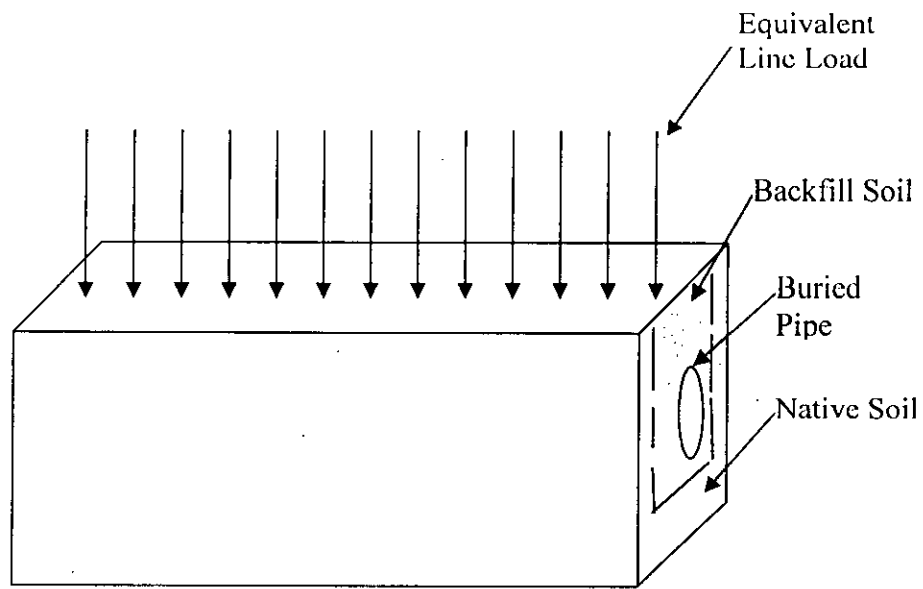


**Figure 3.2 Plain Strain Idealization of Surface load**

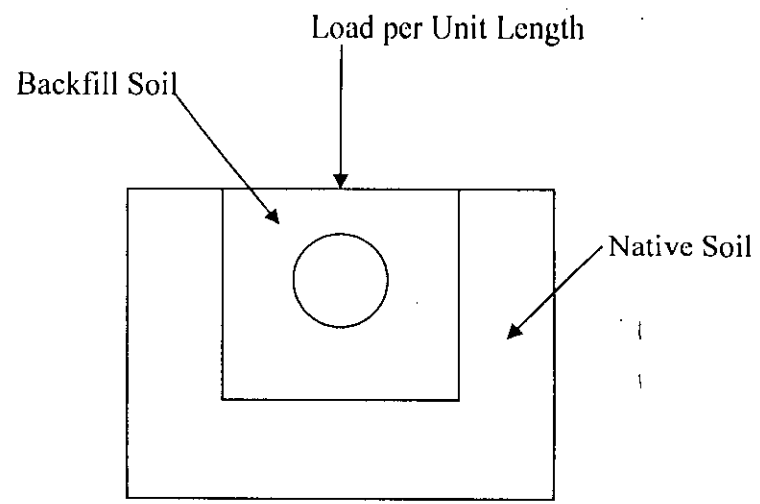


**Figure 3.3 Two Dimensional Idealizations**

For flexible pipes, stress distribution under live load depends on the type of pipe material, diameter of pipe and pipe wall geometry. As discussed earlier, positive arching develop, for flexible pipe, redistributing the stress toward the soils, while the stresses are attracted toward the pipe for stiffer pipe. Analysis with variation of the pipe material properties wall cross-section would be required to capture the arching mechanism for the pipes.

Native soil and backfill soil, on the other hand, have different property. Backfill soil modulus can vary depending upon the degree of compaction during placement. Native soil represents field condition which may be simulated by unique values of soil parameters for a particular case. A study with variation of backfill and native soil properties would be used to understand the effect of the differences in the soil conditions.

Flexible buried pipe have been developed with various wall geometries to obtain higher sectional modulus with minimum utilization of pipe material (Dhar, 2002). Modeling of these non-uniform walls poses another challenge in the finite element analysis. Dhar and Moore (2006) used explicit modeling of the profile to perform axisymmetric analysis. Three-dimensional explicit modeling of the pipe wall was also performed by McGrath et al. (2002). However, Dhar et al. (2004) revealed that idealization of the wall of the profile pipe as beam element with the sectional area and the moment of inertia expressed per length of the pipe can successfully be used to model the global pipe response. Pipe was idealized as a beam element in the present research.

Soil plasticity is also an important parameter that may govern the pipe-soil interaction. However, Dhar et al. (2004) revealed that the effect of soil plasticity on the pipe response is sometime insignificant depending upon the type of loading. A concentrated surface load is expected to cause soil plasticity in the vicinity of the load only, which may diminish at a distances away from the load. Besides the two-dimensional idealization of the three-dimension load required applicability of Boussinesq's Solution which is valid under linear elastic condition. The analysis in the present study was therefore limited to linear elastic analysis.



### 3.3 ASPECTS OF ABAQUS

ABAQUS is a highly sophisticated, general purpose finite element program, designed primarily to model the behavior of solids and structures under externally applied loading. ABAQUS includes the following features:

- Capabilities for both static and dynamic problems
- The ability to model very large shape changes in solids, in both two and three dimensions
- A very extensive element library, including a full set of continuum elements, beam elements, shell and plate elements, among others.
- A sophisticated capability to model contact between solids
- An advanced material library, including the usual elastic and elastic-plastic solids; models for foams, concrete, soils, piezoelectric materials, and many others.
- Capabilities to model a number of phenomena of interest, including vibrations, coupled fluid/structure interactions, acoustics, buckling problems, and so on.

The main strength of ABAQUS, however, is that it is based on a very sound theoretical framework. While no computer program can ever be guaranteed free of bugs, ABAQUS is among the more trustworthy codes. For this reason, ABAQUS is used by a wide range of industries, including aircraft manufacturers, automobile companies, oil companies and microelectronics industries, as well as national laboratories and research universities.

The ABAQUS finite element system mainly includes:

- ABAQUS/Standard, a general-purpose finite element program;
- ABAQUS/Explicit, an explicit dynamics finite element program;
- ABAQUS/CAE, an interactive environment used to create finite element models, submit ABAQUS analyses, monitor and diagnose jobs, and evaluate results; and
- ABAQUS/Viewer, a subset of ABAQUS/CAE that contains only the post processing capabilities of the Visualization module.

ABAQUS/Standard has been used here for analysis of the problem, while ABAQUS/CAE has been used for visualizations of results. ABAQUS FEA takes advantage of the latest high performance parallel computing environments, allowing including details in models previously excluded due to computing limitations. This allows minimizing assumptions while reducing turn around time for high-fidelity results.

### 3.4 FINITE ELEMENT MODEL FORMULATION

Finite element model has proven its superiority by analyzing the complex structures, particularly when analysis of the structure by classical theory is difficult. In finite element analysis, the whole body is divided into a number of elements. Number of element to be used in discretization depends on the type of problem investigated. More element with finer mesh would be required if the non-linear stress field is expected. Special attention is thus required in analyzing the complex zones of a problem. Finite element method works in three steps. First is known as preprocess or modeling of structure, then analysis is performed and finally results are post processed. The structure of interest is subdivided into discrete shapes called elements. Most common element types are one dimensional beams, two dimensional plain stress or plain strain elements and three-dimensional bricks or tetrahedrons. The elements are connected at node points where continuity of displacements fields is enforced.

Finite element analysis was performed in this research in order to investigate the behavior of flexible buried pipes based on two-dimensional idealization. Generation of finite element mesh for buried pipe with backfill and native soil was the first challenge of the modeling. At first, Co-ordinate of center of the buried circle was chosen as a (0, 0). For the research convenience, node number for center of the circle was selected as 110. Then, the first node on the pipe along the positive x-axis on the horizontal line was chosen as 119 with co-ordinate (750, 0), for a pipe with radius of 750 mm. An increment of 100 in node number was provided along the perimeter of the pipe for automatic generation of nodes. As discussed earlier, the use of gap in node number will not affect the computational speed since a frontal technique is used in ABAQUS solution algorithm. But problem was arisen when circle ends since one

node can not possess 2-node number for the case of last node for a circular pipe. Therefore, the increment of node number along the pipe perimeter was stopped before reaching the first node to the node number 7219 (as shown in Figure 3.4). Table 3.1 shows the control nodes and their co-ordinates. Node number increment along radial distance from pipe perimeter was taken 1(one) for the automatic node generation within the soil zone around the pipe. Commands \*NGEN and \*NFILL were used in ABAQUS in automatic node generation. After the node generation, finite elements were generated that define element numbers, connectivity and element types. For the modeling of soil, element numbers were chosen to be 100 less than the number for first node for this element for automatic generation of elements. Thus, element numbers were increased by 100 along the pipe perimeters and by 1(one) toward a radial line from the pipe. Command \*ELEMENT and \*ELGEN were used in ABAQUS for automatic element generation. Appendix A shows the sample data file used for the analysis. However, a problem was arisen in automatic element generation between last node and first node on pipe perimeter. Element is generated in that region manually. Total model was separated in different region. First zone was backfill soil and last one was native soil. Figure 3.4 shows the finite element mesh developed for finite element analysis of the pipe-soil system. Two-dimensional 4-noded plane strain element (CPE4 in ABAQUS) was used to represent the surrounding soil and beam-column element (B21 in ABAQUS) was used to represent the buried pipe wall. It was to be noted that element B21 is a plane stress element. However, modulus of elasticity and Poisson's ratio was adjusted for plain strain representation of the plane stress element (Dhar and Moor, 2007). Cross sectional area (A) and moment of inertia (I) of pipe wall expressed per unit length of the pipe was used for the beam-column element for representation of profile wall pipes. Element number for beam-column element was started from 10001. A total of 72 elements were used to cover the pipe circumference.

A non-linear stress field was expected around a region closer to the pipe under both geostatic and surface loading. A finer mesh was therefore used in the pipe vicinity to provide more accurate results. The mesh was less dense away from the pipe. Boundary of the mesh was placed far enough to avoid the influence of the surface live load. A concentrated surface live load is not expected to affect a large area. However, the boundary was placed approximately at distance of more than 2-times the diameter.

Smooth rigid boundary was chosen along the vertical line on the left and right of the mesh while hinge was used at the bottom of the mesh. Interface between the pipe and the soil assumed to be bonded.

A study was conducted to investigate effect of boundary on the pipe response to identify the distance of boundary from the pipe, required to minimize the boundary effect. Figure 3.5 shows the crown moment with the distance of boundaries from the pipe. Distances on the sides and below the pipe were varied. It is revealed that pipe crown moment reduces as the distance of boundary from pipe increases. However, the moment stabilized beyond a distance of 4200 mm from the center of the pipe. Thus, the boundary effects can be assumed as negligible if placed beyond this distance. Boundaries were therefore placed at a distance of 4200 mm from the center of the pipe for the finite element analysis of the buried pipes under live load.

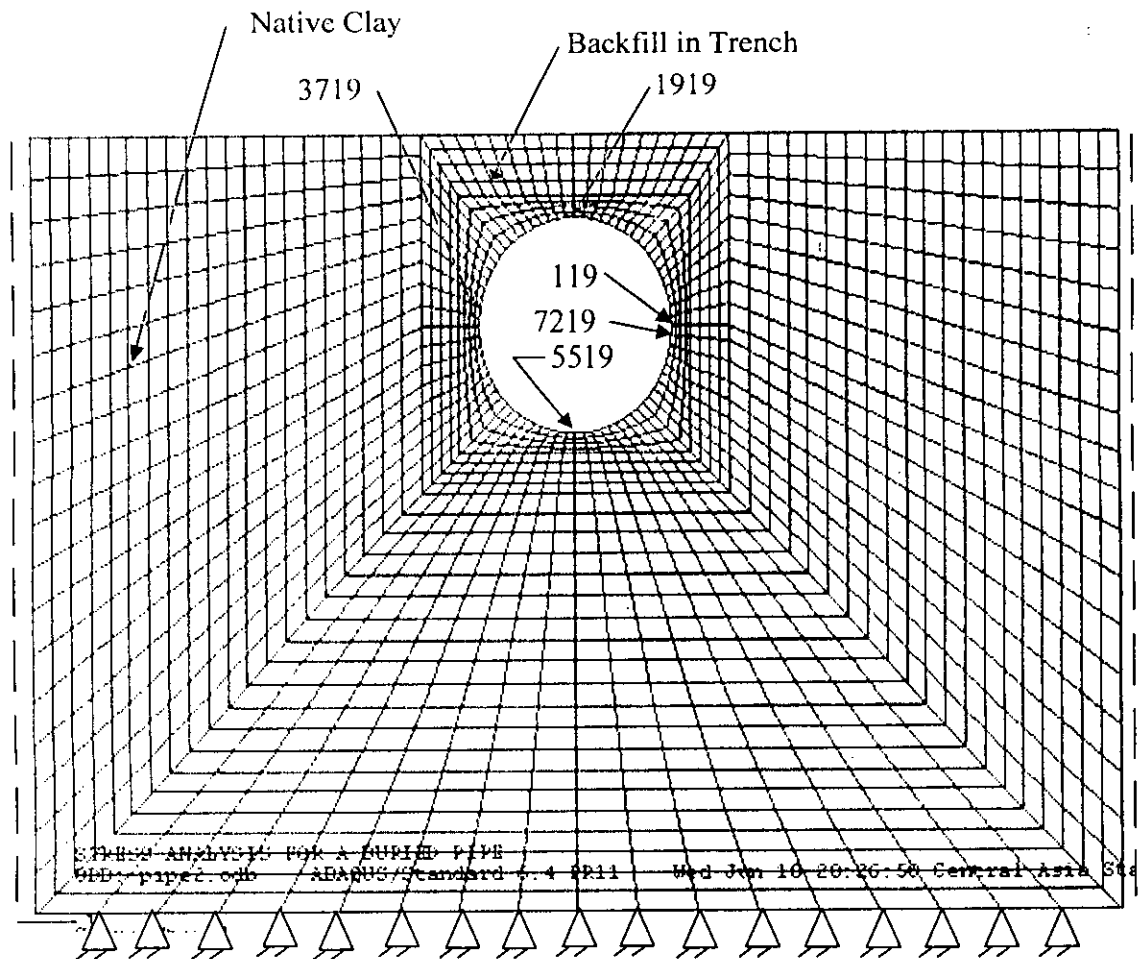


**Figure 3.4 Different Soil Zones in Finite Element Mesh**

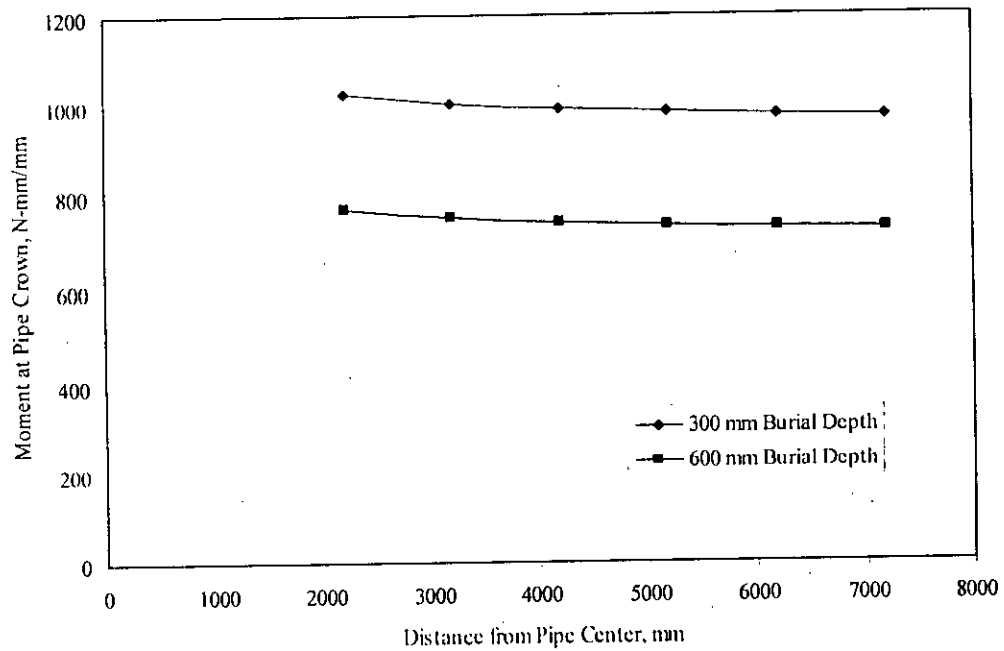


**Figure 3.5 Effects of Boundary Position on Crown Moment**

**Table 3.1 Co-ordinates of Control Nodes**

Node No.	X	Y
119	750	0
1019	530.33	530.33
1919	0	750
2819	-530.33	-530.33
3719	-750	0
4619	-530.33	-530.33
5519	0	-750
6419	530.33	-530.33
7219	747.17	-65.37

### 3.5 MATERIALS USED IN FE ANALYSIS

Plain strain idealization of the three-dimensional problem using Boussinesq's theory requires linear elastic analysis. Thus, linear elastic material parameters were used for modeling of the pipe and surrounding soil. Soil parameters (Modulus of elasticity, Poisson's ratio) depend on the type of soil and the degree of compaction. Granular material (sand or gravel) is generally recommended as the backfill material for pipe. Assuming well-graded or poorly graded sand as the backfill material modulus of elasticity may vary from 5 MPa at the loosest condition to 20 MPa at the densest condition for typical installation according to McGrath (1998). The range of soil modulus (10 Mpa ~ 15 Mpa) was used in this investigation. Poisson's ratio of the soil was used to be 0.2-0.3. Modulus of elasticity of the pipe material was varied from 200 MPa (long term modulus of High Density Polyethylene Pipe) to 210000 MPa (modulus for steel) for investigation of the pipe stiffness on the live load distribution. Unit weight of the soil and pipe material was assumed as zero to demonstrate the effects of surface load only.

### 3.6 VERIFICATION OF FINITE ELEMENT MODEL

Evaluation of the finite element model is required in order to verify if the idealization has reasonably represented the real problem. Evaluation can be performed using available close-form solution or full-scale test measurements. Test result from available literature was used for evaluation of finite element model in this study. McGrath et al. (2001) conducted full-scale pipe tests to improve understanding of the behaviour of large diameter flexible pipe under low fill heights. Field test was conducted maintaining a two lane test road transversely done by test vehicles, a truck with a maximum axle load of 107 kN (24,000 lb) traveling in one lane and a truck with 80 kN (18,000 lb) maximum axle load traveling in the other. Test results of McGrath et al. (2001) were used for evaluation of the finite element mesh developed in this research. This finite element analysis was then extended to investigate the live load affect on the pipe.

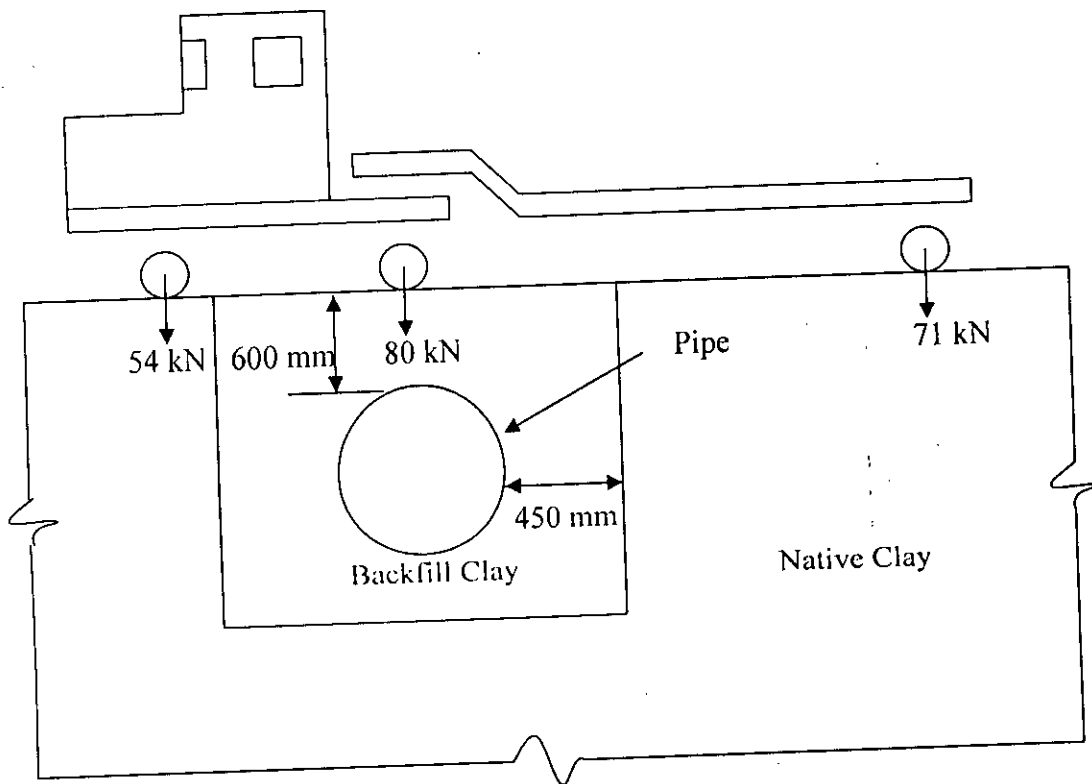


Figure 3.6 Axle Load from 80 kN Axle Truck

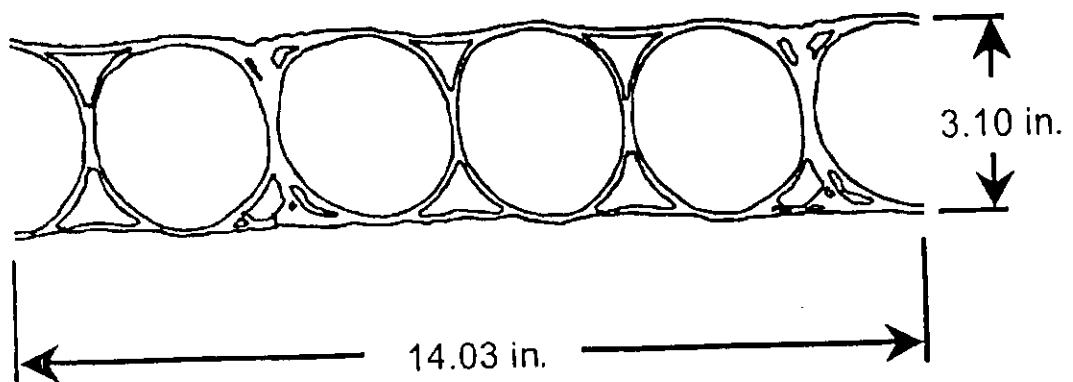
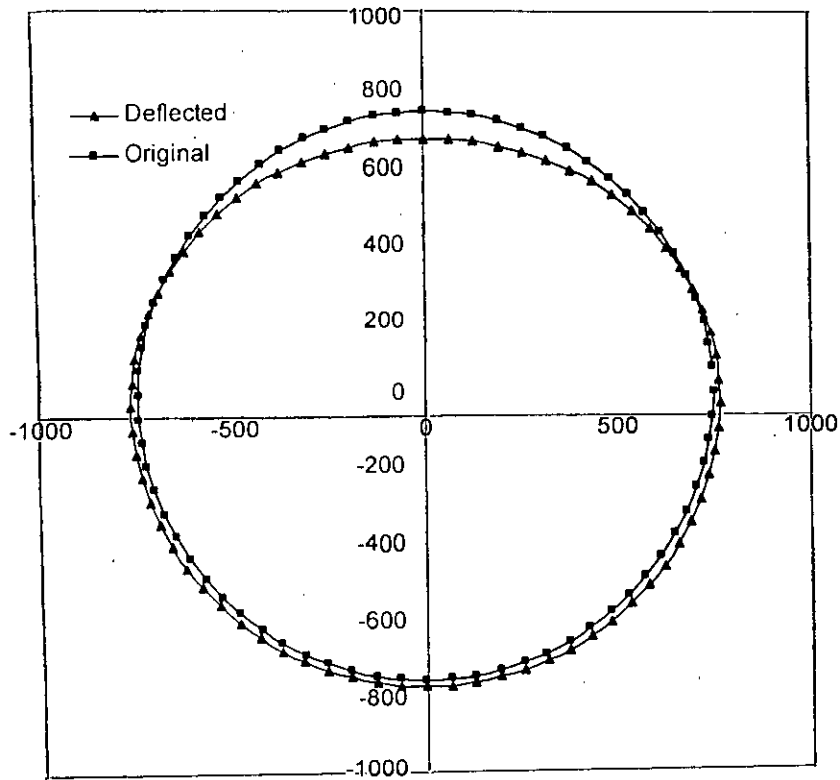


Figure 3.7 One of the Profile of Pipe Wall Used by McGrath et al., (2002)

Figure 3.5 shows on of the test setup used by McGrath et al. (2001). Pipe profile of the pipe wall used in thus test is shown in Figure 3.6. Sectional parameters such as area (A) and moment of inertia (I) of similar profile expressed per unit length of the pipe is available in Dhar (2002). This pipe was 1500 mm diameter high density polyethylene pipe buried at a depth of 600 mm (2 ft). The pipe was installed in a trench of 2400 mm width. This allowed a 450 mm clear space between the pipe spring-line and trench wall. The trench was backfilled using AASHTO type A2 soil compacted to a density of 85-95% of standard proctor density. The surrounding soil was the native soil, which was very stiff clay. Figure 3.5 shows concentrated axle load of 80 kN directly above the crown of the pipe. Vertical deflection of the pipe under this loading condition was measured to be 0.02%. Pipe deflection was measured using deflectometer under the vehicle axle loads. For modeling of the three-dimensional field test, two-dimensional plain strain idealization was used as discussed in section 3.2. The test load was multiplied by a reduction factor to obtain the equivalent plain strain load. An 80 kN axle load was thus corresponding to a line load of 8.3 kN/m. Load was applied in one step only. However, ABAQUS will generate automatically it as thirty increments.

Material parameters for the surrounding soil were chosen based on the typical values for the type of soil used in the test. The native soil was stiff clay, for which the modulus of elasticity was used as 10 MPa and Poison's ratio was used as 0.25. For the backfill soil, which was a granular soil (AASHTO Type A2), elastic modulus was estimated from Selig (1990) for the level of compaction and the initial stress condition. Elastic modulus for HDPE pipes material was chosen as the short time modulus i.e.760 MPa (Arockiasamy et al., 2006).





**Figure 3.8 Pipe Deflections under Concentrated Load**

Figure 3.7 shows the deflected shape of the pipe under the concentrated load at the ground surface above the pipe crown as obtained from the analysis. Unit weight of the soil and the pipe material was neglected during the analysis to obtain the effect of the surface live load only. Figure 3.7 shows the pipe deflection is highest at crown, as expected under concentrated load. Pipe vertical deflection from the analysis was obtained to be 0.018% which was almost same as that measured during the test (i.e.0.02%). Table 3.2 compares the field quantities with finite element model. The finite element model reasonably simulating the field tests conditions. To evaluate the calculation of the finite element analysis further, vertical stress on a horizontal line at a level of 75 mm above the crown was investigated. The investigation was performed using a variation of the pipe modulus. Analysis was performed with the pipe modulus of  $E=210000$  MPa (a modulus of elasticity for steel) and  $E=760$  MPa. Vertical stress at the same level was also calculated using the Boussineq solution that neglects the presence of the pipe.

**Table 3.2 Comparison of Field Quantities with FE Model**

Parameter	Field	FE Model
Pipe	Corrugated HDPE	$A_p = 20 \text{ mm}^2$ $I_p = 15700 \text{ mm}^4$
Backfill Soil	AASHTO Type A2	$E_s = 10 \text{ MPa}$ $\nu_s = 0.25$
Native Soil	Very Stiff Clay	$E_s = 10 \text{ MPa}$ $\nu_s = 0.25$
Deflection	0.02 %	0.018 %

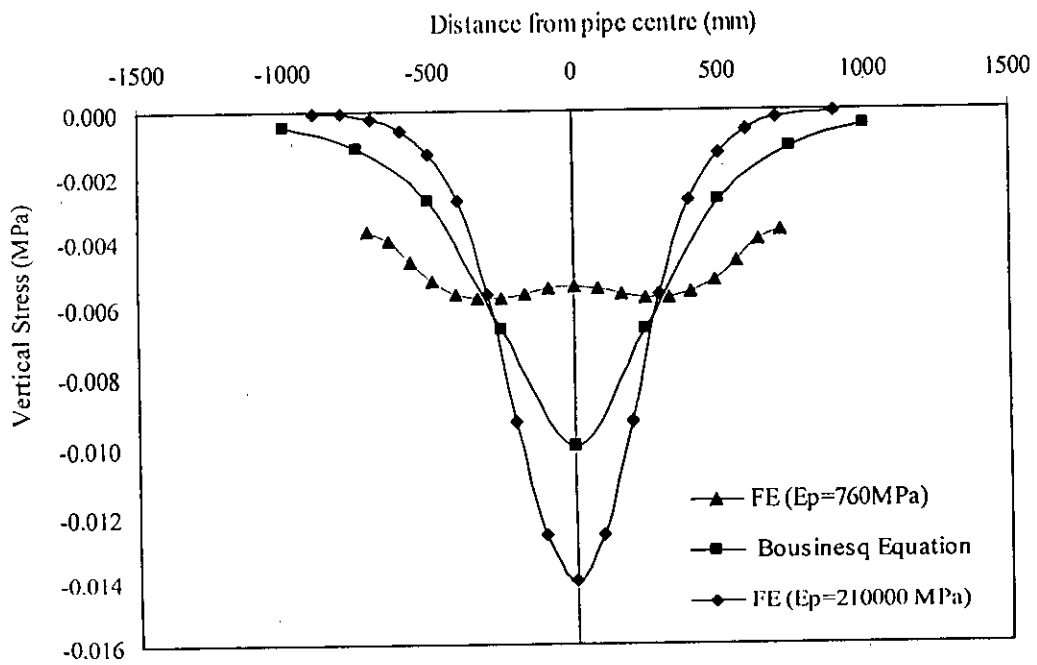


**Figure 3.9 Comparison of Vertical Stress**

Figure 3.8 shows the comparison of vertical stresses calculated. The comparison shows that finite element calculate a greater stress over pipe crown then the Boussinesq's solution for  $E_p=210000$  MPa as expected. Steel pipe with greater stiffness may attract load from the soil toward the pipe due to negative arching. On the other hand, finite element analysis, with HDPE pipe modulus shows less stress over the pipe crown and greater stress to the surrounding soil. For the HDPE pipe with low pipe modulus, positive arching has redistributed the soil stress away to the pipe. Thus, the calculated stresses were found to be less than those obtained from Boussinesq's solution, which neglect the presence of the pipe. The result obtained from finite element was therefore consistent with expected pipe-soil interaction behavior. The model was used for further study of pipe-soil interaction under live load.

## CHAPTER 4

### INVESTIGATION OF PIPES UNDER LIVE LOAD

#### 4.1 INTRODUCTION

Development of finite element model using ABAQUS, for analysis of buried flexible pipe was discussed in Chapter 3. The model has been evaluated using full-scale test results and the known behavior of soil-pipe interaction. The evaluation revealed that stiffness of the pipe material significantly governs the stress field around the pipe under surface load. Other parameters such as pipe wall geometry, depth of soil cover, stiffness of the backfill and in-situ soil may also effect the stress development around the pipe. Understanding the effects of these parameters on the stress development would be required in order to incorporate the effects of live load in the design of the pipes. For pipes with uniform wall, thickness of the pipe could be used as the parameter to define wall geometry. However, flexible pipes with different wall geometries were developed over the last several decades to obtain higher moment of inertia of pipe wall section with minimum utilization of material. Non-uniform walls are modeled through expressing the area and moment of inertia of wall section as per unit length of the pipe. Pipe materials also appeared to vary from different thermoplastic pipes (High-Density Polyethylene, Poly-venylchloride) to steel pipes. Properties of thermoplastic pipes on the other hand vary from its short term modulus to long term modulus. However, considering the surface live load of short duration, the short term modulus may govern the behavior of the pipe under live load.

In this chapter, a parametric study is undertaken so that the behavior of the buried flexible pipe can be understood under different pipe and soil conditions. Different parameters (moment of inertia, sectional area of pipe wall, modulus of pipe material etc.) affect the pipe behavior in different ways. Analyses with variations of different parameters are used to investigate the pipe deformation, internal forces (axial force and bending moment) and soil stresses under those conditions.

Taking the model discussed in Chapter 3, as the reference model, which was compared with test data, parametric study was performed so that the variation can be better understood. Thus, first parametric study was performed with variations of pipe's sectional parameters and modulus of elasticity of pipe material to investigate the effect of pipe parameters. Another parametric study was carried out with change of burial depth of the pipes. Four different burial depths i.e. 300 mm, 600 mm, 1500 mm and 3000 mm were considered to explore the effect. A finite element mesh shown earlier in Figure 3.4 in Chapter 3 has been used in the parametric study for a line load of 8.3 kN/mm.

#### 4.2 EFFECT OF SECTIONAL AREA OF PIPE WALL

Pipe was modeled using the command \*BEAM GENERAL SECTION in ABAQUS which indicates a linear or non linear beam section with no requirement of numerical integration over the section. All sectional properties must be user defined as per this command. At first, pipe sectional area was varied in the analysis keeping other parameters constant. As discussed earlier, sectional properties, expressed per unit length were used in lieu of thickness of pipe to bring the affect of non uniform wall section. Since high density polyethylene (HDPE) pipe was used initially to compare with the field data, its parameters were used at first in the model. A modulus of elasticity of pipe was used as 760MPa (Arockiasamy et al., 2006) for the pipe material and the moment of inertia of pipe wall was  $15700 \text{ mm}^4/\text{mm}$ . Since moment of inertia is directly related to the area of pipe, area of pipe may not be varied independently in reality. However, the area was varied independently i.e.  $A_p = 20 \text{ mm}^2/\text{mm}$ ,  $30 \text{ mm}^2/\text{mm}$  and  $60 \text{ mm}^2/\text{mm}$  for parametric study keeping other parameters as constant.

Table 4.1 summarizes the parameters considered for this study. Two burial depths to correspond the behavior of shallow and deep burial condition were considered. Section 4.6 discusses further about the effects of depths. To reveal the parametric effects vertical stress above the pipe crown, vertical stress distribution along a horizontal line 75mm above the pipe crown was considered. Figure 4.1 depicts the vertical stress distribution along the line above the crown starting from crown to the

**Table 4.1 Parameter Considered for the Effects of Section Area**

Parameter	Value
Pipe Diameter	1500 mm
Burial Depth	300mm, 600mm
Pipe Material Modulus	$E_p = 200 \text{ MPa}, 1000 \text{ MPa}, 10000 \text{ MPa}, 210000 \text{ MPa}$
Soil Parameters	$E_s = 10 \text{ MPa}, \nu_s = 0.25$
Moment of Inertia of Wall	$I_p = 300 \text{ mm}^4/\text{mm}, 7000 \text{ mm}^4/\text{mm}, 15700 \text{ mm}^4/\text{mm}$
Area of Wall	$A_p = 20 \text{ mm}^2/\text{mm}, 30 \text{ mm}^2/\text{mm}, 60 \text{ mm}^2/\text{mm}$

top point of backfill soil for 300 mm of buried depth of the pipe. From graph, it is clear that as the vertical distance increase from crown, vertical stress is also increases and is consistent with classical theory. However, the variation of vertical stress with cross-sectional area is not significant. For all three areas (i.e.  $A_p = 20 \text{ mm}^2/\text{mm}$ ,  $30 \text{ mm}^2/\text{mm}$  and  $60 \text{ mm}^2/\text{mm}$ ) vertical stress is almost same for all points. Figure 4.2 represents the vertical stress distribution for the 600mm buried depth of pipe. It is noticeable that for various cross-sectional area of pipe wall, variation in vertical stress distribution is again insignificant. Almost all curves overlap with one another. Variations in vertical stress distribution do not occur even with the variation of buried depth. According to the classical theory, if the buried depth increases, soil stress will be decreased at crown level. Figure 4.1 and Figure 4.2 also represents this. However, Figure 4.1 and Figure 4.2 do not give a clear picture about the increase in soil vertical stress above pipe crown for two different burial depths. This variation of vertical stress can be better understood if the vertical stresses can be plot on the same diagram. Figure 4.3 plots variation of the vertical stress at crown with the cross sectional area of the pipe for two different burial depths. Vertical stresses were taken for a particular point which was 75 mm above crown. In this diagram, percentage of vertical stress is plotted against the sectional area of pipe. The percentage was expressed with reference to the highest calculated vertical stress for the cases considered. The highest vertical stress occurs for lower buried depth of pipe with the higher cross-sectional area of pipe wall. This graph clearly depicts how the variations in vertical stress occur with the variation of buried depth. It reveals that vertical stress is greater for the pipe at 300 mm buried depth compared to the pipe at 600 mm depth, as expected. The

stresses for 600 mm deep pipe are about one fourth of those for 300 mm deep pipe. The figure also reveals that cross-sectional area of the pipe wall does not influence significantly the stress above pipe crown.

As the vertical stress reaching to the pipe is greater for shallow buried pipe, deflections of the pipes are also expected to be greater. However, this increment may not occur proportionately with vertical stress. A higher sectional area of pipe wall, on the other hand, will cause less deflection under the same stress. Graphs for maximum pipe deformation with sectional area of pipe wall are plotted for different buried depth in Figure 4.4. Figure 4.4 shows similarity with the previous one as plotted for vertical stress analysis. A close look at the graph indicates that for less burial depth deflection is almost twice. Pipe deflection in Figure 4.4 was expressed as percentage of the original pipe diameter. Vertical deflection of the pipe is the maximum under the vertical surface load. Figure 4.4 shows deflection of the pipe decreases with the increase of cross sectional area of pipe wall, as expected.

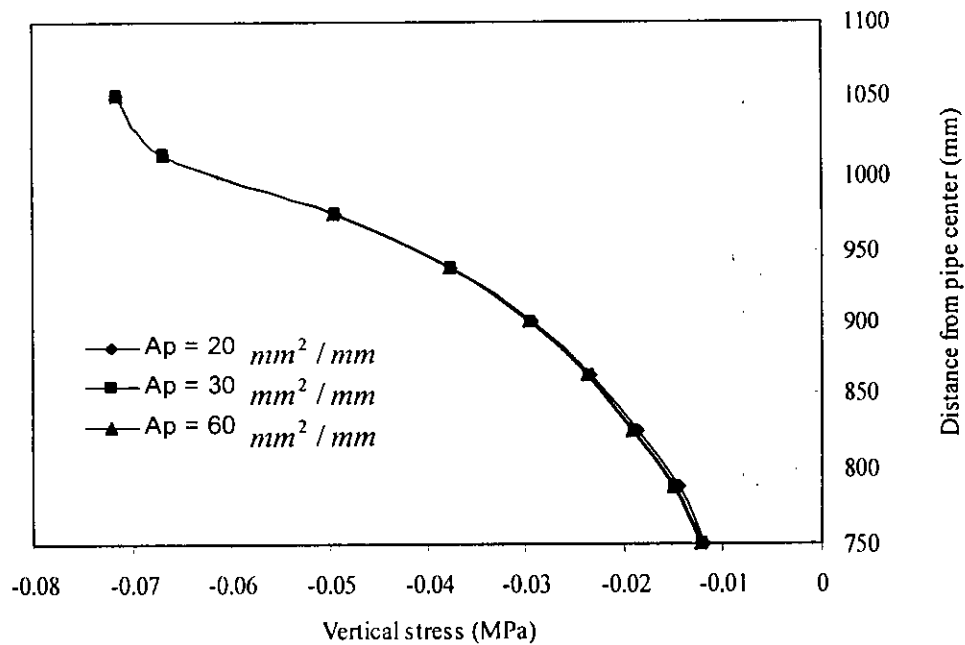


**Figure 4.1 Vertical Stress along Vertical Line above Crown for 300 mm Pipe Burial Depth with Various Areas of Cross-Section**

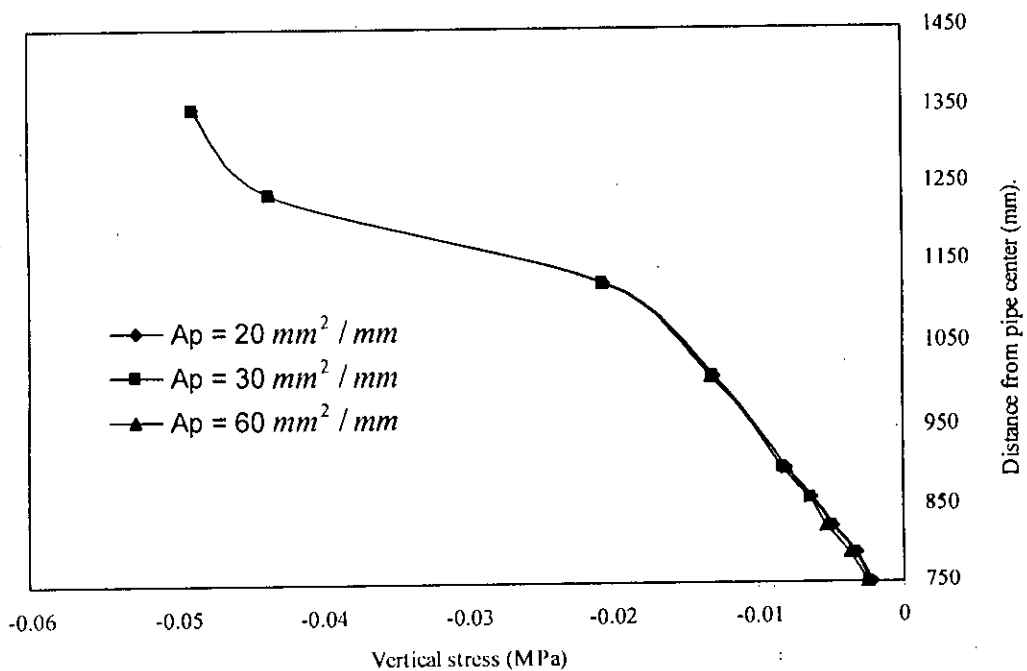


**Figure 4.2 Vertical Stress along Vertical Line above Crown for 600 mm Pipe Burial Depth with Various Areas of Cross Section**

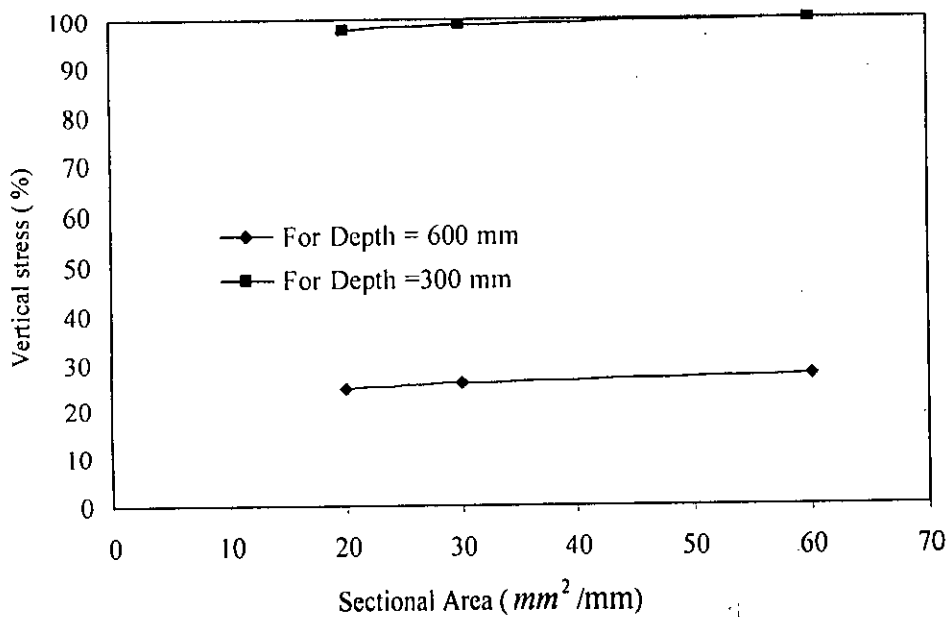


**Figure 4.3 Variation of Vertical Stress at 75mm Above the Pipe Crown for Different Sectional Areas of Pipe Wall**



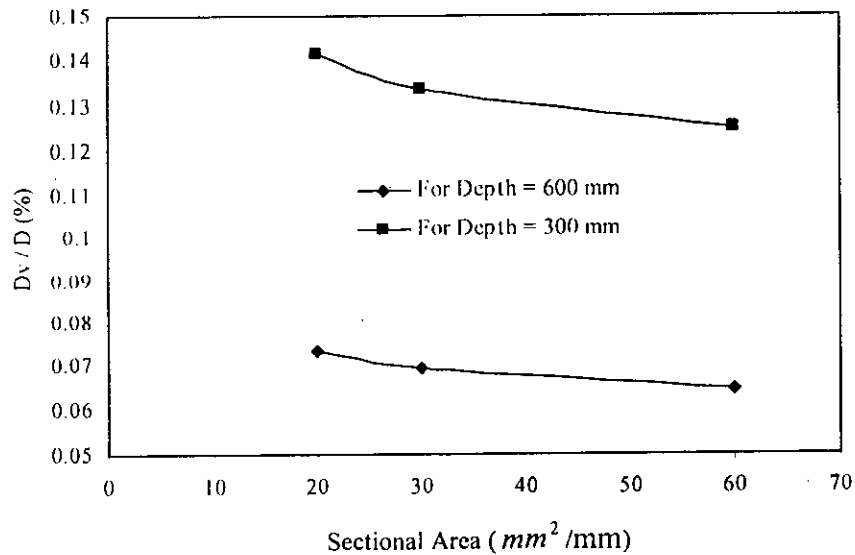


**Figure 4.4 Maximum Pipe Deflection with Cross Sectional Area for Different Depths**

Effects of the surface load on the internal forces of the pipe walls (i.e. axial force and bending moment) under various pipe sectional areas are shown in Figure 4.5 through Figure 4.8. To see the variation of axial force and moment around the pipe was quite difficult in Cartesian co-ordinate system. Thus, polar co-ordinate system was used here to see such variations. Figure 4.5 is a polar diagram representing the variation of thrust (axial force) around the pipe. This graph is plotted for buried depth of 300 mm with a variation in sectional area of pipe. The figure shows that variation of thrust for different sectional area of pipe is not significant. Almost all points indicate the same value for thrust with the variation of sectional area of pipe. It is also clear from the graph that maximum thrust occurs at around 30-degree to 50-degree from the springline for the concentrated surface load. Negative value indicates compressive force of the thrust.

Bending moments on the pipe wall are also not affected by the area of pipe wall section for the thermoplastic pipe with  $E_p = 760$  MPa. Figure 4.6 is a polar diagram which indicates the variation of bending moment around the pipe buried at a depth of 300 mm. The maximum positive moment occurs at the crown of the pipe where maximum negative moment occurs at around 50-degree from the pipe springline. Positive bending moment indicates outward concave deflection and negative moment indicate outward convex deflection of the pipe wall as shown in Figure 4.7. Figure 4.7

shows that outward concave deflection at the crown and outward convex deflection at the shoulder.

Figure 4.8 and Figure 4.9 depicts the wall thrust and bending moment for the pipe at a buried depth of 600 mm, which also demonstrate no effect of cross sectional area. However, the maximum thrust and the maximum bending moment is greater for shallow buried pipe (300 mm). The maximum thrust for the pipe with 300 mm and 600 mm buried depths are 5.29 N/mm and 3.79 N/mm, respectively. The moments for the corresponding pipes are 226.1 N-mm/mm and 76.31 N-mm/mm, respectively. With the increment of buried depth, moment is reduced significantly while the decrease of the thrust is less significant. For a particular point like crown, moment is reduced by about seventy percent when buried depth is doubled.

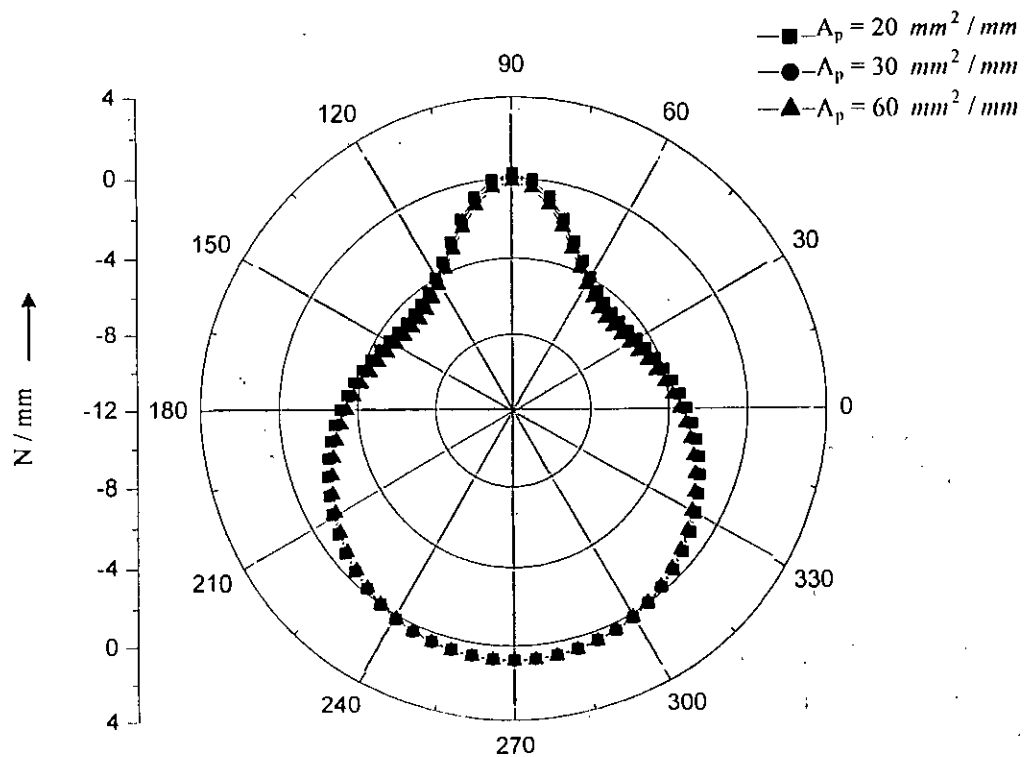


Figure 4.5 Variation of Thrust around the Pipe with Sectional Area for 300 mm Buried Depth of Pipe

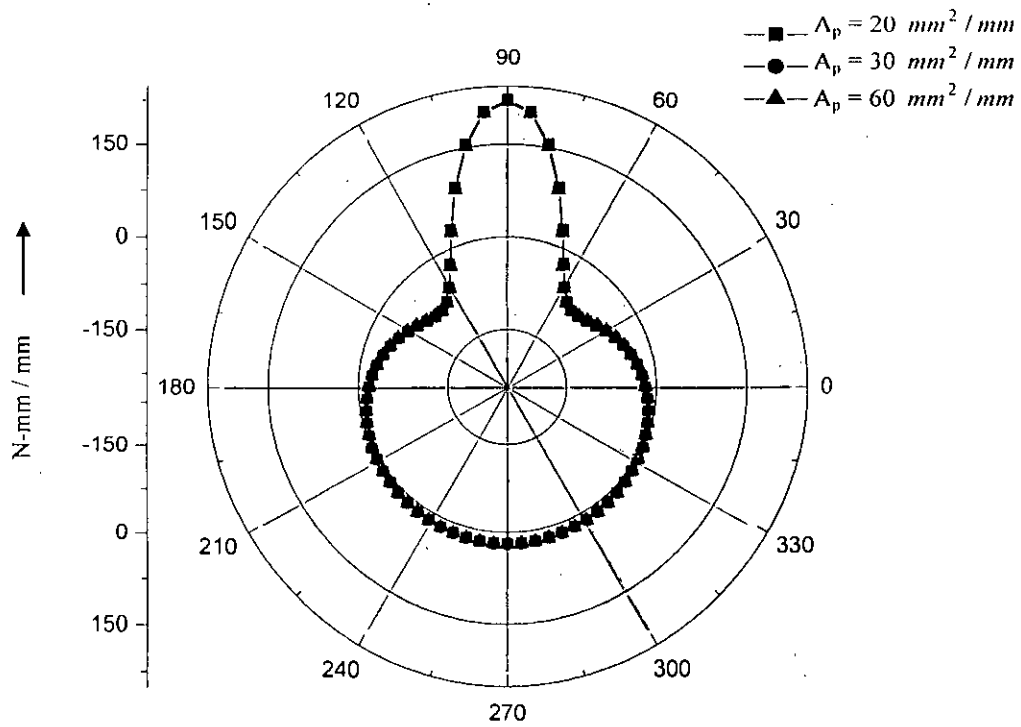


Figure 4.6 Variation of Moment around the Pipe with Sectional Area for 300 mm Buried Depth of Pipe

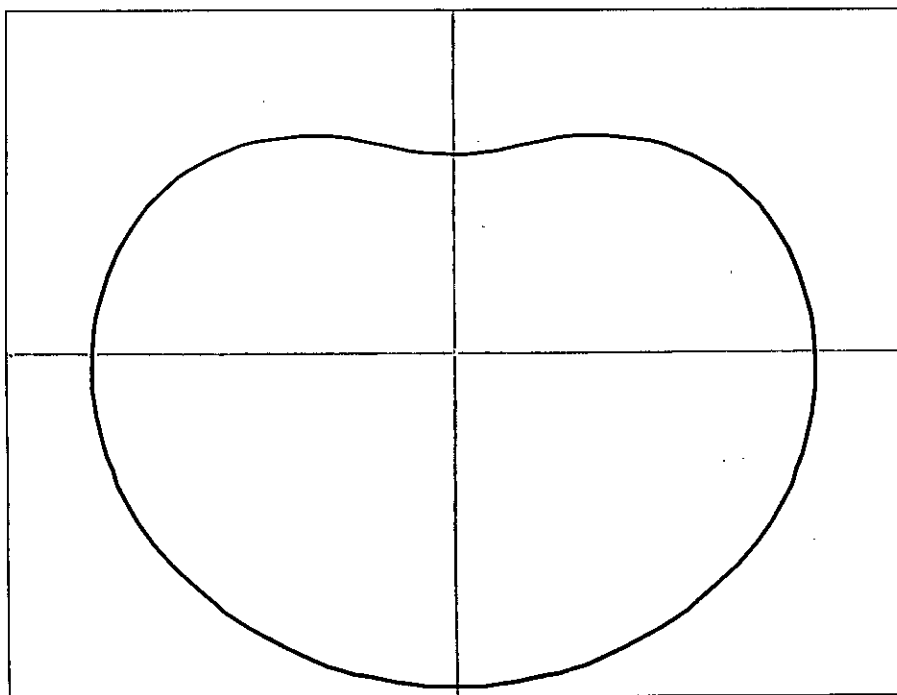


Figure 4.7 Deflected Shape of Pipe under Concentrated Surface Load

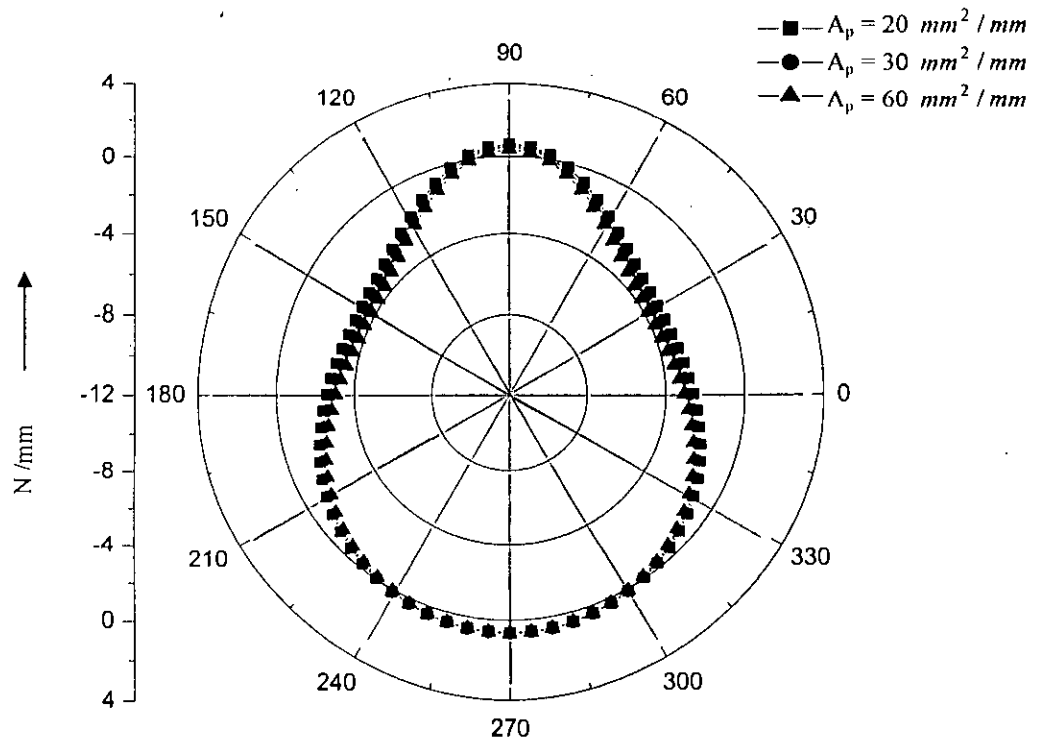


Figure 4.8 Variation of Thrust around the Pipe with Sectional Area for 600 mm Buried Depth of Pipe

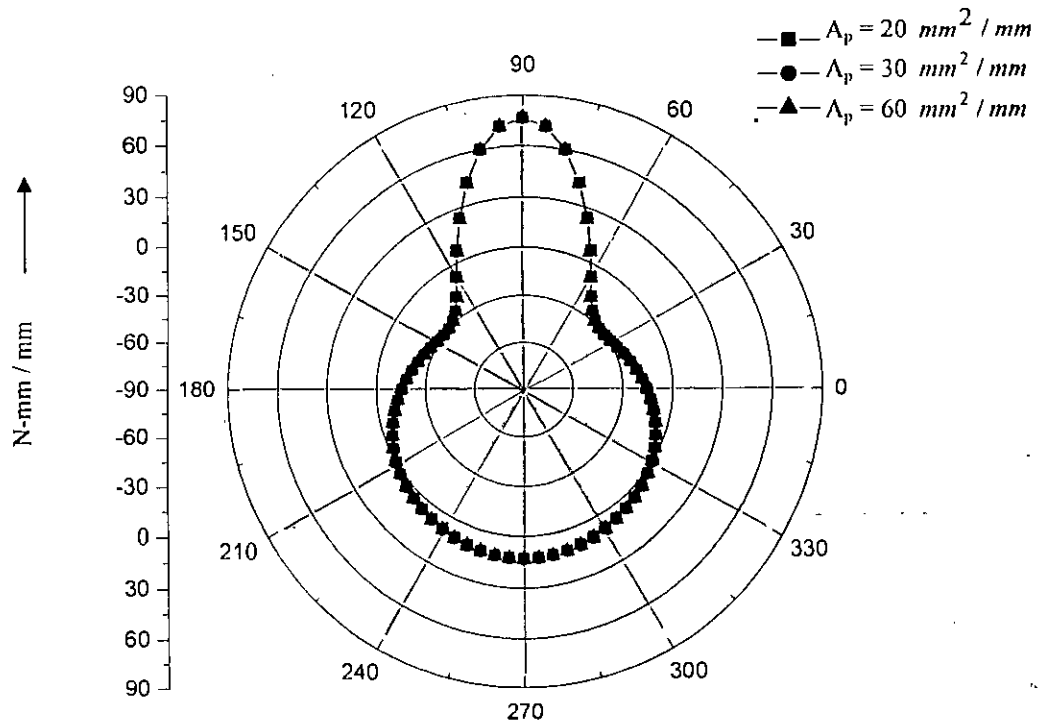
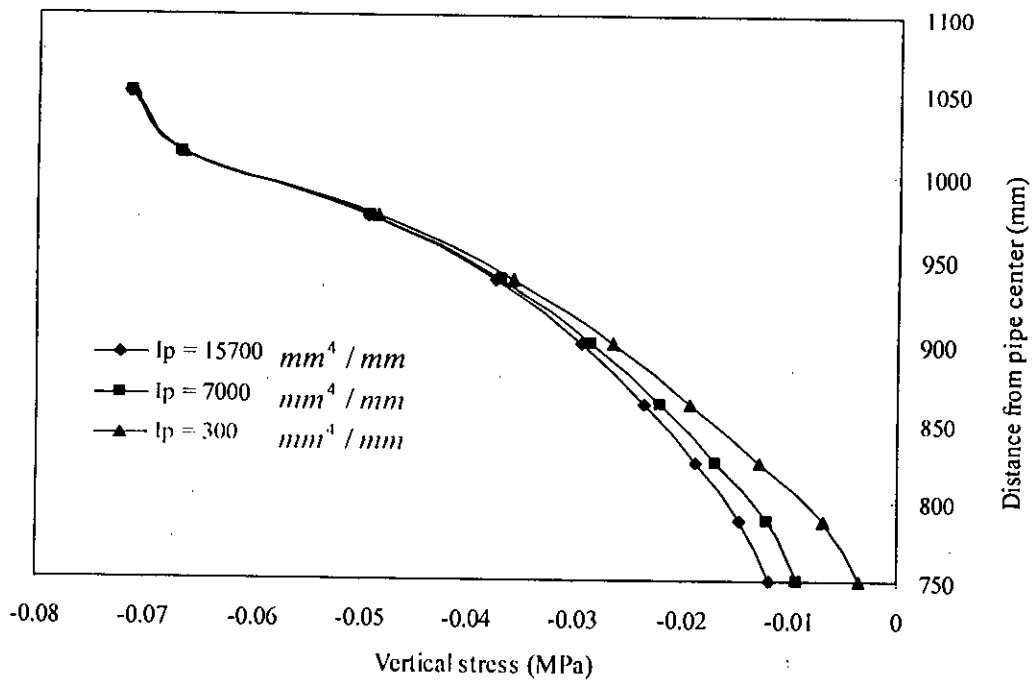


Figure 4.9 Variation of Moment around the Pipe with Sectional Area for 600 mm Buried Depth of Pipe.

### 4.3 EFFECT OF MOMENT OF INERTIA OF PIPE WALL

The moment of inertia is a geometrical property and depends on a reference axis. Moment of Inertia of a pipe's cross-sectional area measures the ability of pipe wall to resist bending. Larger the moment of inertia, less a beam will bend. For flexible pipe, moment of inertia is increased as to make the pipe more economical and stiffer through providing different wall profiles or corrugations. However, corrugation that occurs in the pipe's perimeter varies from manufactures to manufacturers. For different types of corrugation, moment of inertia is also different. Therefore, parametric study with variation of moment of inertia is conducted to identify the effects of this parameter. This parametric study may also help to identify the most efficient and economical sectional properties for pipe. A modulus of elasticity of pipe material was taken as 760MPa, which is short term modulus of HDPE. HDPE pipe with various wall profiles has been developed for buried pipe application. Cross sectional area of pipe wall was used as  $20 \text{ mm}^2$  for this parametric study. Three moments of inertia of pipe i.e.  $I_p = 300 \text{ mm}^4/\text{mm}$ ,  $7000 \text{ mm}^4/\text{mm}$  and  $15700 \text{ mm}^4/\text{mm}$  were considered for the parametric study. Similar moment of inertia for HDPE pipe was reported in Dhar (2002). To see the parametric effects, vertical stress distribution above the pipe crown, vertical stress distribution along the line which was 75mm above the pipe crown was considered first. Deflection of the pipe was then investigated. Figure 4.10 plots vertical stress along a vertical line above crown. Figure 4.10 shows that for all moment of inertia, graph is same up to 950mm level above crown. Then, the curves are diverged. For low moment of Inertia, vertical stress is less. But for high moment of inertia vertical stress is greater. Since high moment of inertia indicates high bending stiffness, the pipe can sustain a greater stress. On the other hand, pipe with less moment of inertia takes less stress due to arching effect. Figure 4.10 and Figure 4.11 shows the vertical stress distribution along the crown at different buried depths with different moment of inertias. Comparison between the graphs indicates that vertical stress is greater for buried depth of 300 mm than 600 mm for any particular point. Figure 4.11 also shows that divergence of curves occurs at level 950mm. But in compare to the Figure 4.10 degree of divergence is less, indicating less effects for the deeper pipe.

Obviously, for any point above the pipe, vertical stress for 300 mm buried depth will be greater than the 600 mm buried depth due to closeness to the load. Vertical soil stress right above the crown (75 mm) is plotted with the moment of inertia of pipe wall for two burial depths of pipe in Figure 4.12. The vertical stress in percentage with reference to the maximum stress is plotted in the figure as before. Figure 4.12 shows large difference in the vertical stress distribution for different burial depths. The vertical stress above crown appeared to increase with the increase of moment of inertia in both cases. However, the pipe deflection appeared to decrease with the increase of the moment of inertia as shown in Figure 4.13. The deflection appears to be related linearly with the moment of inertia of the pipe wall for the deeper pipe, while the pipe deflection is non-linear for the pipe with shallow burial depth.



**Figure 4.10 Vertical Stress along Vertical Line above Crown for 300 mm Pipe Burial Depth with Various Moment of Inertias**

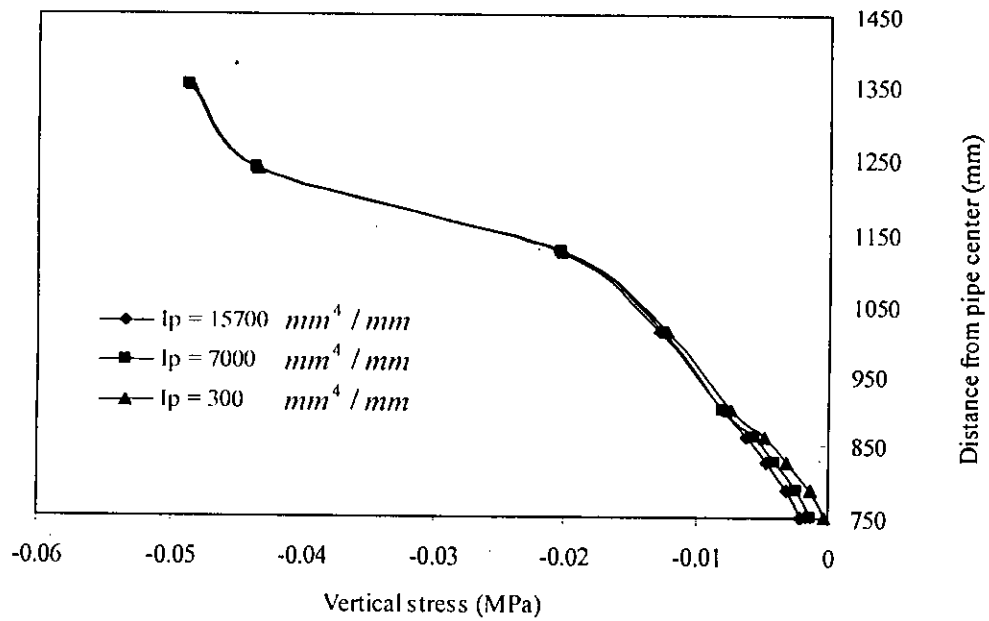


**Figure 4.11 Vertical Stress along Vertical Line Above Crown for 600 mm Pipe Burial Depth with Various Moment of Inertias**

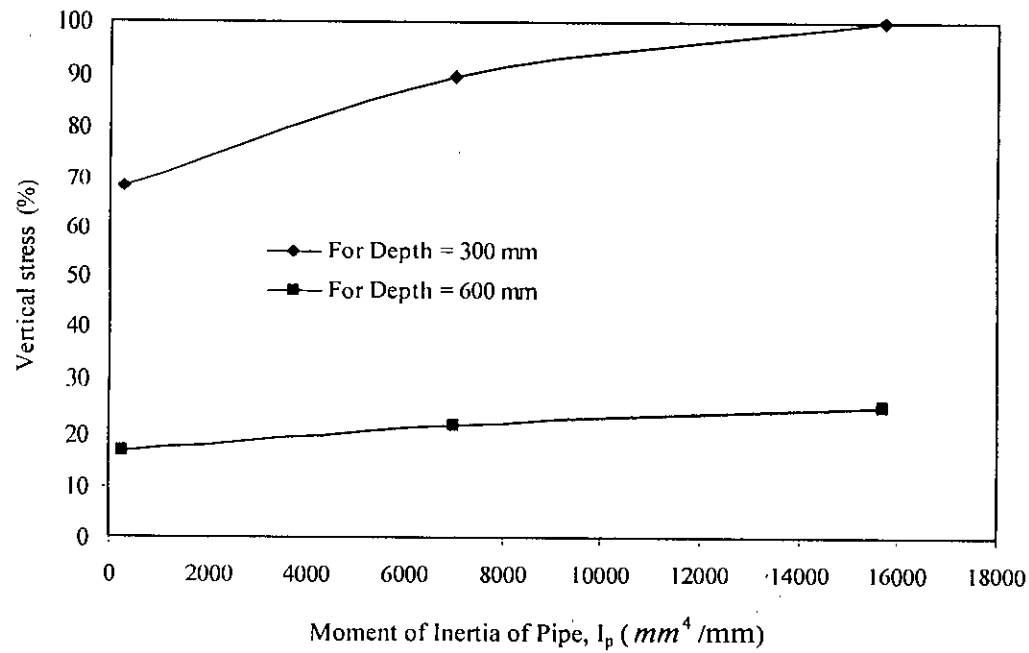


**Figure 4.12 Variation of Vertical Stress at 75mm above the Crown for Different Section Modulus of Pipe**

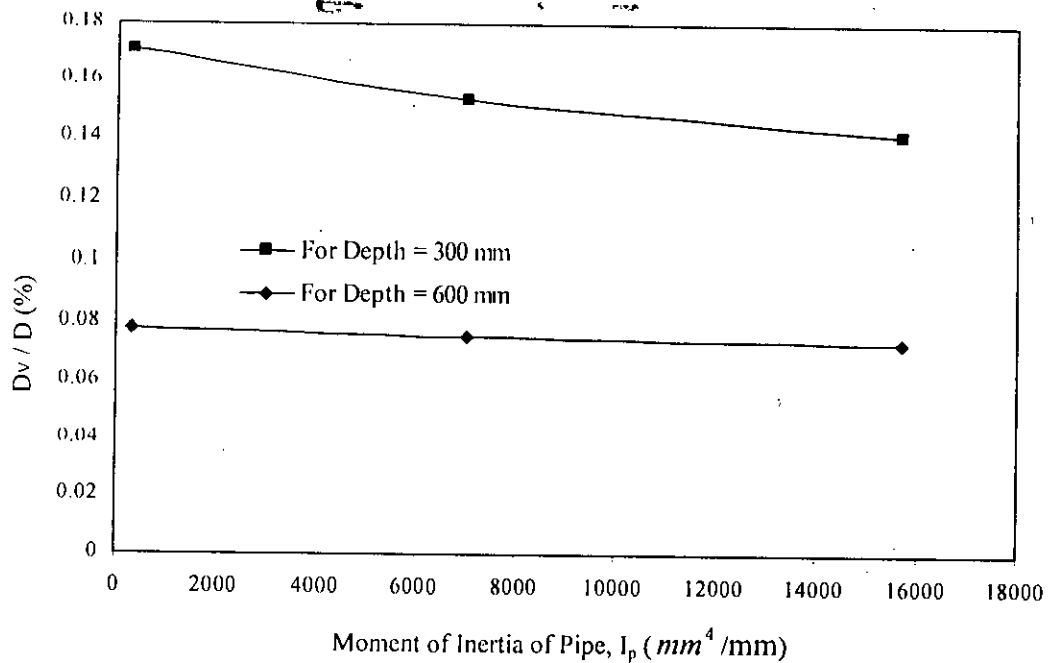


**Figure 4.13 Maximum Pipe Deflections with Sectional Moment of Inertia for Different Depths**

658501

Figure 4.14 shows variation of thrust along the perimeter of pipe for different moment of inertia in polar coordinate system for a burial depth of 300 mm. For different moment of inertia variation in thrust is not significant. This indicates that wall thrust is independent on the sectional parameters (area and moment of inertia of cross-section) of the pipe wall.

Figure 4.15 shows a polar co-ordinate plot of the variation of moment along the perimeter of pipe for different moment of inertia of the wall. The figure shows that the wall bending moment is significantly affected by the moment of inertia of the pipe section. The higher the moment of inertia, the greater the bending moment at pipe crown. However, bending deflection is less for the pipe with higher moment of inertia of wall section, as discussed with reference to Figure 4.13. The effects of pipe burial depths on the thrust and bending moment for variation of the wall moment of inertia are revealed from Figure 4.16 and 4.17. The figures plot thrust and moment for the pipe with 600 mm burial depths. It is also demonstrated that the wall thrust is not affected by the moment of inertia of the cross-sectional area, while the bending moment is significantly affected. However, the magnitude of the bending moment is much less for the deeper pipe (Figure 4.17) than those for shallow buried pipe (Figure



4.15). Table 4.2 shows the maximum bending moments for the two burial depths for various moment of inertias. Table indicates that at shoulder moment is negative for all cases but at crown moment is always positive. The moment is negative at springline and it becomes positive when it reaches to the crown.

**Table 4.2 Maximum Bending Moments for Variation of  $I_p$**

Burial Depths	Moments of Inertia ( $\text{mm}^4/\text{mm}$ )	Crown Moment (N-mm/mm)	Shoulder Moment (N-mm/mm)
300 mm	300	8.73	-1.73
	7000	131.5	-40.47
	15700	226.1	-80.08
600 mm	300	1.99	-0.6209
	7000	39.19	-14.15
	15700	76.28	-28.74

The studies described above demonstrate that moment of inertia of the pipe wall significantly govern the stress distribution due the concentrated surface load for the pipe investigated. The stresses influence the deformation mechanism of the pipe. The moment of inertia defines the bending stiffness of the pipe wall for a particular modulus of elasticity of the pipe material. To explore the mechanics, further investigation with variation of the modulus of pipe material has been performed, as discussed in the following section.

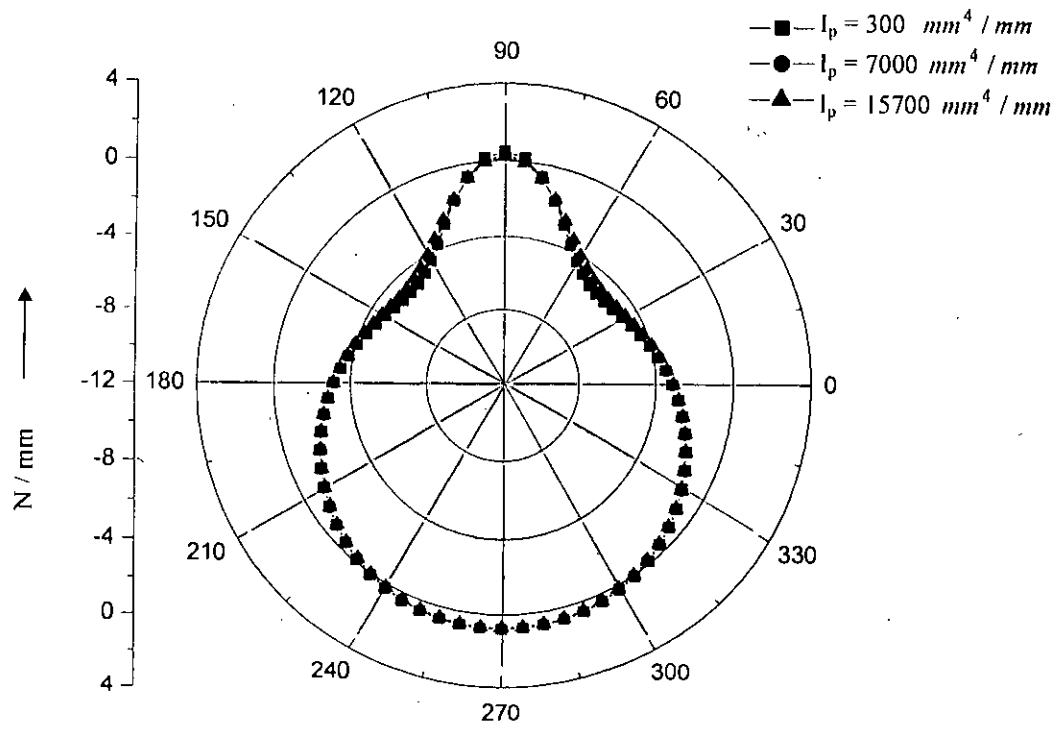


Figure 4.14 Variation of Thrust around the Pipe with Moment of Inertia for 300 mm Buried Depth of Pipe

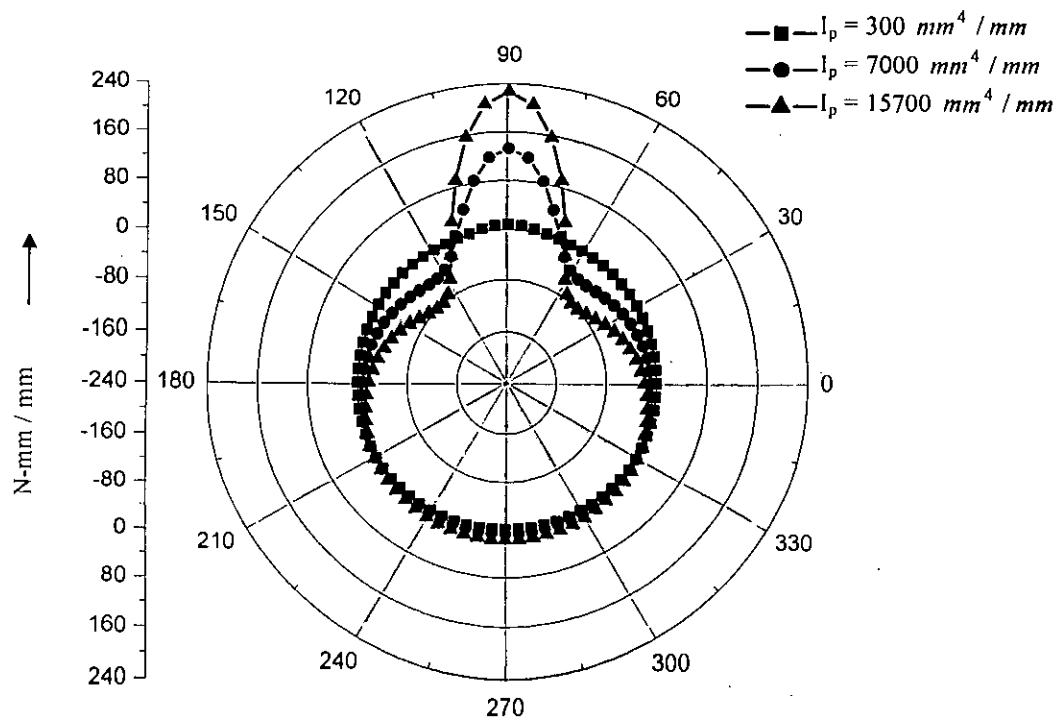


Figure 4.15 Variation of Bending Moment around the Pipe with Moment of Inertia for 300 mm Buried Depth of Pipe

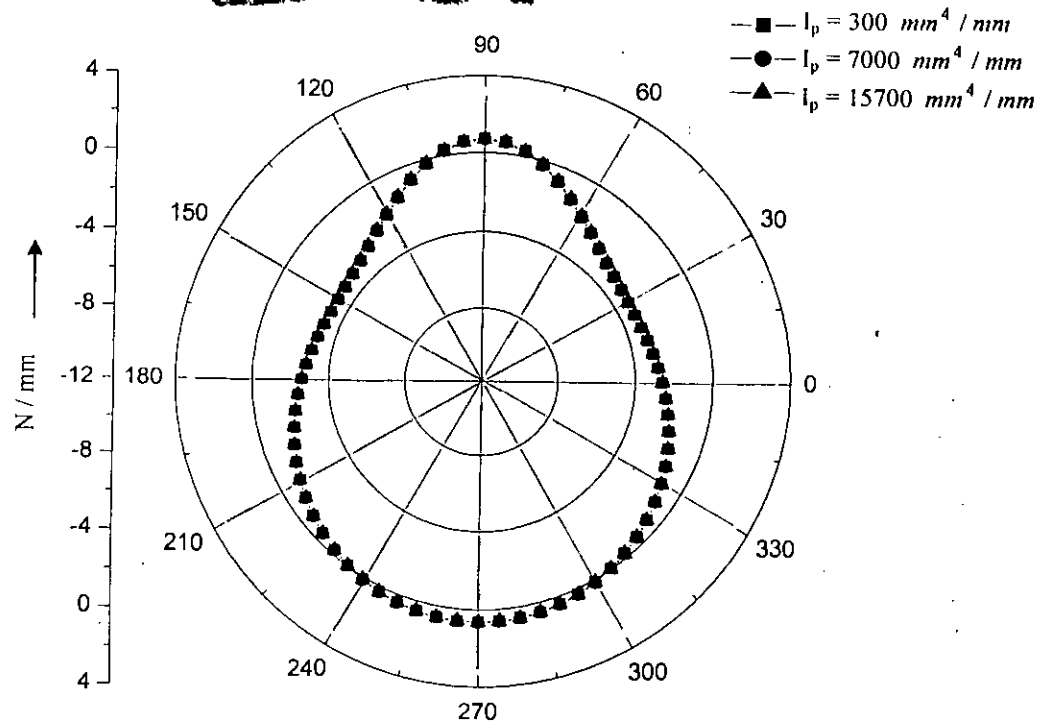


Figure 4.16 Variation of Thrust around the Pipe with Moment of Inertia for 600 mm Buried Depth of Pipe

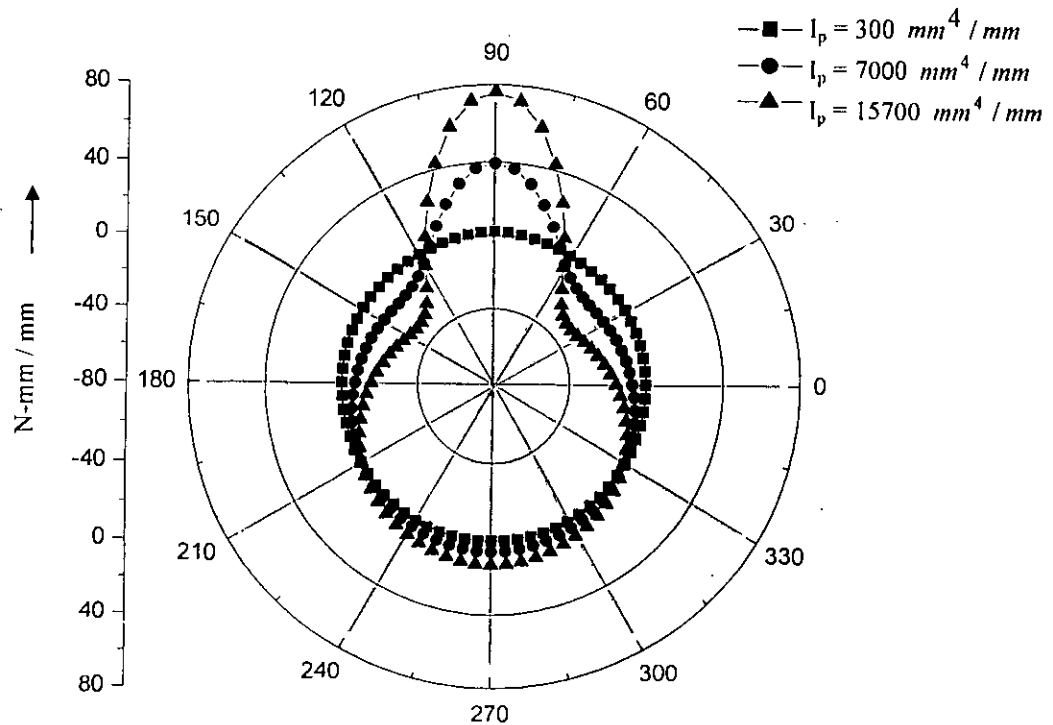
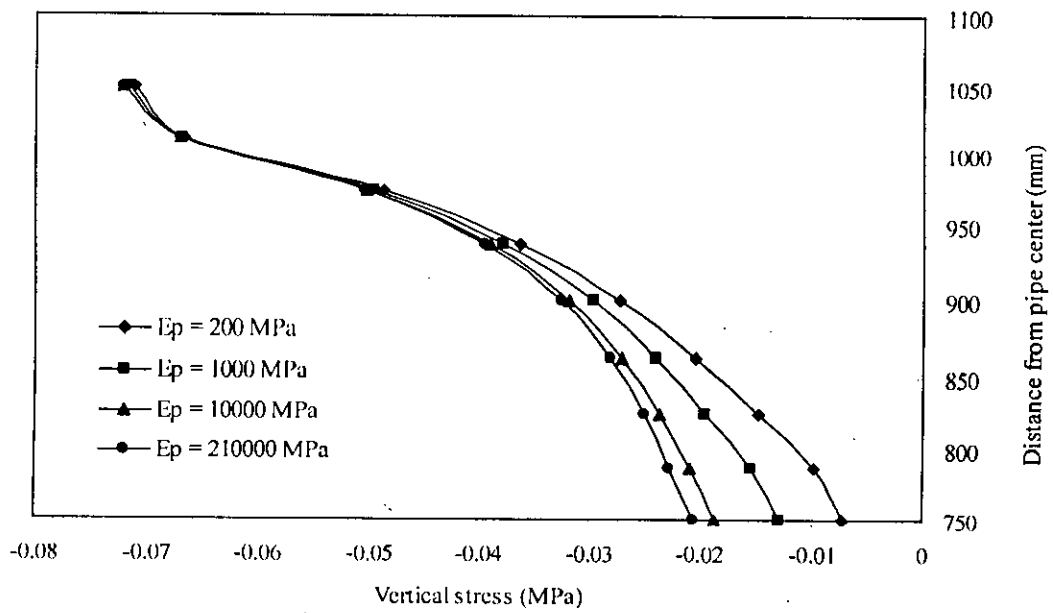


Figure 4.17 Variation of Bending Moment around the Pipe with Moment of Inertia for 600 mm Buried Depth of Pipe

#### 4.4 EFFECT OF MODULUS OF ELASTICITY OF PIPE MATERIAL

Starting from plastic pipe to metal pipe, flexible pipe can vary with a wide range depending on the material properties, which may affect the distribution of live load around the pipe. In general, if section modulus increases pipe will be stiffer and attract more loads reducing the distribution of stress in the soil mass. It will also deform less due to stiffness. A parametric study with variation of material modulus has been conducted to understand the mechanics. While parametric study was performed with the variation of the material modulus of pipe, pipe sectional area was used as  $20 \text{ mm}^2/\text{mm}$  and moment of inertia was used as  $15700 \text{ mm}^4/\text{mm}$ . For native and backfill soil, a modulus of 10 MPa was used. The modulus for pipe material was varied as 200 MPa, 1000 MPa, 10000 MPa and 210000 MPa to cover a wider range starting from long-term modulus of thermoplastic material to the modulus of steel.

A parametric study for two different buried depths was first performed, for the effects of pipe modulus on vertical stress distribution. Figure 4.18 shows the variation of vertical stress along the crown for pipe with 300 mm buried depth. Significant difference in vertical stress occurs at a level which is just above the crown up to 1000mm above the crown. The stress was greater for pipe with higher modulus of elasticity. Obviously, high material modulus indicates high stiffness and therefore high load resistance capabilities to receive more stress than the others. For 600 mm burial depth, Figure 4.19 is plotted to explore the vertical distribution of the stresses. Similar behavior and variation is revealed as those for pipe with soil cover of 300mm above the crown, as shown in Figure 4.18. However, the magnitude of stress is less for the deeper pipe. Figure 4.20 shows the comparison of vertical stress distribution at 75mm above the crown for the two burial depths. The vertical stresses are expressed as a percentage of the maximum vertical stress as before. This graph reveals that vertical stress at this level is almost double for the pipe with 300 mm burial depth than for the pipe 600 mm burial depth, which is consistent with the theory. It is also revealed that vertical stress increases with the increase of pipe material modulus initially, which is almost constant for material modulus of above 10000 MPa. Thus for pipe with very high material modulus, the effect of live load appears to be less dependent of the pipe stiffness.



**Figure 4.18 Vertical Stress above the Crown for 300 mm Burial Depth of Pipe, with Various Pipe Material Modulus**

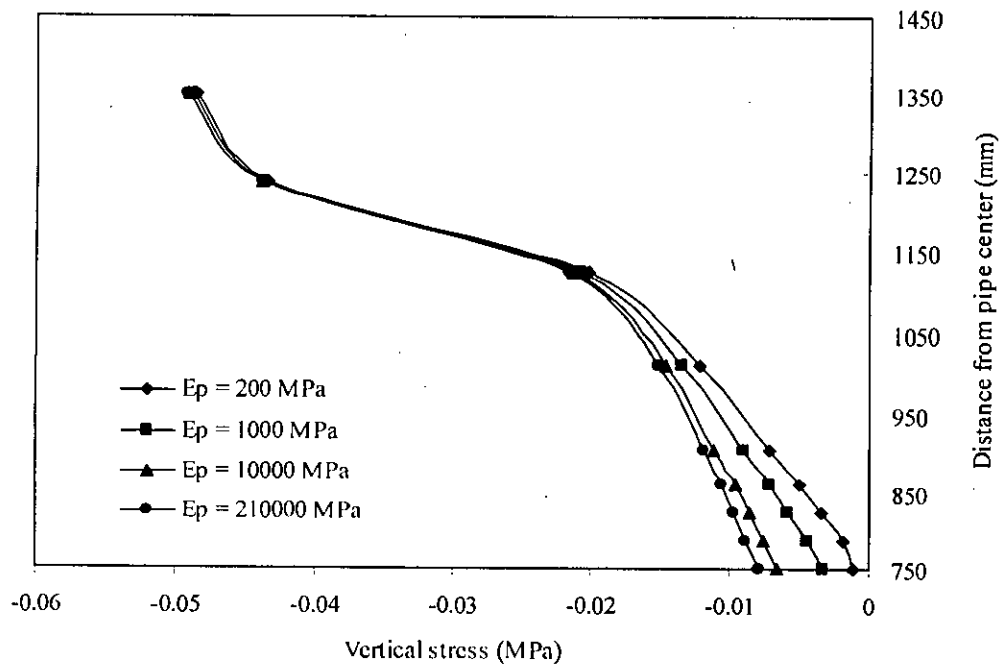


**Figure 4.19 Vertical Stress above the Crown for 600 mm Burial Depth of Pipe, with Various Pipe Material Modulus**

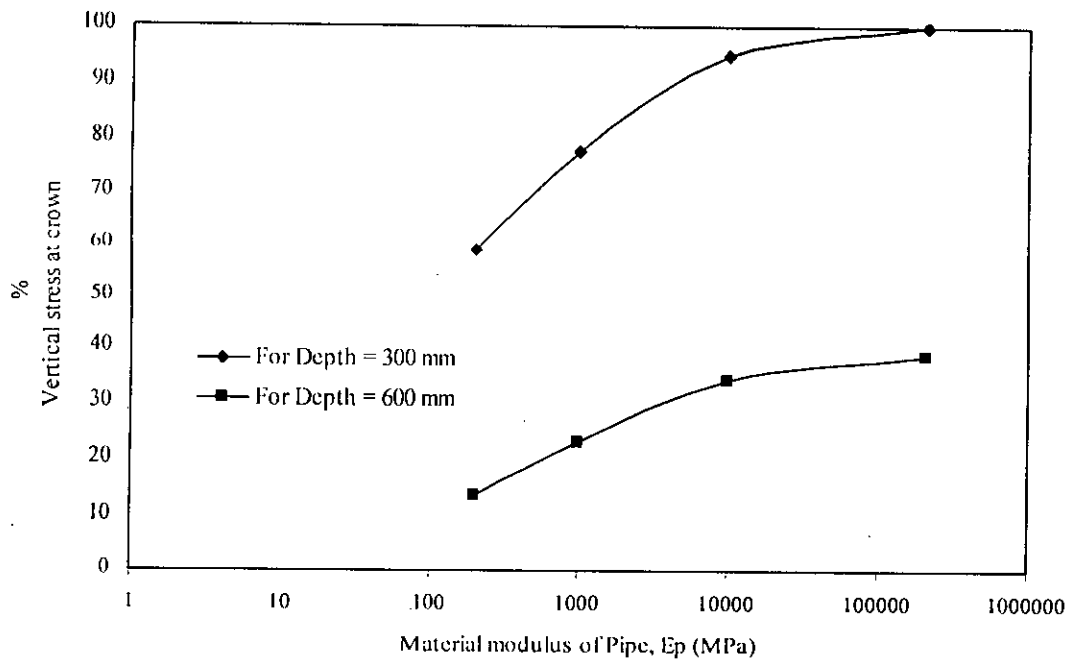


**Figure 4.20** Variation of Vertical Stress at 75mm Above the Crown for Different Material Modulus of Pipe

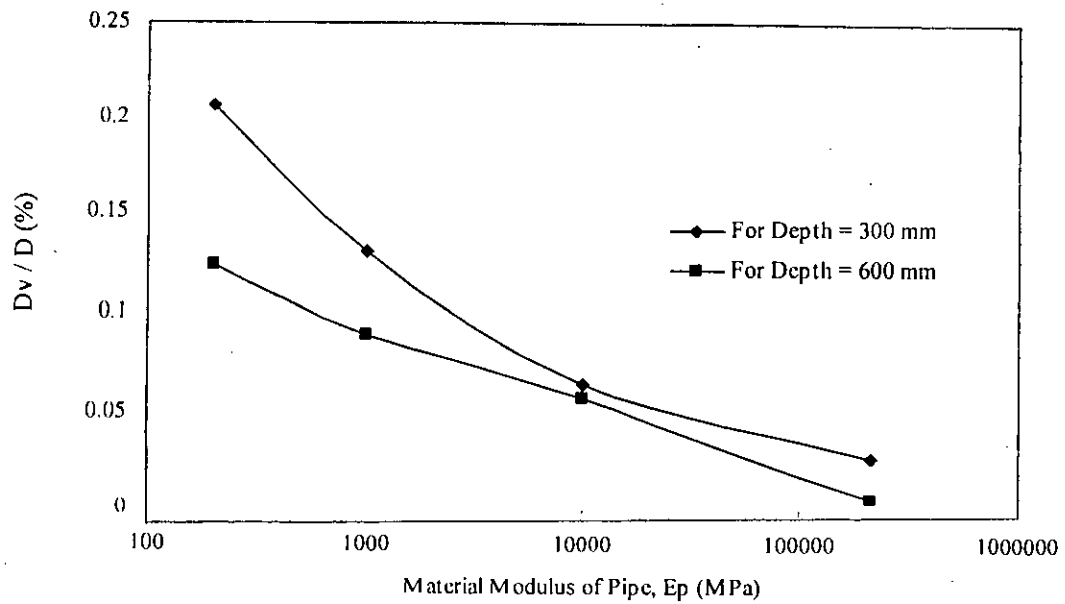


**Figure 4.21** Maximum Deflection of Pipe for Variation of Pipe Material Modulus

Figure 4.21 shows pipe deflection with modulus of pipe material under the surface load. From the figure, it is clear that as the material modulus of pipe increases, the pipe becomes stiffer. Therefore, it can take more stress with less deflection than the others. Although the vertical stress is greater for the stiffer pipe, it deforms less. Variation of pipe deflection with modulus is greater initially, which stabilizes for very high moduli for pipe materials for the pipe at 300 mm depth. However, for the pipe at 600 mm depth, the initial effect on deflection is less. This indicates that the pipe at shallow burial is greatly influenced due to pipe modulus than the deeper pipe.

Figure 4.22 shows variation of thrust along the perimeter of pipe for different material modulus of pipe material, in polar coordinate system for pipe with 300 mm burial depth. Variation of bending moment for the same pipe is plotted in Figure 4.23. It is revealed that the thrust is less influenced by the material modulus of the pipe. However, the moment is significantly affected by the modulus. For increase of pipe modulus from 200 MPa to 210000 MPa, the maximum thrust was increased by 10 %. For the corresponding modulus the positive moment at the crown was increased to 10 times and the negative moment at the shoulder was increased to 17 times. Thus the shoulder moments were affected more significantly than the crown moment. Variation of moment is significant when section modulus increased from 1000 MPa to 10000 MPa.

For 600 mm burial depth, graphs are plotted in Figure 4.24 and Figure 4.25. Figure 4.24 describes thrust around the pipe for variation in material modulus of pipe. The thrust is also less affected in this case. Keeping the similarity with 300 mm burial depth as mentioned in Figure 4.22. For increase of pipe modulus from 200 MPa to 210000 MPa, the maximum thrust was increased by 55 % for the pipe. Figure 4.25 describes the variation for moment around the pipe for 600 mm burial depth. The positive bending moment at crown was increased by 1370 % and the negative bending moment at the shoulder was increased by 2440 % for the change of pipe modulus from 200 MPa to 210000 MPa. Thus, the wall thrusts and moments are more significantly affected by pipe modulus for the deeper pipe. This may be due to the fact that the effects of the surface load are localized at the crown and shoulder for the shallow buried pipe. However, the stresses are distributed over the whole pipe circumference for deeply buried pipe. The mechanism will be discussed further with

reference to the study of the effect of burial depth. The magnitude of the maximum moment is much less for the deeper pipe (600 mm).

It is also noticed from Figure 4.23 and Figure 4.25 that locations of the maximum negative moment at the shoulder are affected by the pipe modulus. With the increase of the pipe modulus, the point of maximum negative moment move from the shoulder toward the springline. The locations of maximum compressive thrust which occur at the shoulder are also affected. However, the influence is less for the thrust than the moment.

For the stiffer pipes with pipe modulus of 10,000 MPa and 210000 MPa the effect of surface load extend through the whole circumference of the pipe, as revealed from Figure 4.23 and Figure 4.25. Positive bending moment at the invert also increased for the pipe with those two moduli. However, moment increases at the invert are less than those at the crown. For the pipe with  $E_p = 210000$  MPa the invert moment is 45% of the crown moment for the burial depth of 300 mm and is 51 % for the burial depth of 600 mm. The invert moment is 5 to 27 % and 11 to 38 % of crown moment for the other pipes with burial depth of 300 mm and 600 mm, respectively. For the pipe with low material modulus the effects of surface load are demonstrated around the crown and shoulder only.



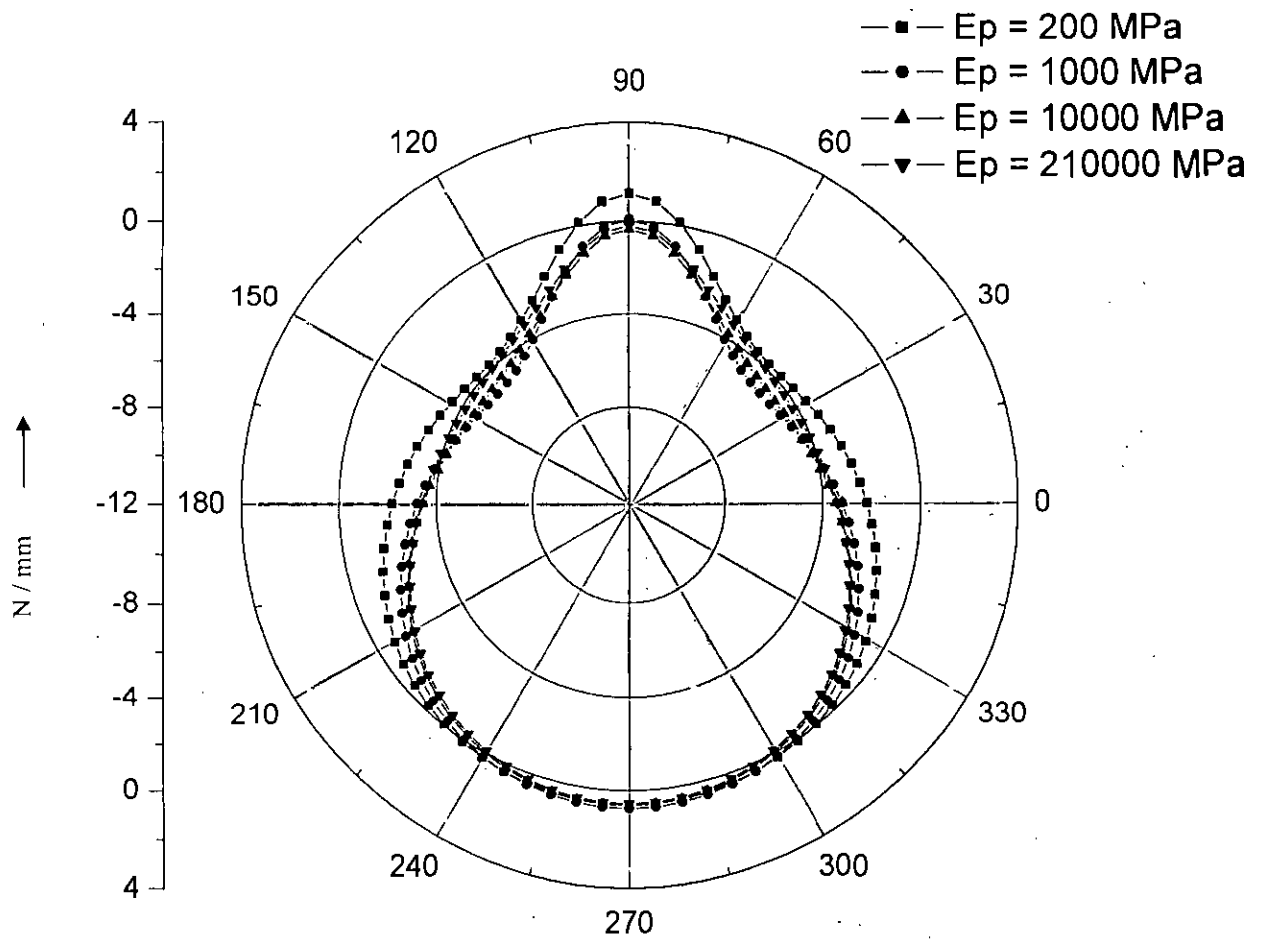


**Figure 4.22 Variation of Thrust around the Pipe with Pipe Material Modulus for  
 300 mm Pipe Buried Depth**

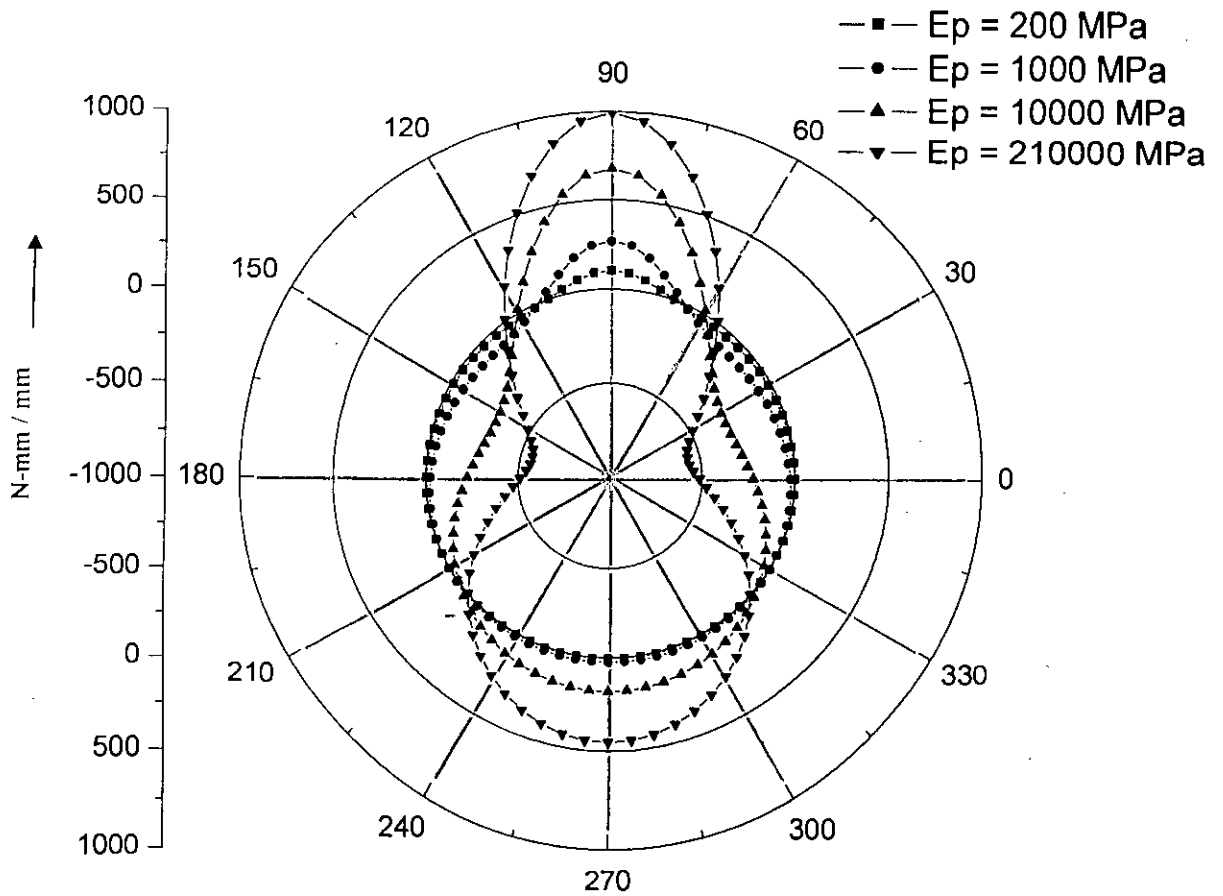


**Figure 4.23 Variation of Bending Moment around the Pipe with Pipe Material Modulus for 300 mm Pipe Buried Depth**

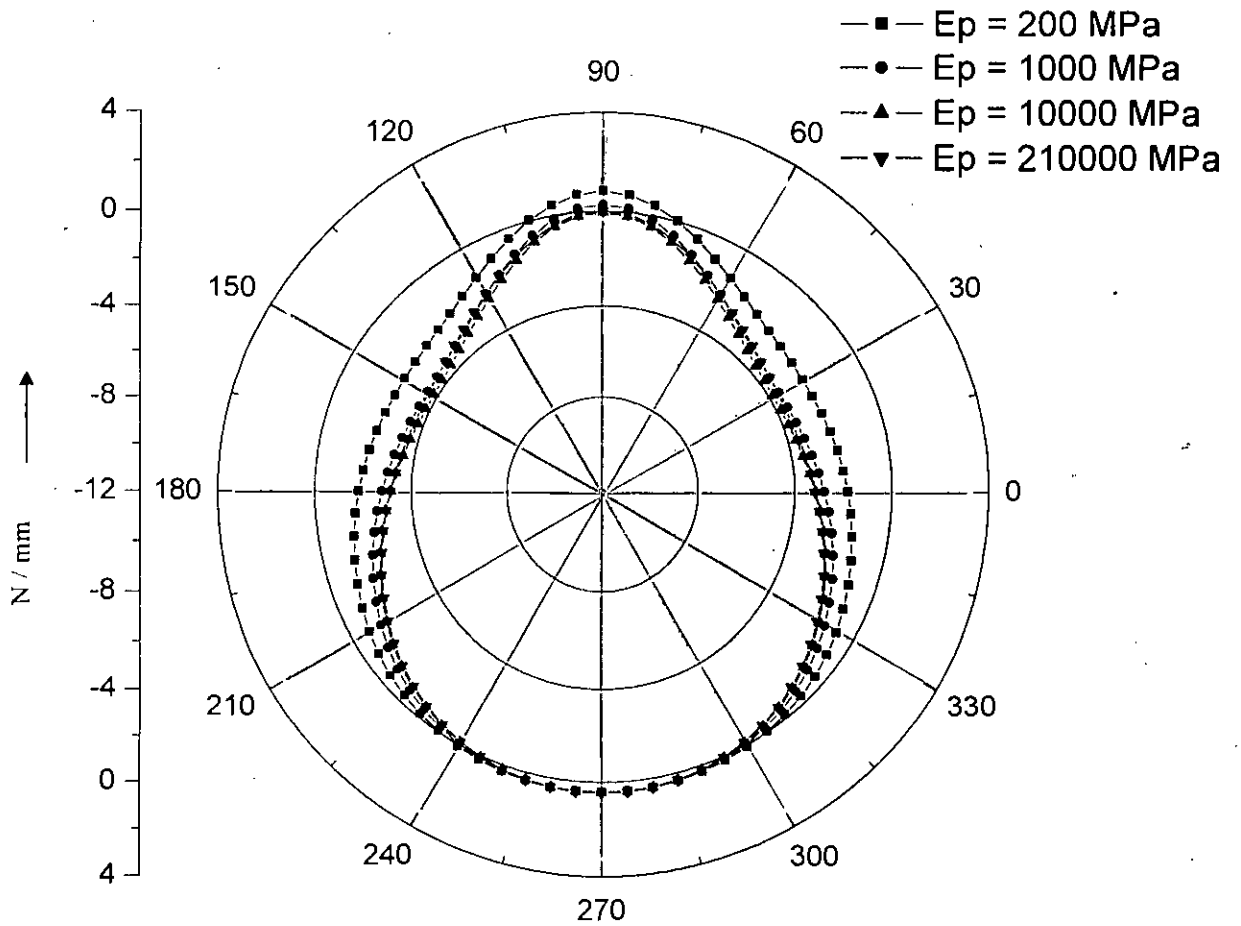


**Figure 4.24 Variation of Thrust around the Pipe with Pipe Material Modulus for  
 600 mm Pipe Buried Depth**

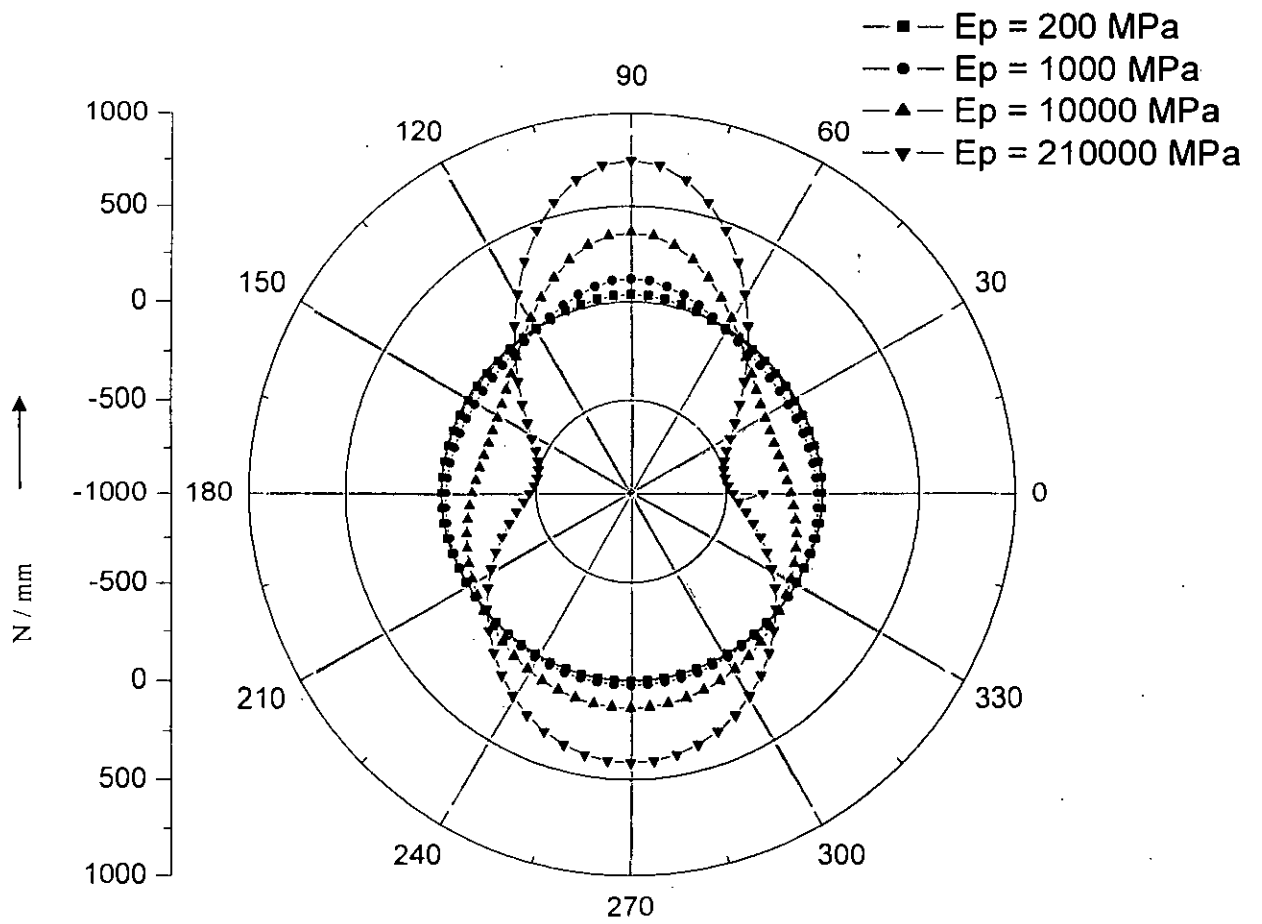


**Figure 4.25 Variation of Thrust around the Pipe with Pipe Material Modulus for:  
600 mm Pipe Buried Depth**

Therefore, it can be concluded that material modulus of pipe significantly affect the moment that come along the pipe periphery. In case of moment, variation in the maximum moment is less times for pipe with 300 mm burial depth than the pipe with 600 mm burial depth. However, the magnitude of the moment is greater for shallow pipe. Thrusts calculated for 300 mm buried depth is about 10 to 56 % greater than the pipe with 600 mm burial depth when material modulus is increased. Vertical stress is almost two times for 600 mm burial depth than 300 mm burial depth of pipe.

#### 4.5 EFFECT OF RELATIVE STIFFNESS

The investigation of the effects individual parameters on the live load distribution has been discussed in the previous sections. This section focuses on the investigation based on the relative stiffness of the pipe-soil system. Dhar (2003) and Dhar and Kabir (2006) used relative stiffness such as, bending stiffness ( $\frac{E_p I_p}{E_s R^3}$ ) and hoop stiffness ( $\frac{E_p A_p}{E_s R}$ ) for calculation pipe deflection for buried flexible pipes. Here, R is pipe radius,  $E_p$  and  $E_s$  are pipe and soil modulus, respectively,  $A_p$  and  $I_p$  are area and moment of Inertia, respectively, of pipe wall section. These two stiffness have been used for investigation of live loads under different conditions. Figure 4.26 indicates the graphs of relative bending stiffness and maximum moment that occurs around the pipe. The maximum bending moment occurred at the crown for the pipes under concentrated surface load. The figure shows that as the value of relative bending stiffness increase, moment also increases. But moment increases sharply in a zone of intermediate stiffnesses. Similar effect occurs whatever the depth is. However, this proves a direct relationship between the relative bending stiffness and moment around the pipe. At any point on the graph, for 300 mm buried depth, moment is greater than 600 mm buried depth. The increase of moment with the bending stiffness is initially linear. The rate of increase is greater for an intermediate range of the relative bending stiffness, which stabilize again for higher stiffness. Thermoplastic pipe with material modulus of 700 to 3000 MPa appears to fall in the intermediate stiffness region, indicating greater dependency on the soil-pipe interaction under surface load. To

explore the moments around pipe circumference polar diagram is plotted in Figure 4.27 for few stiffness values as indicated by circles in Figure 4.26.

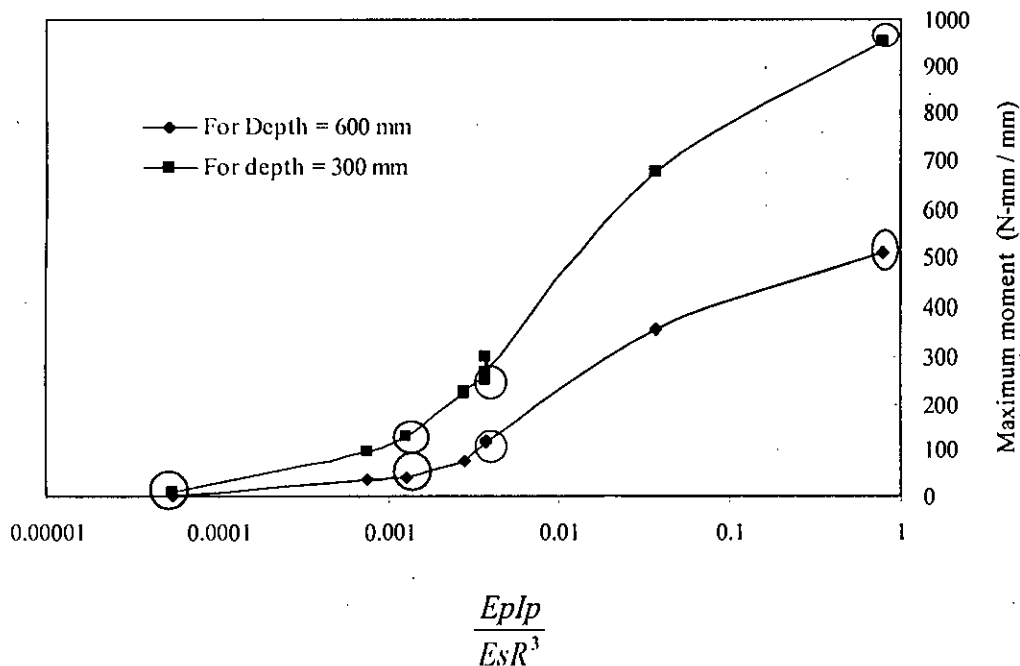


Figure 4.26 Variation of Maximum Moment with  $\frac{Eplp}{EsR^3}$

Figure 4.27 indicates the diagram that represents the moment around the pipe for 300 mm burial depth with four particular relative stiffnesses. According to Figure 4.27 the maximum moment occurs for the maximum relative bending stiffness. Similarly, the minimum moment occurs for the minimum relative bending stiffness. The highest relative bending stiffness for pipe occurs when material modulus for pipe was the highest. Figure 4.27 describes the variation of moment around the pipe with relative bending stiffness for burial depth of 600 mm as circled in the Figure 4.26. The Figure also shows that as the value of relative bending stiffness increases, value for moment is also increases.

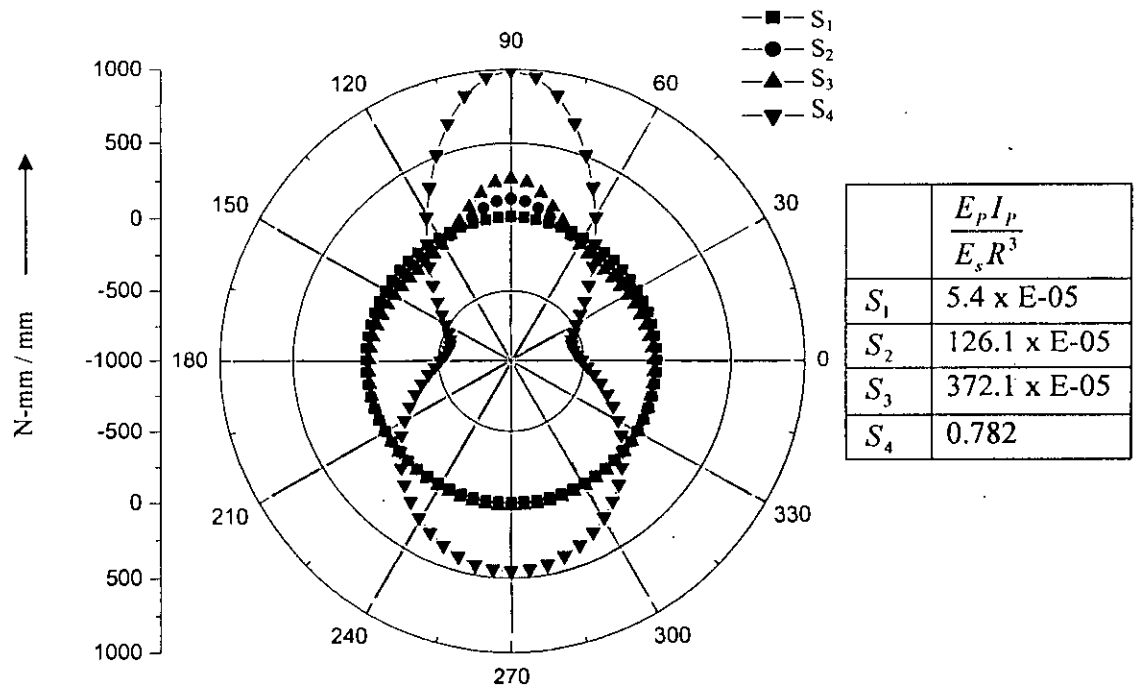


Figure 4.27 Variation of Bending Moment with Relative bending Stiffness around the Pipe for 300 mm Pipe Burial Depth

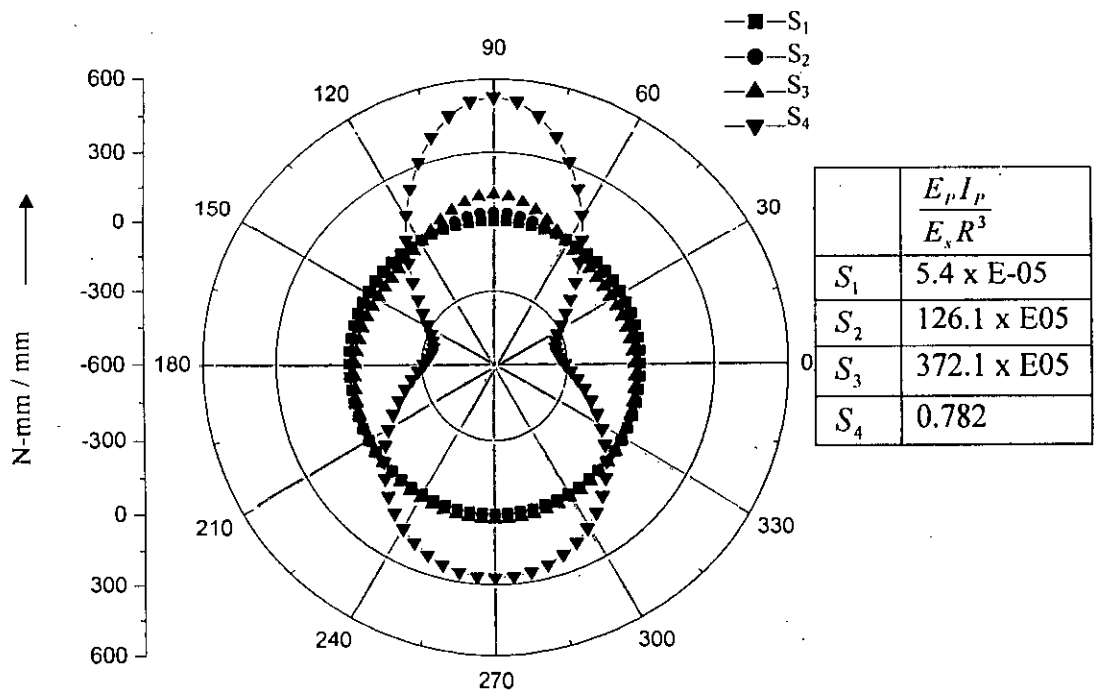


Figure 4.28 Variation of Bending Moment with Relative bending Stiffness around the Pipe for 600 mm Pipe Burial Depth

Therefore, a summary can be drawn that there are a relationship in between relative bending stiffness and moment along the pipe periphery. The maximum moment occurs for maximum relative bending stiffness and this relationship is almost linear for pipe with low relative stiffness and then become non-linear. Most of the thermoplastic pipe falls in the non-linear zone, indicating strong dependency of the effects on pipe parameters. Burial depth of the pipe has also influence on the moment development of the pipe wall.

Relative hoop stiffness is also an important factor that may govern the thrust around the pipe. However, as seen earlier area of cross-section of pipe does not have significant effect on the development of thrust on pipe wall under concentrated surface load. Thus, the variation in thrust is expected due to stiffness of the pipe material with respect to the surrounding soil. Figure 4.29 represents the variation of the axial force (thrust) with relative hoop stiffness that occurs around the pipe for both 300 mm and 600 mm burial depth. The thrust was maximum at an angle of 35 to 45° from the springline for burial depth of 300 mm and at an angle of 25 to 30° for burial depth of 600 mm of the pipe. As discussed earlier, with the increase of burial depth, the effect of live load thrust moves toward the springline of the pipe. The figure revealed that the magnitude of thrust increase with increase of stiffness initially, which finally become constant for pipe with high hoop stiffness ( $>10$ ). Thus, for stiffer pipe thrust appeared to depend on the burial depth of the pipe and independent on the hoop stiffness, while for very flexible pipes (i.e. thermoplastic pipe). The thrust depends on the relative hoop stiffness of the pipe-soil system.



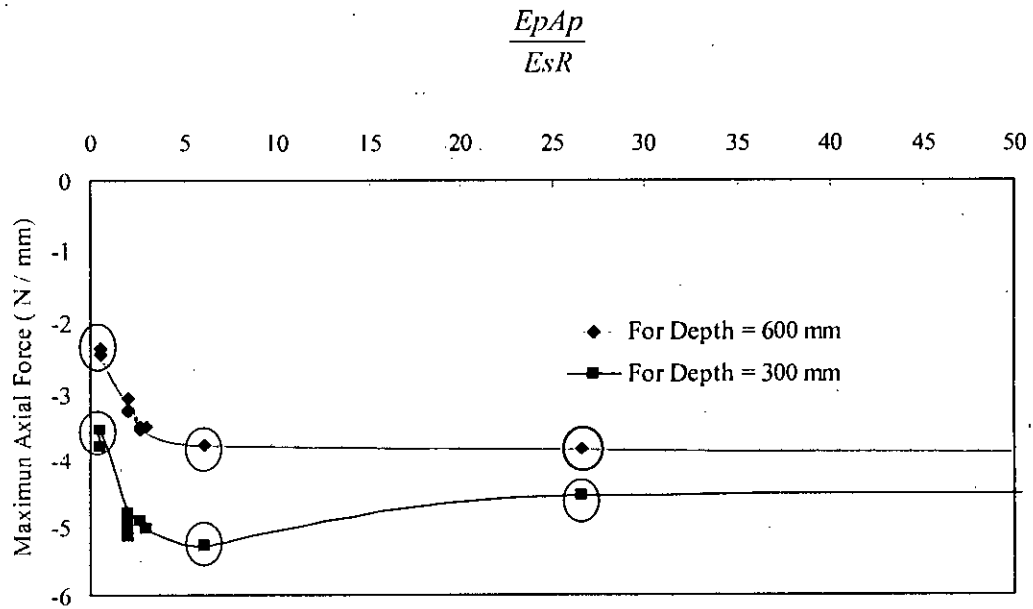


Figure 4.29 Variation of Maximum Thrust with  $\frac{E_p A_p}{E_s R}$

Figure 4.30 shows the polar diagram for thrust around the pipe perimeter for 300 mm burial depth of pipe for different relative hoop stiffness (as circled in Figure 4.29) along with the maximum one. Figure 4.30 indicates that for different relative hoop stiffness values, all graphs are overlapped with one another for pipe with high relative hoop stiffness and the difference is insignificant. It is seen from the diagram that the maximum value of thrust occurs in between angle of 30 to 60 degree from the springline. The minimum value occurs at the crown. Figure 4.31 indicates the thrust along the pipe perimeter for pipe with 600 mm burial depth considering the points as circled in Figure 4.29. This diagram also indicates less significant change in thrust with the variation of relative hoop stiffness. However, variation of the thrust is evident at the shoulder.

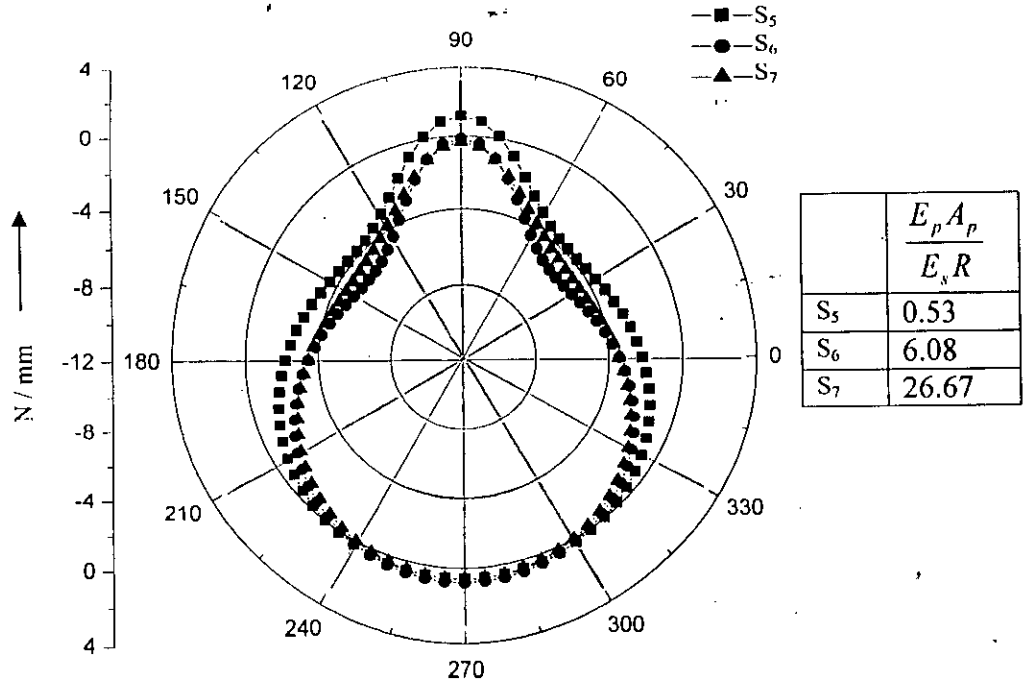


Figure 4.30 Variation of Thrust around the Pipe with Relative Hoop Stiffness for 300 mm Buried Depth of Pipe

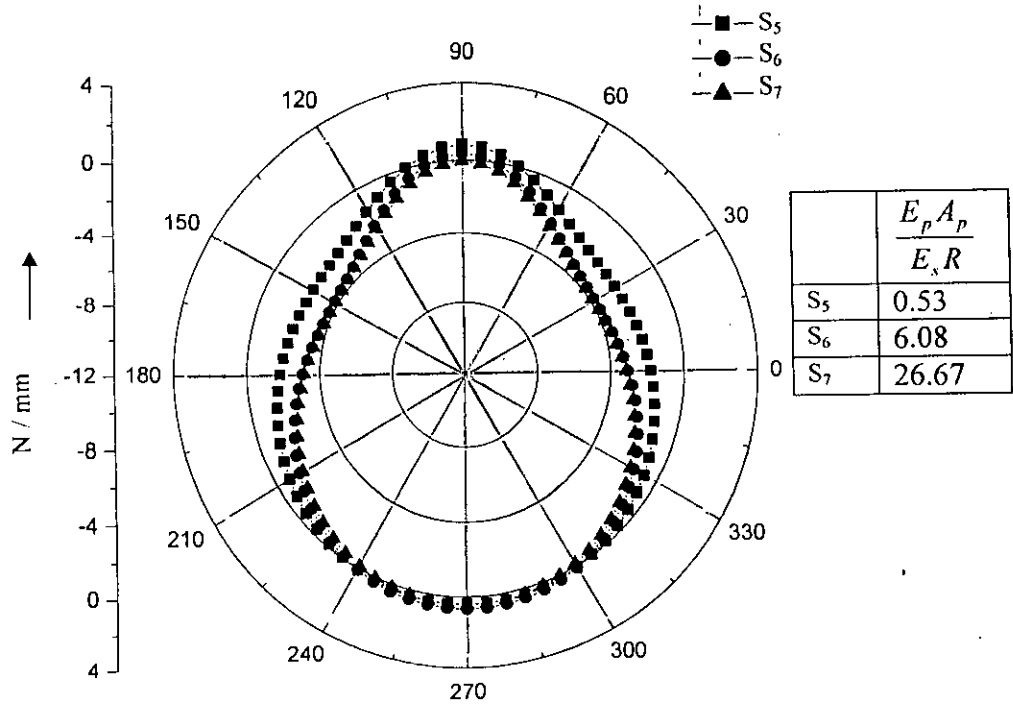


Figure 4.31 Variation of Thrust around the Pipe with Relative Hoop Stiffness for 600 mm Buried Depth of Pipe

#### 4.6 EFFECT OF BURIAL DEPTH

The study discussed above reveals that the burial depth of pipe affects the soil-structure interaction behavior under surface load significantly. As a general point of view, as the buried depth decreases, stress reaching to pipe increases if other things remain the same under concentrated surface load. Therefore, higher burial depth indicates less stress due to vehicular load. However, dead load that comes from the backfill soil increases with the increase of burial depth. The effect of surface live load was only considered in this research as the loading condition. A concentrated load was applied as a surface load above pipe crown as mentioned earlier. To understand the buried pipe behavior effectively for different burial condition, analysis were performed with different burial depth of the pipes such as; 300 mm, 600 mm, 1500 mm and 3000 mm. Finite element meshes were developed similar to that discussed in Chapter 3 (Figure 3.4), with increase of a zone of mesh on top. Element size was maintained at the top zone as same as the zone underneath. The number of element in a horizontal line was also maintained to be the same. Figure 4.32 indicates a sample finite element mesh that is used for modeling of pipe with higher buried depths. Load was applied on top of the mesh on a point directly above the pipe crown to represent the concentrated surface load. The boundary conditions for the mesh were the same as those discussed in Chapter 3.

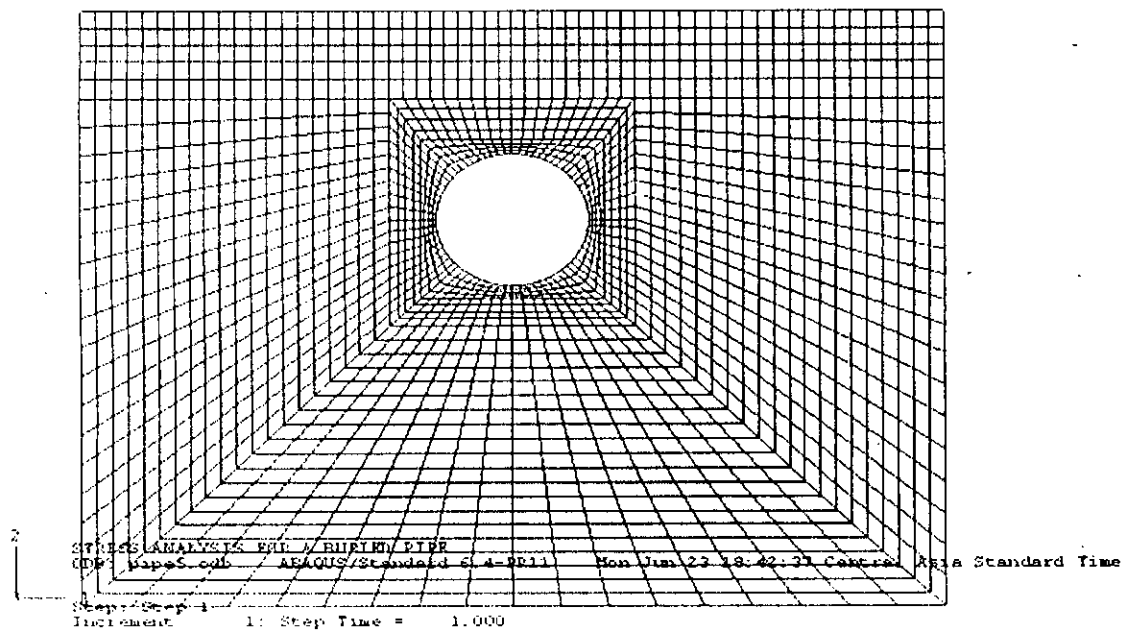


Figure 4.32 Finite Element Mesh Used for the Study with Various Burial Depths

Figure 4.33 depicts the variation of vertical stress above pipe's crown with a ratio of buried depth to pipe diameter. For all the cases presented in the figure only material modulus of pipe and burial depth was varied while other parameters were kept as the same. It was found, as in the previous study, that material modulus of pipe affects live load distribution significantly. Graph is also plotted in Figure 4.33 for the stress at a level of pipe crown according to Boussinesq's equation for live load distribution. To compare the results of Boussinesq's equation with the finite element output, as shown in Figure 4.33, the depth at which stress was calculated by Boussinesq's equation was also divided by pipe diameter. It is to be noted that the Boussinesq's solution calculate the soil stress in a homogenous isotropic and elastic soil mass. Thus, the presence of pipe is neglected. Figure 4.33 reveals that Boussinesq's equation over-predict the stress for each of the flexible pipe except the one with  $E_p = 210000$  MPa (steel pipe). As expected, arching in flexible pipe cause redistribution of stress toward the soil, resulting in these reduction. However for the pipe with  $E_p = 210000$  MPa, Boussinesq's equation gives almost the same stress for pipe with greater burial depth (depth greater than pipe diameter). However, for shallow depth the Boussinesq's solution may under-predict the stress for the pipes with high material moduli as a result of development of negative arching. Thus, for shallow buried pipes, pipe-soil interaction analysis would be required to calculate the soil stresses due to surface load.

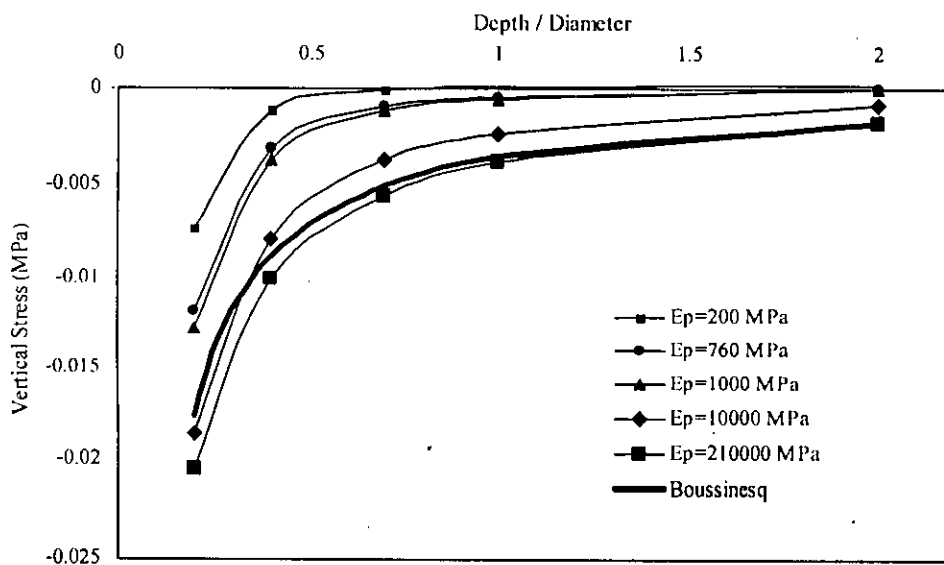
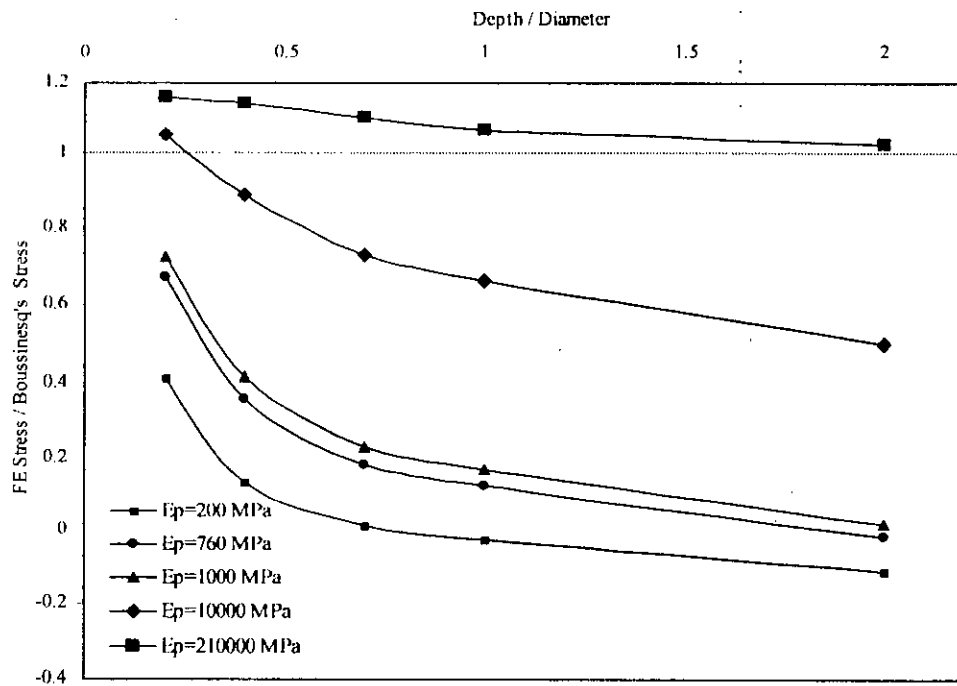


Figure 4.33 Variation of Vertical Stress above Crown for Different Burial Depth

It is revealed from Figure 4.33 that the effects of surface load for thermoplastic pipe with material modulus between 200-1000 MPa are minimized if the burial depth is greater than the diameter of the pipe. To illustrate this elaborately, ratio of the finite element results to Boussinesq's stresses are plotted against burial depth in Figure 4.34. It is revealed that for material modulus between 200-1000 MPa, vertical stress is a fraction of the Boussinesq's stress at every point i.e. vertical stress is lower than the Boussinesq's stress whatever the depth is. For a material modulus of 210000 MPa, the vertical stress is greater than Boussinesq's stress due to the development of negative arching. For shallow burial depths pipe attract more stress than deep burial depth. With the increase of buried depth the ratio of FE to Boussinesq's stress approaches to 1, indicating that the stress can reasonably be estimated using Boussinesq's equation.



**Figure 4.34 Variation of Vertical Stress with Boussinesq's Stress above Crown for Different Burial Depth**

Vertical stress pattern along the horizontal line above crown at the different level are plotted for the pipe with a burial depth of 600 mm in Figure 4.35. Figure 4.35 indicates a comparison of soil stresses at different level for thermoplastic pipe having a material modulus of 760 MPa. Figure 4.35 indicate that as the distance from pipe crown increases vertically, variation with Boussinesq's are reduced. At a level of 75

mm from the crown the ratio of the FE vertical stress to the Boussinesq's stress is 0.5 whereas at a level of 262 mm from the crown the ratio is 0.70, indicating the stress closer to that from Boussinesq's solution for the farther point. Table 4.3 compares the calculated vertical stress with the stress from Boussinesq's equation on a vertical line above pipe crown.

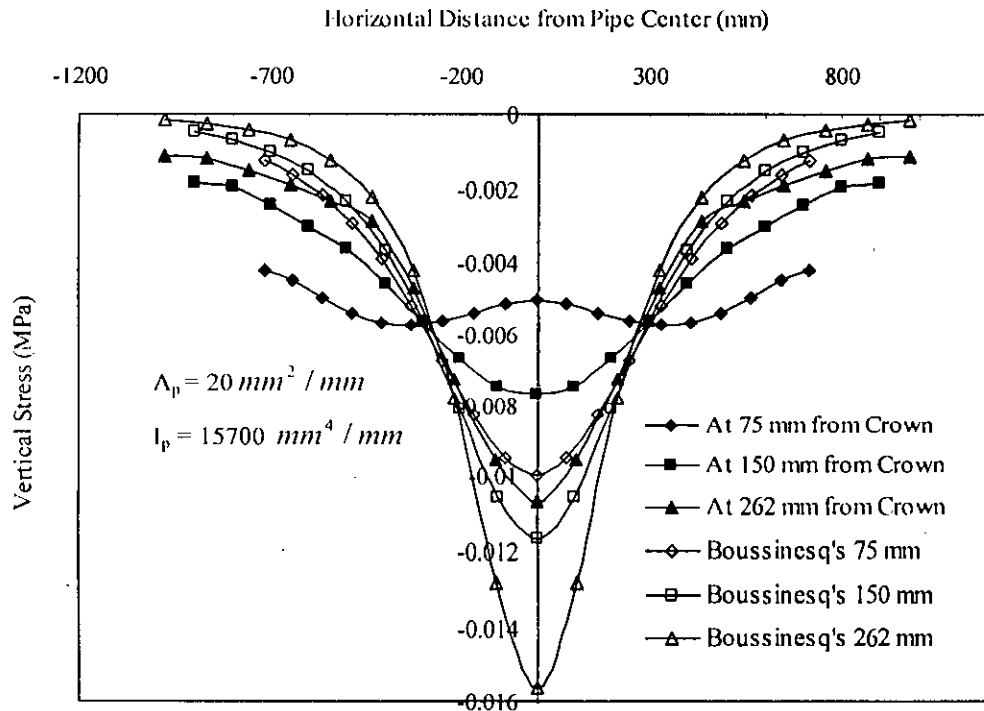


**Figure 4.35 Vertical Stress Comparison for 600 mm Burial Depth of Pipe with  $E_p = 760 \text{ MPa}$**

**Table 4.3 Comparison of Stresses 75 mm above Pipe Crown for HDPE Pipe (Burial Depth = 600 mm)**

Distance Above Crown (mm)	FE Vertical Stress (MPa)	Vertical Stress from Boussinesq's Equation (MPa)	Ratio (FE/Boussinesq's)
75	-0.005	-0.010	0.519
150	-0.008	-0.012	0.658
262	-0.011	-0.016	0.689

Figure 4.36 indicates vertical soil stress at three different levels for pipe with material modulus of  $E_p = 210000$  MPa and a burial depth of 600 mm. It is revealed from the figure that as the distance from pipe crown increase, the variation between the FE stresses with Boussinesq's stress decrease. Right above the crown the finite element analysis calculated a greater stress than that obtained from Boussinesq's equation. This indicates the development of negative arching for the stiffer steel pipe. However, with the increase of the distance from pipe crown finite element over-predict the vertical stress compared to the Boussinesq solution. Table 4.4 reveals a comparison of ground stresses at different level above pipe crown calculated using two methods.

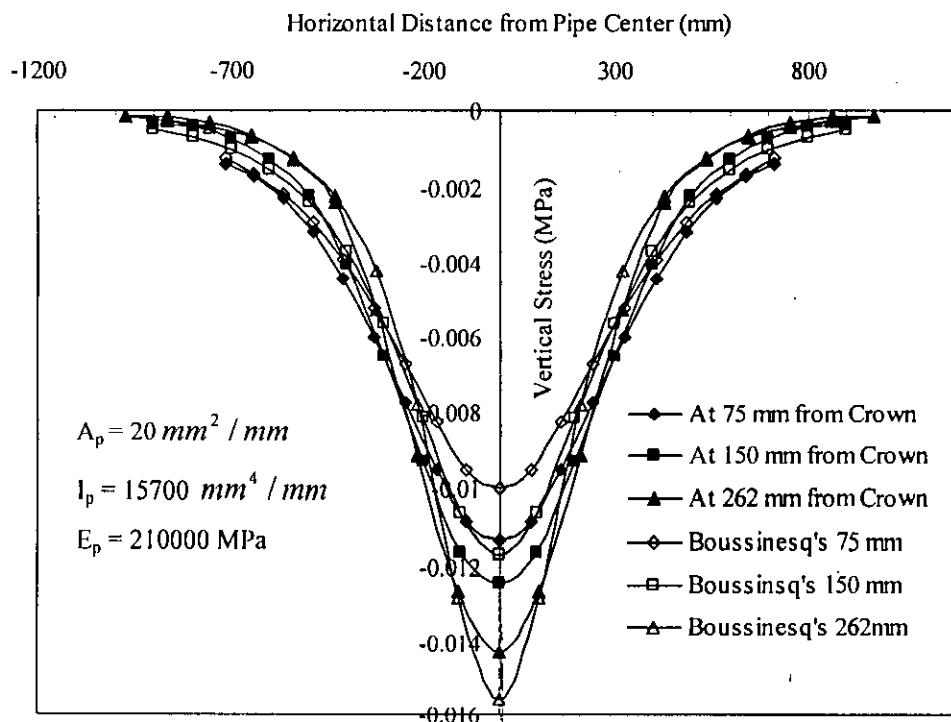


Figure 4.36 Vertical Stress Comparison for 600 mm Burial Depth of Pipe with  $E_p = 210000$  MPa

**Table 4.4 Comparison of Stresses 75 mm above Pipe Crown for Steel Pipe  
(Burial Depth = 600 mm)**

<b>Distance Above Crown (mm)</b>	<b>FE vertical Stress (MPa)</b>	<b>Vertical Stress from Boussinesq's Equation (MPa)</b>	<b>Ratio (FE/Boussinesq's)</b>
75	-0.013	-0.010	1.28
150	-0.014	-0.012	1.15
262	-0.015	-0.016	0.98

Figure 4.37 compares the soil stress above the pipe crown for the thermoplastic pipe with  $E_p = 760$  MPa and the pipe burial depth of 300 mm. Pipe material modulus of 760 MPa, Moment of inertia of  $15700 \text{ mm}^4$  and area of  $20 \text{ mm}^2$  was considered for the calculation. Soil stress at different level above crown is plotted in Figure 4.37 along with the stress from Boussinesq's equation. Calculation showed that for shallow (at 300mm) buried pipe, the ratio of FE vertical soil stress with Boussinesq is 0.88 at a level of 75 mm above crown. As the distance from pipe crown increase, this ratio also increases i.e. at 150 mm level above crown this ratio becomes 0.94, indicating the FE stress to be closer to those from Boussinesq's solution. Table 4.5 compares FE and Boussinesq stress in the ground above the pipe crown. Thus, as the distance above crown increases, variation in vertical stress between Boussinesq's equation and FE model decreases. The increase of the difference (decrease of the ratio) in Table 4.5 for the distance of 225 mm above pipe crown is attributed to the closeness of the point to the concentrated load for the pipe with 300 mm burial depth. Soil stress in the vicinity of the load is non-linear and may be affected by the coarseness of the FE meshes. However, the stress at that point was of little interest and therefore not considered further.

Since pipe material modulus effect the soil stress at different levels significantly, at 300 mm burial depth, graphs are also plotted in Figure 4.38 to see the variation of soil stress for the pipe with material modulus of 210000 MPa. This figure also indicate that soil stress in the pipe vicinity deviate from the Boussinesq stress to a greater extend than the ground points away from the pipe. A comparison of the ground



stresses for a 300 mm burial depths a steel pipe is shown in Table 4.6. The stress at 225 mm above pipe crown again indicated a greater difference between calculation using FE and Boussinesq's equation due to the closeness of load as discussed above.

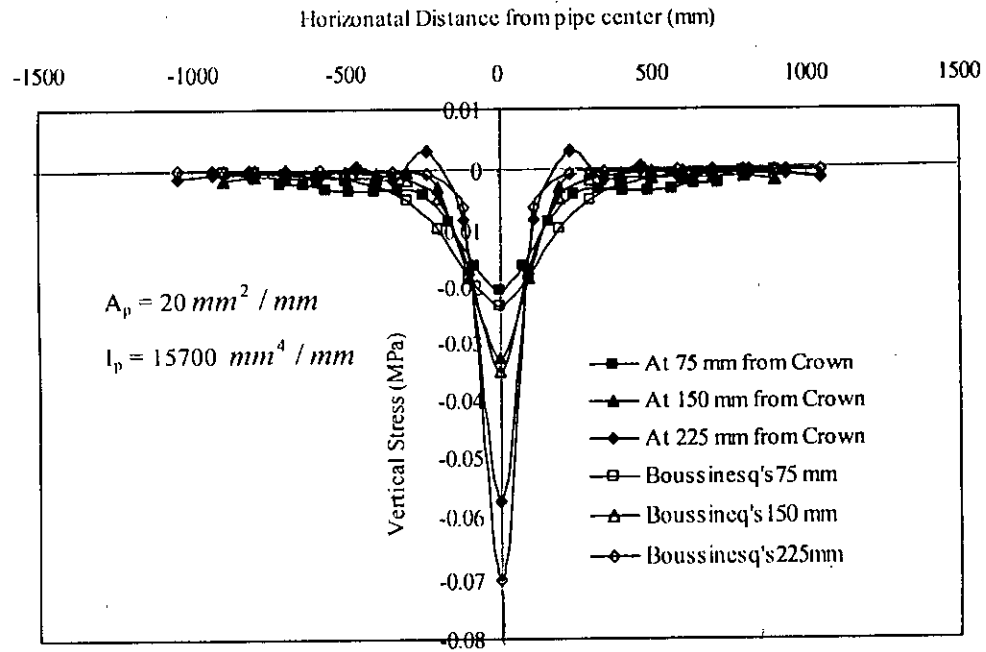
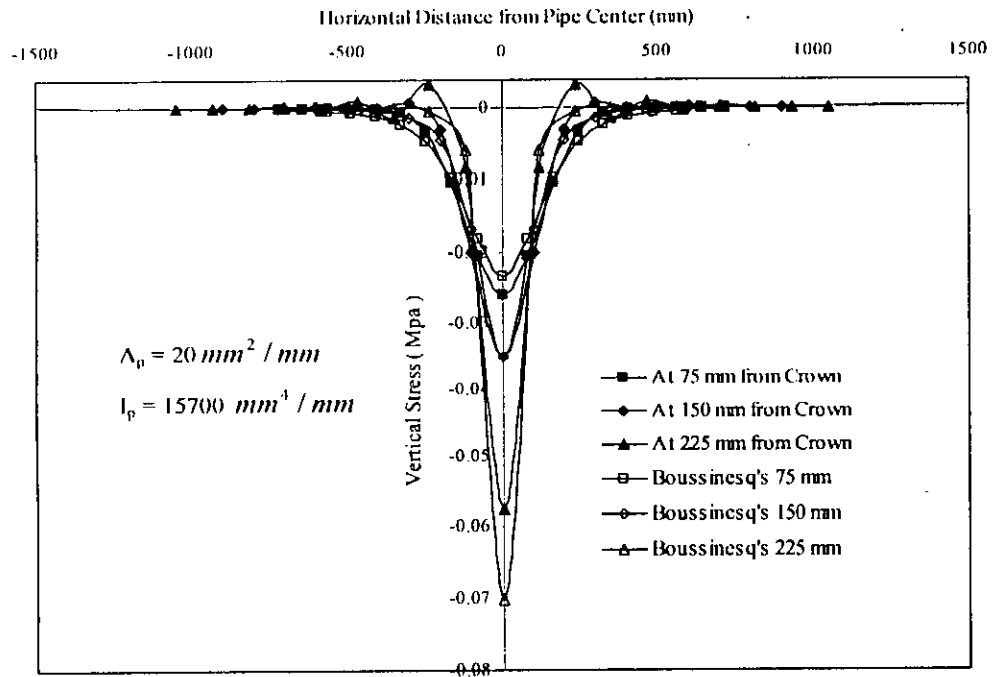


Figure 4.37 Vertical Stress Comparison for 300 mm Burial Depth of Pipe with  $E_p = 760$  MPa (HDPE Pipe)

Table 4.5 Comparison of Stresses 75 mm above Pipe Crown for HDPE Pipe (Burial Depth = 300 mm)

Distance Above Crown (mm)	FE Vertical Stress (MPa)	Vertical Stress from Boussinesq's Equation (MPa)	Ratio (FE/Boussinesq's)
75	-0.021	-0.023	0.883
150	-0.033	-0.035	0.935
225	-0.057	-0.070	0.819



**Figure 4.38 Vertical Stress Comparison for 300 mm Burial Depth of Pipe with  $E_p = 210000 \text{ MPa}$**

**Table 4.6 Comparison of Stresses 75 mm above Pipe Crown for Steel Pipe (Burial Depth = 300 mm)**

Distance Above Crown (mm)	FE vertical Stress (MPa)	Vertical Stress from Boussinesq's Equation (MPa)	Ratio (FE/Boussinesq's)
75	-0.026	-0.023	1.11
150	-0.035	-0.035	1.00
225	-0.058	-0.070	0.82

It is interesting to note from Figures 4.35 and Figure 4.37 that stress distribution at 75 mm above crown is different for the pipes with burial depths of 300 mm and 600 mm. For the pipe with 300 mm burial depth, the vertical stress above the pipe crown is the maximum, while the stress is the minimum for other cases of thermoplastic pipes. For the steel pipe the maximum stress occurred above crown (Figure 4.36 and Figure 4.38) for both 300 mm and 600 mm burial depths. To see the variation further, graphs are plotted for vertical stress 75mm above the crown for pipes with different burial depths in Figure 4.39. This figure indicates that the crown stress is the minimum for deeper flexible pipes. A jump occurred for reducing depth from 1500 mm to 600 mm. For other deeper burial depths, all graphs are almost similar in shape, although the stresses were less for deeper pipe. The graph is not similar for 300 mm burial depth of pipe. It shows increase of stress above the crown, indicating a different mechanism of load distribution for shallow buried flexible pipe.

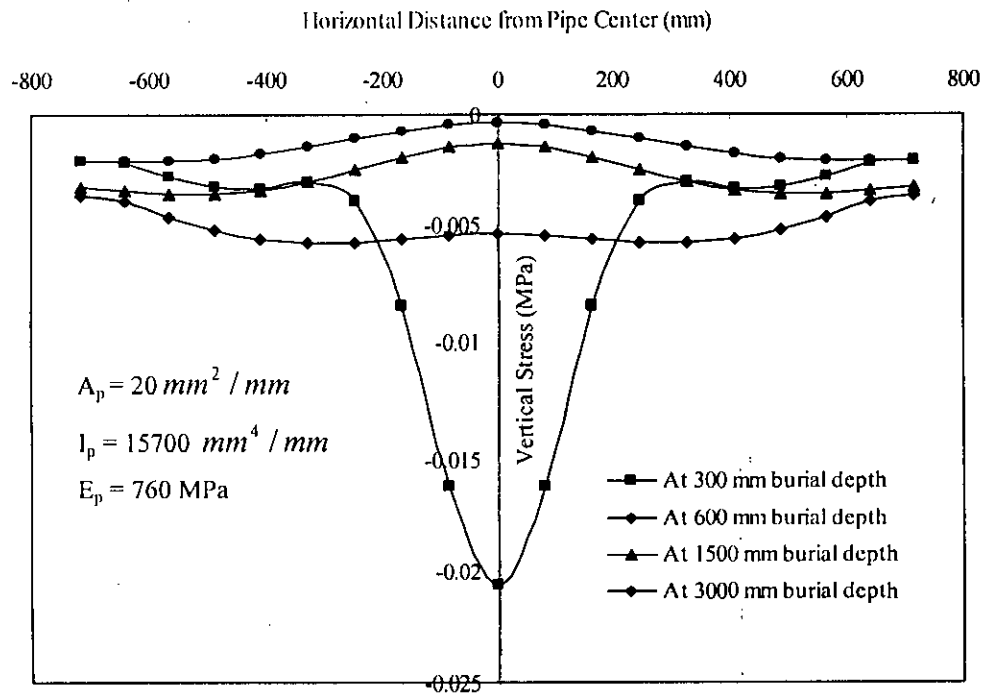


**Figure 4.39 Variation of Vertical Stress at 75 mm above Crown for Different Burial Depths**

Figure 4.40 depicts the soil stress developed underneath the pipe due to surface line load. Stress on a horizontal line 75 mm below pipe invert are plotted in the figure. The vertical soil stress is almost zero below the pipe invert in Figure 4.40 for each of the burial depths, which increase with the distance from the pipe invert. Thus, the vertical soil stress distribution is completely different for soil above and below pipe. At a level of 75 mm above pipe crown, maximum soil stress occurs directly above the pipe crown. At a distance from pipe center, ratio for vertical soil stress at invert level to that above crown is 0.18 for a burial depth of 300 mm. It indicates that vertical soil stress at the haunch location is a fraction of the crown stress. It is also clear from the graph that as the burial depth increases, difference between the vertical stress distributions tends to be negligible. All graphs are resembles to a one as the burial depth increases. Again, the curvature in distributing the vertical stress from the point below pipe invert is reduced as the burial depth increases whereas for 300 mm burial depth vertical stress distribution curve posses sharp curvature.

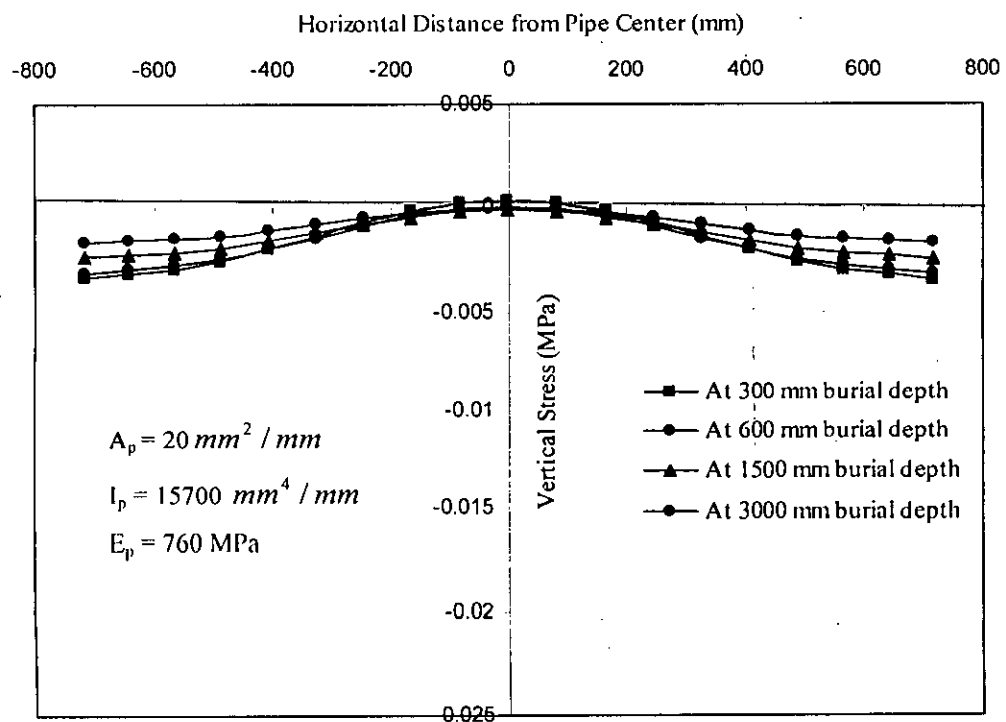


**Figure 4.40 Variation of Vertical Stress at 75 mm below Invert  
for Different burial Depths**

Figure 4.41 shows the lateral stresses developing on the sides of the pipe due to surface load. It reveals that the stress is concentrated above the springline level of the pipe, particularly for shallow burial depths. The point of the maximum stress is at the shoulder level. However, with the increase of burial depth the point of the maximum stress moves toward springline. The magnitude of the maximum stress is also reduced with the increase of burial depths, as expected. The concentration of the stress above the springline level indicate the effect of concentrated surface loads is localized in the upper part of the pipe for shallow buried pipe. The stress is distributed toward the lower part and the horizontal stress distribution become symmetric about springline for deeply buried pipe, indicating distribution of effects over the whole pipe. This observation confirms the findings with reference to thrust and bending moments (Figure 4.22 and Figure 4.24).

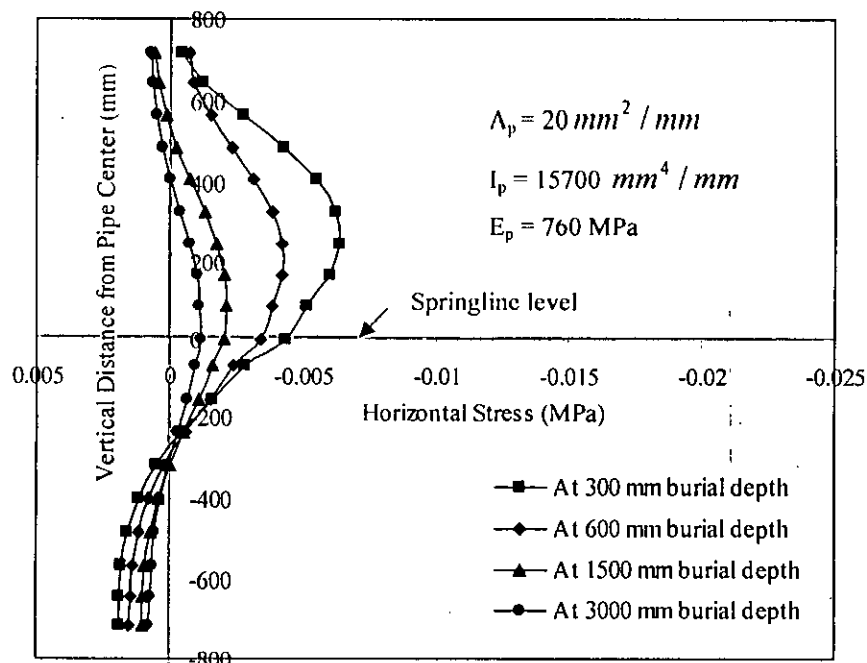


Figure 4.41 variation of Horizontal Stress at 75 mm from Springline for Different Burial Depth

## 4.7 COMPARISON WITH DESIGN CODES

As discussed earlier, the design codes estimate the live load as a uniformly distributed load calculated based on an assumed load spreading rate. Different load spreading rate was followed at different code. ASCE, AASHTO, CANADIAN etc. codes are available for comparison with the observed data. Almost all codes use the same load spreading rate (1.75 times the depth) for surface live load as discussed earlier. However, AASHTO recommended a lower load spreading rate (1.15 to 1 time depth).

AASHTO gives an averaged soil stress value throughout a horizontal level above the pipe. Figure 4.42 compare the pipe stress calculated above the crown with the values according AASHTO and ASCE codes for the pipe with 300 mm burial depth. AASHTO code with load spreading over 1.15 times the pipe depth and ASCE code with load spreading over 1.75 times the pipe depth is revealed in Figure 4.42. The stresses calculated using finite element analysis and Boussinesq's equation averaged (using trapezoidal rule) over the pipe crown are also shown in the figure. The comparison reveals that the stresses calculated using design codes are less than the maximum stress, however, much greater than the average of the stresses.

Figure 4.43 also depicts that soil experience more stress at the same level if the pipe has higher material modulus even in case of average values. For both thermoplastic and steel pipes, average soil stress is greater than the average Boussinesq's stresses. But this data are not comparable with the AASHTO. For a burial depth of 300 mm, AASHTO indicates the highest value among the curves and Boussinesq solution indicates the lowest values. All values are averaged for a soil stress at a level of 75 mm above the crown. All averaged values are somewhat closer to one other but the design codes indicate higher values. Thus, the design codes give more conservative values than that may occur actually.

Graphs are plotted as shown in Figure 4.43 for 600 mm burial depth of pipe. It is revealed that AAHTO gives the maximum soil stress whereas ASCE yields lowest value even for the deeper pipe. But difference between these soil stresses, for all these cases, is not as large as occurred in Figure 4.42. Here, AASHTO yields more reasonable value (close to the average calculated stress) than those in Figure 4.42.

Thus, for deeper pipe the design codes yields a better estimation of live load stresses over buried pipe.

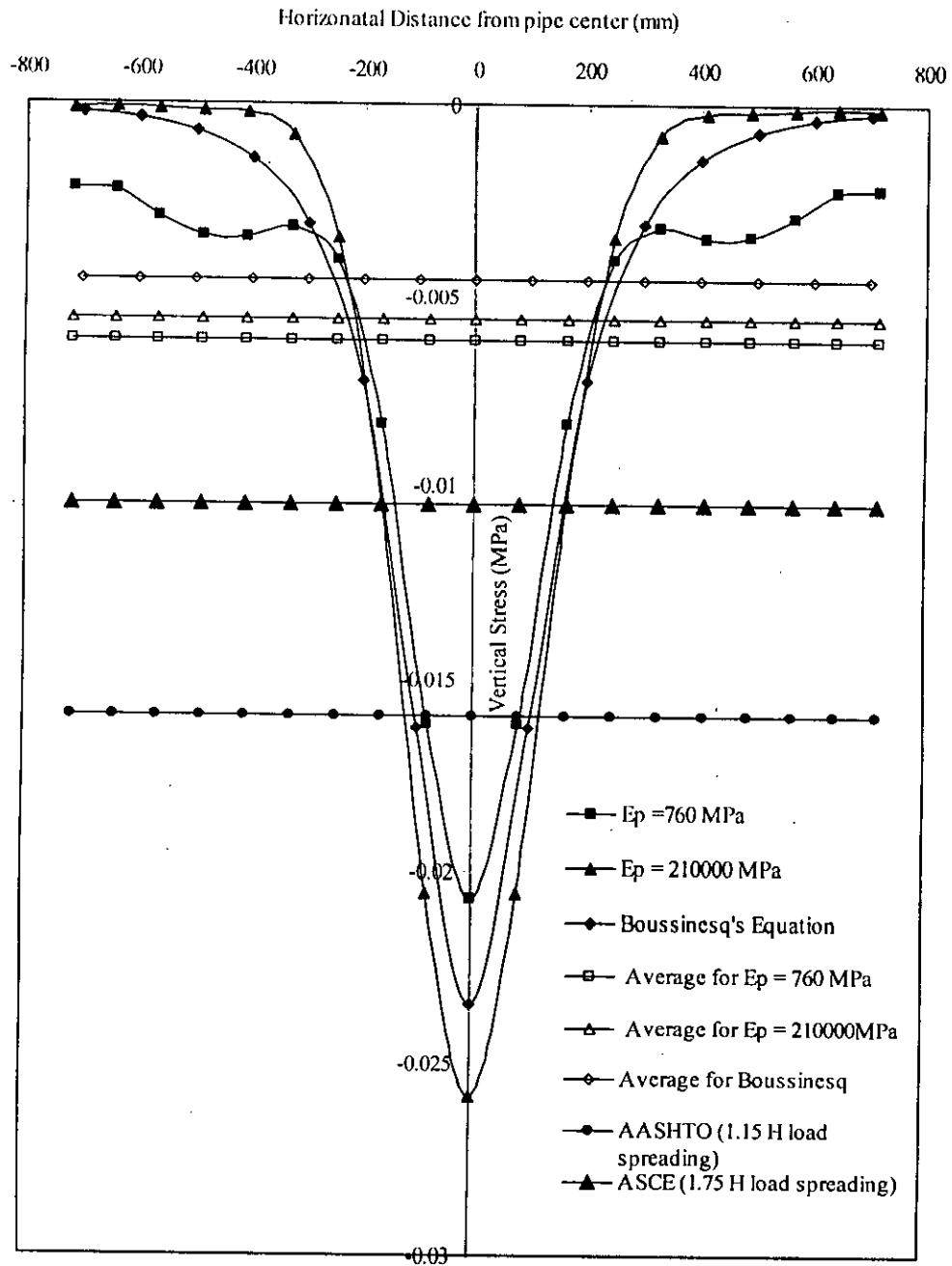


Figure 4.42 Comparison of Soil Stresses for Pipe with 300 mm Burial Depth at 75 mm above Crown

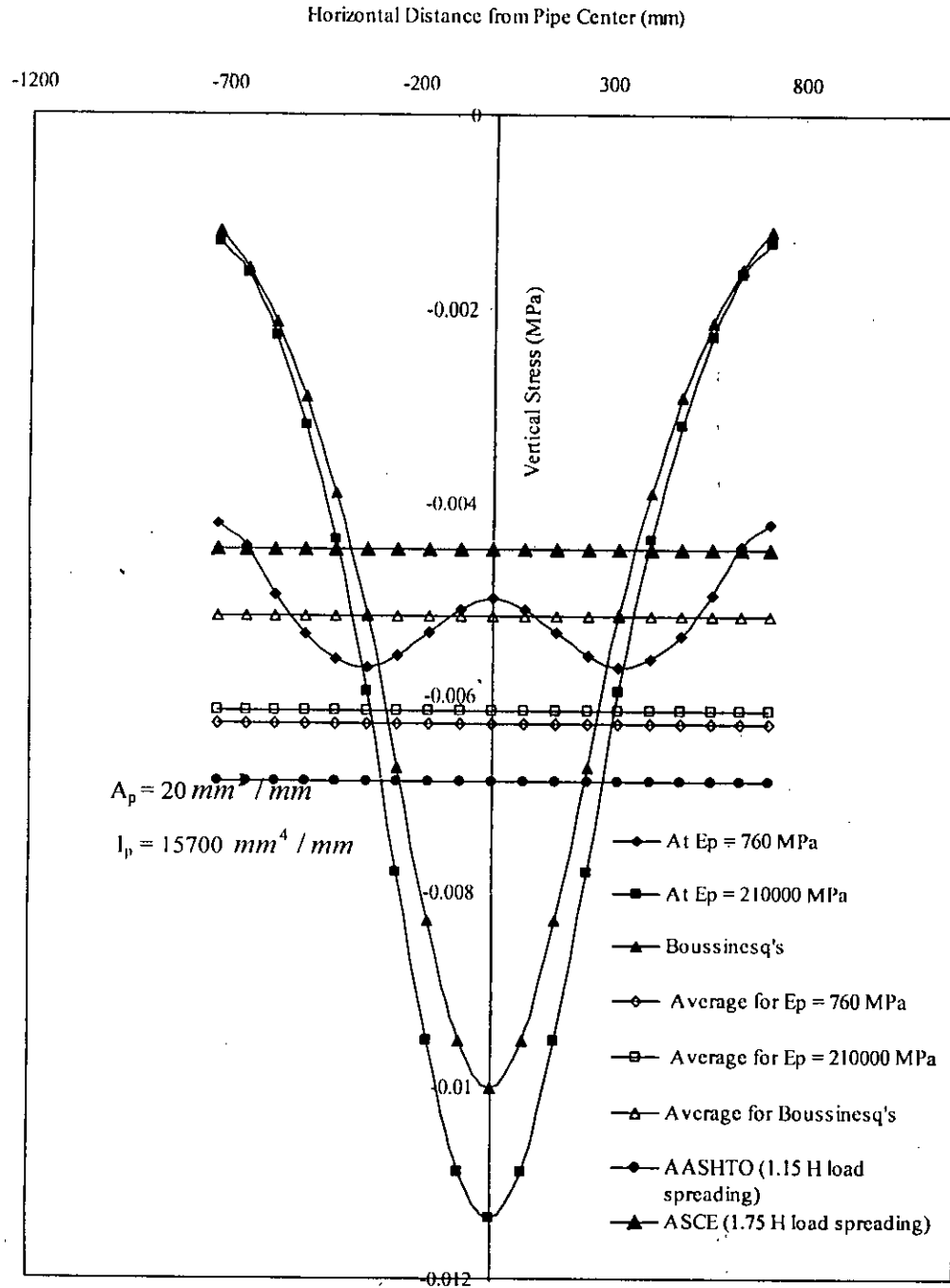


Figure 4.43 Comparison of Soil Stresses for Pipe with 600 mm Burial Depth



## CHAPTER 5

### CONCLUSIONS AND RECOMMENDATIONS

#### 5.1 INTRODUCTION

Use of flexible pipe is gaining popularity day by day due to its various advantages. Significant research concerning the soil-structure interaction phenomena has been conducted in recent years to develop a better understanding of the complex soil-pipe interaction. A large portion of the works focused on the soil-pipe interaction under earth load. Two-dimensional plain-strain analyses are generally used for modeling of the pipe-soil system. However, the surface load of finite dimension from vehicular traffic (i.e. wheel load) over the pipe makes the problem as three dimensional. The wheel loads are idealized as a concentrated load in AASHTO standard design code (AASHTO, 1996), while idealization as a distributed load over the area of tire footprint is used in AASHTO LRFD design code (AASHTO, 1998). The load is then assumed to produce a uniform pressure at the level of pipe crown, estimated based on a load spreading with depth. Researchers have analyzed the problems with buried pipes and culverts using two-dimensional idealization of the three dimensional loads (Fernando and Carter, 1998; Taleb and Moore, 1999; Jayawickrama et al., 2002; McGrath et al., 2002). Fernando and Carter (1998) analyzed solid uniform-wall buried pipes under surface patch loads using a three-dimensional semi-analytical finite element analysis. In this analysis, a two dimensional finite element mesh, similar to a plane strain model, was used to model the pipe-soil system. Fourier integral transform techniques were then used for an equivalent two-dimensional representation of the field quantities and loadings in longitudinal direction. In other analyses (Taleb and Moore, 1999; Jayawickrama et al., 2002; McGrath et al., 2002), the Boussinesq's solution for a vertical load at the surface of an elastic half-space was used to convert the three-dimensional loading to an equivalent two-dimensional load. The approach of conversion of the three-dimensional load into the equivalent two-dimensional load has been used in this research for investigation of the pipe-soil system under surface

concentrated load. A parametric study was carried out to assess the effects of various geometric and material parameters on the behavior of pipes under the surface load. Pipe deformations, internal forces (axial force and bending moment) and soil stresses are investigated using variations of those parameters. This chapter summarizes the findings of this research work. Thus, recommendations are also made for the future study for the better understanding of the behavior of flexible pipe under surface load.

## 5.2 FINDINGS FROM THE STUDY

Two-dimensional finite element analysis appeared as an effective tool for analysis of buried pipe under three-dimensional loading. The analysis successfully predicted the behavior of a pipe measured in full-scale test under concentrated surface load. The three-dimensional load was converted into equivalent line load through relation recommended in Jayawickrama et al (2002). After evaluation of the finite element model with full-scale test, study was conducted to investigate pipe behavior under different conditions. Mesh around the pipe vicinity was kept finer than the zone away from the pipe to capture the non linear stress field expected around the pipe. Particular attention was given in the parametric study for large diameter flexible pipe under different burial depth. Sectional area, sectional modulus and material modulus of pipe were also considered for the parametric study. The specific findings from this research are summarized as below:

- A two dimensional model developed taking soil-structure interaction into the consideration to analysis the flexible pipe under surface load can be used to calculate internal forces in plane of pipe section, which usually governs the pipe design. Two dimensional analyses successfully simulated the pipe response measured in full-scale tests under live load.
- Concentrated surface load above the pipe crown induces compressive thrust at the pipe shoulder, positive bending moment (Outward concave bending) at the crown and negative bending moment at the invert.

- Sectional parameter of pipe wall has significant effects on the live load distribution for buried flexible pipes. Although sectional area of pipe wall do not affect largely, moment of inertia of pipe wall affect the thrust and moments that develop around the pipe. The effects are very significant on the bending moment.
- Material modulus of pipe also affects the thrust and moment developing around the pipe circumference. However, the influence is small on thrusts, while the bending moment is significantly affected. Positive moments develop at the crown and invert and negative moment develops at the shoulder for pipes with high material modulli.
- For a particular pipe, the effects of the surface load reduced rapidly with the depths of soil cover up to a depth of half of the pipe diameter, beyond which the effect reduced steadily.
- The influences of surface loads are localized within a zone around the pipe crown for shallow buried pipes ( $<0.5D$ ) and for pipes with low material modulus. However, the influence extends downward covering the full pipe circumference for deeper pipes and pipes with high material modulus.
- Soil stresses that develop above the pipe crown, below invert and on the sides yields a better understanding of the of the stress distribution for flexible pipe. Mechanism of the stress distribution was different for shallow and deep burial condition for High-Density polyethylene pipe.
- Boussinesq solution always over-predicts the crown level stress for HDPE pipe. However for stiffer (steel) pipe, Boussinesq equation under predicts the stress for shallow burial condition and over predict for deep burial condition. These are due to development of arching from soil-pipe interaction. When the pipe is very flexible, arching in the soil causes redistribution of stress away from the pipe, resulting in less stress over pipe crown. Negative arching, on the other hand, may develop for stiffer pipe that cause attraction of load from the soil toward the pipe.

- AASHTO yields conservative value of soil stress for buried pipe for greater burial depth.

### 5.3 RECOMMENDATIONS FOR FUTURE STUDY

The overall behavior of large diameter buried flexible pipe under surface load was analyzed in this research based on two-dimensional idealization of the three dimensional load. The analysis was limited to linear elastic material parameters. Load directly on top of pipe crown that covered to worst case scenario was only considered. Future research in the area of surface load study may include the following:

- Investigation of the pipe under unsymmetric loading where load to be placed away from the pipe crown. Thus the effects of multiple wheels can be taken into consideration.
- A design chart can be developed for use in design codes based on more studies on pipe with deep and shallow burial depths. A wide range of pipe diameter and wall profile can be taken into consideration for a rigorous study.
- Simplified equation can be developed to incorporate live load effects for buried flexible pipe design.
- For gaining confidence in analysis of pipe, a physical model may be developed and experiments can be carried out to compare with the finite element result.
- Inelastic modeling of soil and pipe can be considered in future study to investigate effects of non-linear inelastic material behavior on the pipe response.

- Non-linear soil behavior like consolidation, creep etc. can be incorporated in soil-pipe interaction analysis to identify the effects of more realistic non-linear material behavior.
  
- Full-scale field tests are also recommended through measuring pipe strains, pipe deflection, soil stress and deformation to develop a better understanding about the field performance of the pipes.

## REFERENCES

AASHTO (1998) "LRFD Bridge Design Specifications", 2<sup>nd</sup> ed. AASHTO, Washington, D.C.

AASHTO (1996) "Standard Specifications for Highway Bridges", 16<sup>th</sup> ed. AASHTO, Washington, D.C.

ASCE (1993) "Standard Practice for Direct Design of Buried Precast Concrete Pipe Using Standard Installation (SIDD)", ASCE 15-93, New York.

Arockiasamy, M., O. Chaallal, and T. Limpeteepakarn. (2006) "Full-Scale Field Tests on Flexible Pipes under Live Load Application", Journal of Performance of Constructed Facilities, ASCE, Vol.20, No.1, 2006.

CAN/CSA (2001) Canadian Highway Bridge Design Code.

Burns, J.Q. and Richard, R.M. (1964) "Attenuation of Stresses for Buried Cylinder" Proceedings of Symposium on soil-structure interaction, University of Arizona, pp: 379-392

Cameron, A. D., (2006) "Analysis of Buried Flexible Pipes in Granular Backfill Subjected to Construction Traffic"

Dhar, A.S (2003) "The Development of a Simplified Equation for Deflection of Buried Pipe", ASCE, International Pipe line 2003 Conference, Baltimore, MD, USA. July 13-16, PP: 1096-1105.

Dhar,A.S (2002) "Limit States of Profiled Thermoplastic pipes under Deep Burial", Ph.D. Thesis, Department of Civil and Environmental Engineering, The University of Western Ontario, Canada.

Dhar, A.S. and Kabir, M.A. (2006) "A Simplified Soil-Structure Interaction Band Method for Calculating Deflection of Buried Pipe", Geotechnical Symposium in Roma, University of Roma, "La Sapienza". Italy, March 2006.

Dhar,A.S. and Moor,I.D. (2006) "Evaluation of Local Bending in Profile Wall Polyethylene pipe" Journal of Transportation Engineering, ASCE,Vol.132, No.11,PP.898-906

Dhar,A.S., Moor,I.D. and McGrath,T.J.(2004) "Thermoplastic Culvert Deformation and Strain Evaluation using Two Dimensional Analysis" Journal of Geotechnical and Geo-environmental Engineering, ASCE, Vol.130,No.2.PP-199-208.

Dhar, A.S., Siddique, M.S.A. and Sinha, A.N (2004) "Deflection of Polyvinyl Chloride Pipes in Clayey Backfill", Transportation Research Record.1892, Journal of the Transportation Research Board, pp.221-226.

Dhar, A.S., Moore,I.D. and McGrath, T. J. (2002) "Evaluation of Simplified Design Methods for Buried Thermoplastic Pipe" Proc.,Pipelines 2002 Conference. ASCE, Cleveland, Ohio, Aug.4-7, 2002.

Dhar, A.S. and Noor, M.A. (2007) "Simplified Soil-Structure Interaction Methods for Buried Pipe Design", Research Report, Committee for Advanced Studies and Research, Bangladesh University of Engineering and Technology, Dhaka, Bangladesh.

Fernando, N. S.M., and Carter, J. P. (1998) "Elastic Analysis of Buried Pipes under Surface Patch Loadings" Journal of Geotechnical and Geo-environmental Engineering, Vol.124, No.8, August.

Haggag, A.A. (1989) "Structural Backfill Design for Corrugated-Metal Buried Structures" Ph.D. dissertation, Amherst, University of Massachusetts.

Hall,W.J. and Newmark, N.M. (1977) "Seismic Design Criteria for Pipeline Facilities", In Proceedings of the Conference on the Current State of Knowledge of Lifeline Earthquake Engineering, ASCE, New York.

Heger, F.J., Liepins, A.A., and Selig, E.T. (1985) "SPIDA: An Analysis and Design System for Buried Concrete Pipe" Advances in Underground pipeline Engineering, Proceedings of ASCE, pp: 143-154

Hoeg, K. (1968) "Stress Against Underground Cylinder" Journal of soil Mechanics and Foundation Engineering, ASCE, Vol.94, SM4, 833-858

Jayawickrama, P.W., A.L. Amarasiri, and P.E.Regino (2002) "Minium Cover Requirements for Large-Diameter High-Density Polyethylene Pipe Installed with Granular Backfill" presented at 81<sup>st</sup> Annual meeting of the Transportation Research Board, Washington, D.C.

Katona, M.G., Smith, J.M., Odello, R.S., and Allgood, J.R. (1976) "CANDE- A Modern Approach for the Structure design and Analysis of Buried Culverts" Report No.FHWA-RD-77-5, Federal Highway Administration, Washington, D.C., October

Katona, M.G., Vittes, P.D., Lee, C.H., and Ho., H.T. (1981) "CANDE -1980:Box Culverts and Soil Models" Report No.FHWA/RD-80/172, Federal Highway Administration, Washington, D.C., May

McGrath, T.J. (1998) "Design Method for Flexible pipe. A Report to the AASHTO Flexible Culvert Liaison Committee." Simpson Gumpertz & Heger, Inc., Arlington, Mass.

McGrath, T.J., and Boyton, J. (2002) "Performance of Thermoplastic Culvert Pipe under Highway Vehicle Loading", 81<sup>st</sup> Transportation Research Board Annual meeting, Washington, D.C.

Molin, J. (1981) "Flexible Pipes Buried in Clay" Proc., International Conference on Underground Plastic Pipe (J. Schrock, ed.), ASCE, Reston, Va., pp.332-337.

Moore, I.D. (2000) "Culverts and Buried Pipelines" Chapter 18, Geotechnical and Geoenvironmental Handbook, Edited by R.K. Rowe, Kluwer publisher, pp: 541-568

Moore, I. D. (1993) "Structural Design of Profiled Polyethylene Pipe" Part 1 - Deep Burial. Research Report, University of Western Ontario, Geotechnical Research Centre, GEOT-8-93, March.

Moore, I.D., and Brachman, R.W.I. (1994) "Three Dimensional Analysis of flexible Circular Culverts" J. of Goetech. Engrg., ASCE, 120(10), 1829-1844.

Moser, A. P. (2001) "Buried Pipe Design" McGraw - Hill.

Musser, S.C. (1989) "CANDE -89 User Manual" Report No.FHWA-RD-89-169, Federal Highway Administration, Mclean, VA

Noor, M.A. and Dhar, A.S. (2003) " Three Dimensional Response of Buried pipe Under Vehicular Loads" proceedings of the ASCE International Conference on Pipeline Division of ASCE, Baltimore, Maryland.

PCA (1944) "Vertical Pressure on Culverts under Wheel Loads on Concrete Pavement Slabs"

Sargand,S.M. and Masada T. (2007) "Long-Term Monitoring of Pipe under Deep Cover" Final Report to Ohio Department of Transportation, Ohio, USA.

Selig, E.T. (1990) "Soil Properties for Plastic Pipe Installations" ASTM Special Technical Publication 1093, Buried Plastic Pipe Technology, W. Conshohocken, Pa, pp: 141-158



Spangler, M.G. (1941) "The Structural Design of Flexible Pipe Culverts" Bulletin 153. Iowa Engineering Experiment Station. Ames, Iowa.

Taleb, B., and I.D. Moore. (1999) "Metal Culvert Response to Earth Loading: Performance of Two-Dimensional Analysis" Transportation Research Record: Underground and Other Structural Design Issues 1656:25-36. Paper No: 99-0532

Watkins, R.K., and Spangler, M. G. (1958) "Some Characteristics of Modulus of Passive Resistance of Soil; A Study of Similitude" Proc., 37<sup>th</sup> Annual Meeting, Vol. 37, Highway Research Board, Washington, D.C., 576-583.

Westergaard, H. M., (1926) "Stresses in Concrete Pavements Computed by Theoretical Analysis"

Wong, L.S., Allouche, E.N. and Moore, I.D. (2002) "Long-term Monitoring and Analysis of Full Scale Concrete Pipe Test Beds" ASCE Pipeline 2002 Conference, Cleveland, OH, USA

# APPENDIX

## CODES USED IN THE ANALYSIS

\*\*\*\*\*

FOR BURIAL DEPTH = 300 mm

\*\*\*\*\*

\*HEADING

STRESS ANALYSIS FOR A BURIED PIPE

\*\*

\*\*

\*PREPRINT, ECHO=YES, HISTORY=YES, MODEL=YES

\*\*

\*RESTART, WRITE, FREQ=1

\*\*

\*\*

\*FILE FORMAT, ZERO INCREMENT

\*\*

\*\*\*\*\*

\*\* MESH GENERATION

\*\*\*\*\*

\*\* NODE DEFINITION

\*\*\*\*\*

\*\* Dimensions are in N,mm

\*\*\*\*\*

\*NODE

101, 0.0, 0.0

119, 750.0, 0.0

1919, 0.0, 750.0

123, 900.0, 0.0

127, 1200.0, 0.0

147, 4200.0, -1200.0

1023, 900.0, 900.0

1027, 1200.0, 1050.0

1047, 4200.0, 1050.0

1923, 0.0, 900.0

1927, 0.0, 1050.0

2823, -900.0, 900.0

2827, -1200.0, 1050.0

2847, -4200.0, 1050.0

3719, -750.0, 0.0

3723, -900.0, 0.0

3727, -1200.0, 0.0

4623, -900.0, -900.0

4627, -1200.0, -1200.0

4647, -4200.0, -4200.0  
5523, 0.0, -900.0  
5527, 0.0, -1200.0  
5519, 0.0, -750.0  
6423, 900.0, -900.0  
6427, 1200.0, -1200.0  
6447, 4200.0, -4200.0  
7219, 747.146, -65.3668  
7223, 900.0, -78.74  
7227, 1200.0, -104.9864  
7247, 4200.0, -1500.0

\*\*\*\*\*

**\*\*NODE GENERATION**

\*\*\*\*\*

\*NGEN, LINE=C, NSET=HOLE1  
119, 1919, 100, 101  
\*NGEN, LINE=C, NSET=HOLE2  
1919, 3719, 100, 101  
\*NGEN, LINE=C, NSET=HOLE3  
3719, 5519, 100, 101  
\*NGEN, LINE=C, NSET=HOLE4  
5519, 7219, 100, 101  
\*\*NGEN, LINE=C, NSET=HOLE5  
\*\*119, 7219, 7100, 101  
\*NGEN, NSET=OUTER1  
123, 1023, 100  
\*NGEN, NSET=OUTER1  
1023, 1923, 100  
\*NGEN, NSET=OUTER2  
1923, 2823, 100  
\*NGEN, NSET=OUTER2  
2823, 3723, 100  
\*NGEN, NSET=OUTER3  
3723, 4623, 100  
\*NGEN, NSET=OUTER3  
4623, 5523, 100  
\*NGEN, NSET=OUTER4  
5523, 6423, 100  
\*NGEN, NSET=OUTER4  
6423, 7223, 100  
\*NGEN, NSET=OUTER5  
123, 7223, 7100

\*\*\*\*\*

**\*\* NODE FILL**

\*\*\*\*\*

\*NFILL, NSET=PLATE1, BIAS=1  
HOLE1, OUTER1, 4, 1  
\*NFILL, NSET=PLATE2, BIAS=1  
HOLE2, OUTER2, 4, 1  
\*NFILL, NSET=PLATE3, BIAS=1  
HOLE3, OUTER3, 4, 1  
\*NFILL, NSET=PLATE4, BIAS=1  
HOLE4, OUTER4, 4, 1

\*\*\*\*\*

\*\* ELEMENT CONNECTIVITY DEFINITION

\*\*\*\*\*

\*ELEMENT, TYPE=CPE4  
19, 119, 120, 220, 219  
\*ELEMENT, TYPE=CPE4  
1819, 1919, 1920, 2020, 2019  
\*ELEMENT, TYPE=CPE4  
3619, 3719, 3720, 3820, 3819  
\*ELEMENT, TYPE=CPE4  
5419, 5519, 5520, 5620, 5619  
\*ELEMENT, TYPE=CPE4  
7119, 7219, 7220, 120, 119

\*\*\*\*\*

\*\*ELEMENT GENERATE

\*\*\*\*\*

\*ELGEN, ELSET=HAUNCH  
19, 4, 1, 1, 18, 100, 100  
\*ELGEN, ELSET=HAUNCH  
1819, 4, 1, 1, 18, 100, 100  
\*ELGEN, ELSET=HAUNCH  
3619, 4, 1, 1, 18, 100, 100  
\*ELGEN, ELSET=HAUNCH  
5419, 4, 1, 1, 17, 100, 100  
\*ELGEN, ELSET=HAUNCH  
7119, 4, 1, 1, 1, 7100, 100

\*\*\*\*\*

\*\* BEAM ELEMENT

\*\*\*\*\*

\*ELEMENT, TYPE=B21, ELSET=PIPE  
10001, 119, 219  
\*ELGEN, ELSET=PIPE  
10001, 71, 100, 1, 1  
\*ELEMENT, TYPE=B21, ELSET=PIPE  
10072, 7219, 119

\*\*\*\*\*

\*\*MIDDLE ZONE

\*\*\*\*\*

\*NGEN, NSET=OUTER  
127, 1027, 100  
\*NGEN, NSET=OUTER  
1027, 1927, 100  
\*NGEN, NSET=OUTER  
1927, 2827, 100  
\*NGEN, NSET=OUTER  
2827, 3727, 100  
\*NGEN, NSET=OUTER  
3727, 4627, 100  
\*NGEN, NSET=OUTER  
4627, 5527, 100  
\*NGEN, NSET=OUTER  
5527, 6427, 100  
\*NGEN, NSET=OUTER

```

6427, 7227, 100
*NSET, NSET=INNER, GENERATE
123, 7223, 100
*NFILL, NSET=SOILB, BIAS=1
INNER, OUTER, 4, 1
*****
**      ELEMENT CONNECTIVITY MIDDLE
*****
*ELEMENT, TYPE=CPE4
23, 123, 124, 224, 223
*ELGEN, ELSET=BACKS
23, 4, 1, 1, 71, 100, 100
*ELEMENT, TYPE=CPE4
7123, 7223, 7224, 124, 123
*ELGEN, ELSET=BACKS
7123, 4, 1, 1, 1, 7100, 100
*****
** OUTER NODE
*****
*NGEN, NSET=OUTER11
147, 1047, 100
*NGEN, NSET=OUTEROUT
2847, 4647, 100
*NGEN, NSET=OUTEROUT
4647, 6447, 100
*NGEN, NSET=OUTEROUT
6447, 7247, 100
**
*NSET, NSET=MIDDLE, GENERATE
2827, 7227, 100
*NFILL, NSET=SOILN, BIAS=1
MIDDLE, OUTEROUT, 20, 1
*NSET, NSET=MIDDLE11, GENERATE
127, 1027, 100
*NFILL, NSET=SOILN, BIAS=1
MIDDLE11, OUTER11, 20, 1
*****
**      ELEMENT CONNECTIVITY OUTER
*****
*ELEMENT, TYPE=CPE4
2727, 2827, 2828, 2928, 2927
*ELGEN, ELSET=NATIVS
2727, 20, 1, 1, 44, 100, 100
*ELEMENT, TYPE=CPE4
7127, 7227, 7228, 128, 127
*ELGEN, ELSET=NATIVS
7127, 20, 1, 1, 1, 7100, 100
*ELEMENT, TYPE=CPE4
27, 127, 128, 228, 227
*ELGEN, ELSET=NATIVS
27, 20, 1, 1, 9, 100, 100

```

```

*****
**      ELEMENT PROPERTIES
*****
*BEAM GENERAL SECTION, ELSET PIPE, SECTION GENERAL
20, 15700, 10000, 15700, 10000

760,300
*SOLID SECTION, MATERIAL=SOILB, ELSET=HAUNCH
*SOLID SECTION, MATERIAL=SOILB, ELSET=BACKS
*SOLID SECTION, MATERIAL=SOILN, ELSET=NATVLS
*****
**      MATERIAL PROPERTY DEFINITION
*****
*MATERIAL, NAME=SOILB
*ELASTIC
10, 0.25
*MATERIAL, NAME=SOILN
*ELASTIC
10, 0.25
*****
**      TIME INDEPENDENT BOUNDARY CONDITIONS
*****
*NSET, NSET=BOTTOM, GENERATE
4647, 6447, 100
*NSET, NSET=LEFT, GENERATE
2847, 4647, 100
*NSET, NSET=RIGHT, GENERATE
147, 1047, 100
*NSET, NSET=RIGHT, GENERATE
6447, 7247, 100
*****
**BOUNDARY CONDITION
*****
*BOUNDARY
RIGHT, YSYMM
LEFT, YSYMM
BOTTOM, PINNED
*****
** SPECIFIC OUTPUT REQUESTS
*****
*NSET, NSET=PIPNO, GENERATE
119, 7219, 100
*NSET, NSET=HOR1012.5, GENERATE
1024, 2824, 100
*NSET, NSET=HOR900, GENERATE
1023, 2823, 100
*NSET, NSET=HOR866, GENERATE
1022, 2822, 100
*NSET, NSET=HOR825, GENERATE
1021, 2821, 100
*ELSET, ELSET=VERT, GENERATE
1819, 1827, 1
*ELSET, ELSET=VERT, GENERATE

```

```

1719, 1727, 1
*ELSET, ELSET=HOR900, GENERATE
923, 2623, 100
*ELSET, ELSET=HOR825, GENERATE
921, 2621, 100
*****
** SURFACE LOADS
*****
*STEP
*STATIC
*CLOAD
1927, 2, -8.3
*****
** OUTPUT COMMANDS
*****
*NODE PRINT, NSET=PIPNO
COORD, U
*NODE PRINT, NSET=HOR825
COORD
*NODE PRINT, NSET=HOR866
COORD
*NODE PRINT, NSET=HOR900
COORD
*NODE PRINT, NSET=HOR1012.5
COORD
*EL PRINT, POSITION=AVERAGED AT NODES, ELSET=PIPE
SF
*EL PRINT, POSITION=AVERAGED AT NODES, ELSET=VERT
S, E
*EL PRINT, POSITION=AVERAGED AT NODES, ELSET=HOR825
S, E
*EL PRINT, POSITION=AVERAGED AT NODES, ELSET=HOR900
S, E
*END STEP

```

\*\*\*\*\*

FOR BURIAL DEPTH = 600 mm

\*\*\*\*\*

\*\*

\*HEADING  
STRESS ANALYSIS FOR A BURIED PIPE

\*\*

\*\*

\*PREPRINT, ECHO=YES, HISTORY=YES, MODEL=YES

\*\*

\*RESTART, WRITE, FREQ 1

\*\*

\*\*

\*FILE FORMAT, ZERO INCREMENT

\*\*

\*\*\*\*\*

\*\* MESH GENERATION

\*\*\*\*\*

\*\* NODE DEFINITION

\*\*\*\*\*

\*NODE

101, 0.0,	0.0
119, 750.0,	0.0
1919, 0.0,	750.0
123, 900.0,	0.0
127, 1200.0,	0.0
147, 4200.0,	-1200.0
1023, 900.0,	900.0
1027, 1200.0,	1350.0
1047, 4200.0,	1350.0
1923, 0.0,	900.0
1927, 0.0,	1350.0
2823, -900.0,	900.0
2827, -1200.0,	1350.0
2847, -4200.0,	1350.0
3719, -750.0,	0.0
3723, -900.0,	0.0
3727, -1200.0,	0.0
4623, -900.0,	-900.0
4627, -1200.0,	-1200.0
4647, -4200.0,	-4200.0
5523, 0.0,	-900.0
5527, 0.0,	-1200.0
5519, 0.0,	-750.0
6423, 900.0,	-900.0
6427, 1200.0,	-1200.0
6447, 4200.0,	-4200.0
7219, 747.146,	-65.3668
7223, 900.0,	-78.74
7227, 1200.0,	-104.9864
7247, 4200.0,	-1500.0



\*\*\*\*\*

\*\*NODE GENERATION

\*\*\*\*\*

\*NGEN, LINE=C, NSET=HOLE1  
119, 1919, 100, 101

\*NGEN, LINE=C, NSET=HOLE2  
1919, 3719, 100, 101

\*NGEN, LINE=C, NSET=HOLE3  
3719, 5519, 100, 101

\*NGEN, LINE=C, NSET=HOLE4  
5519, 7219, 100, 101

\*\*NGEN, LINE=C, NSET=HOLES  
\*\*119, 7219, 7100, 101

\*NGEN, NSET=OUTER1  
123, 1023, 100

\*NGEN, NSET=OUTER1  
1023, 1923, 100

\*NGEN, NSET=OUTER2  
1923, 2823, 100

\*NGEN, NSET=OUTER2  
2823, 3723, 100

\*NGEN, NSET=OUTER3  
3723, 4623, 100

\*NGEN, NSET=OUTER3  
4623, 5523, 100

\*NGEN, NSET=OUTER4  
5523, 6423, 100

\*NGEN, NSET=OUTER4  
6423, 7223, 100

\*NGEN, NSET=OUTER5  
123, 7223, 7100

\*\*\*\*\*

\*\* NODE FILL

\*\*\*\*\*

\*NFILL, NSET=PLATE1, BIAS=1  
HOLE1, OUTER1, 4, 1

\*NFILL, NSET=PLATE2, BIAS=1  
HOLE2, OUTER2, 4, 1

\*NFILL, NSET=PLATE3, BIAS=1  
HOLE3, OUTER3, 4, 1

\*NFILL, NSET=PLATE4, BIAS=1  
HOLE4, OUTER4, 4, 1

\*\*\*\*\*

\*\* ELEMENT CONNECTIVITY DEFINITION

\*\*\*\*\*

\*ELEMENT, TYPE=CPE4  
19, 119, 120, 220, 219

\*ELEMENT, TYPE=CPE4  
1819, 1919, 1920, 2020, 2019

\*ELEMENT, TYPE=CPE4  
3619, 3719, 3720, 3820, 3819

\*ELEMENT, TYPE=CPE4  
5419, 5519, 5520, 5620, 5619

\*ELEMENT, TYPE=CPE4

7119, 7219, 7220, 120, 119

\*\*\*\*\*

\*\*ELEMENT CONNECTIVITY

\*\*\*\*\*

\*ELGEN, ELSET=HAUNCH

19, 4, 1, 1, 18, 100, 100

\*ELGEN, ELSET=HAUNCH

1819, 4, 1, 1, 18, 100, 100

\*ELGEN, ELSET=HAUNCH

3619, 4, 1, 1, 18, 100, 100

\*ELGEN, ELSET=HAUNCH

5419, 4, 1, 1, 17, 100, 100

\*ELGEN, ELSET=HAUNCH

7119, 4, 1, 1, 1, 7100, 100

\*\*\*\*\*

\*\* BEAM ELEMENT

\*\*\*\*\*

\*ELEMENT, TYPE=B21, ELSET=PIPE

10001, 119, 219

\*ELGEN, ELSET=PIPE

10001, 71, 100, 1, 1

\*ELEMENT, TYPE=B21, ELSET=PIPE

10072, 7219, 119

\*\*\*\*\*

\*\* MIDDLE ZONE

\*\*\*\*\*

\*NGEN, NSET=OUTER

127, 1027, 100

\*NGEN, NSET=OUTER

1027, 1927, 100

\*NGEN, NSET=OUTER

1927, 2827, 100

\*NGEN, NSET=OUTER

2827, 3727, 100

\*NGEN, NSET=OUTER

3727, 4627, 100

\*NGEN, NSET=OUTER

4627, 5527, 100

\*NGEN, NSET=OUTER

5527, 6427, 100

\*NGEN, NSET=OUTER

6427, 7227, 100

\*NSET, NSET=INNER, GENERATE

123, 7223, 100

\*NFILL, NSET=SOILB, BIAS=1

INNER, OUTER, 4, 1

\*\*\*\*\*

\*\* ELEMENT CONNECTIVITY MIDDLE

\*\*\*\*\*

\*ELEMENT, TYPE=CPE4

23, 123, 124, 224, 223

\*ELGEN, ELSET=BACKS

23, 4, 1, 1, 71, 100, 100

\*ELEMENT, TYPE=CPE4  
7123, 7223, 7224, 124, 123  
\*ELGEN, ELSET=BACKS  
7123, 4, 1, 1, 1, 7100, 100  
\*\*\*\*\*

\*\* OUTER NODE  
\*\*\*\*\*

\*NGEN, NSET=OUTER11  
147, 1047, 100  
\*NGEN, NSET=OUTEROUT  
2847, 4647, 100  
\*NGEN, NSET=OUTEROUT  
4647, 6447, 100  
\*NGEN, NSET=OUTEROUT  
6447, 7247, 100  
\*NSET, NSET=MIDDLE, GENERATE  
2827, 7227, 100  
\*NFILL, NSET=SOILN, BIAS=1  
MIDDLE, OUTEROUT, 20, 1  
\*NSET, NSET=MIDDLE11, GENERATE  
127, 1027, 100  
\*NFILL, NSET=SOILN, BIAS=1  
MIDDLE11, OUTER11, 20, 1  
\*\*\*\*\*

\*\* ELEMENT CONNECTIVITY OUTER  
\*\*\*\*\*

\*ELEMENT, TYPE=CPE4  
2727, 2827, 2828, 2928, 2927  
\*ELGEN, ELSET=NATIVES  
2727, 20, 1, 1, 44, 100, 100  
\*ELEMENT, TYPE=CPE4  
7127, 7227, 7228, 128, 127  
\*ELGEN, ELSET=NATIVES  
7127, 20, 1, 1, 1, 7100, 100  
\*ELEMENT, TYPE=CPE4  
27, 127, 128, 228, 227  
\*ELGEN, ELSET=NATIVES  
27, 20, 1, 1, 9, 100, 100  
\*\*\*\*\*

\*\* ELEMENT PROPERTY  
\*\*\*\*\*

\*BEAM GENERAL SECTION, ELSET=PIPE, SECTION=GENERAL  
20, 15700, 10000, 15700, 10000  
  
760, 300  
\*SOLID SECTION, MATERIAL=SOILB, ELSET=HAUNCH  
\*SOLID SECTION, MATERIAL=SOILB, ELSET=BACKS  
\*SOLID SECTION, MATERIAL=SOILN, ELSET=NATIVES  
\*\*\*\*\*

\*\* MATERIAL PROPERTY DEFINITION  
\*\*\*\*\*

\*MATERIAL, NAME=SOILB

```

*ELASTIC
10, 0.25
*MATERIAL, NAME=SOILN
*ELASTIC
10, 0.25
*****
**      TIME INDEPENDENT BOUNDARY CONDITIONS
*****
*NSET, NSET=BOTTOM, GENERATE
4647, 6447, 100
*NSET, NSET=LEFT, GENERATE
2847, 4647, 100
*NSET, NSET=RIGHT, GENERATE
147, 1047, 100
*NSET, NSET=RIGHT, GENERATE
6447, 7247, 100

*****
**BOUNDARY CONDITION
*****
*BOUNDARY
RIGHT, YSYMM
LEFT, YSYMM
BOTTOM, PINNED
*****
** SPECIFIC OUTPUT REQUESTS
*****
*NSET, NSET=PIPNO, GENERATE
119, 7219, 100
*NSET, NSET=HOR1012.5, GENERATE
1024, 2824, 100
*NSET, NSET=HOR900, GENERATE
1023, 2823, 100
*NSET, NSET=HOR866, GENERATE
1022, 2822, 100
*NSET, NSET=HOR825, GENERATE
1021, 2821, 100
*ELSET, ELSET=VERT, GENERATE
1819, 1827, 1
*ELSET, ELSET=VERT, GENERATE
1719, 1727, 1
*ELSET, ELSET=HOR900, GENERATE
923, 2623, 100
*ELSET, ELSET=HOR825, GENERATE
921, 2621, 100
*****
**      SURFACE LOADS
*****
*STEP
*STATIC
*CLOAD
1927, 2, -8.3

```

```
*****
** OUTPUT COMMANDS
*****
*NODE PRINT, NSET=PIPNO
COORD, U
*NODE PRINT, NSET=HOR825
COORD
*NODE PRINT, NSET=HOR866
COORD
*NODE PRINT, NSET=HOR900
COORD
*NODE PRINT, NSET=HOR1012.5
COORD
*EL PRINT, POSITION=AVERAGED AT NODES, ELSET=PIPE
SF
*EL PRINT, POSITION=AVERAGED AT NODES, ELSET=VERT
S, E
*EL PRINT, POSITION=AVERAGED AT NODES, ELSET=HOR825
S, E
*EL PRINT, POSITION=AVERAGED AT NODES, ELSET=HOR900
S, E
*END STEP
```

\*\*\*\*\*

**FOR BURIAL DEPTH = 1500 mm**

\*\*\*\*\*

\*HEADING

STRESS ANALYSIS FOR A BURIED PIPE

\*\*

\*\*

\*PREPRINT, ECHO=YES, HISTORY=YES, MODEL=YES

\*\*

\*RESTART, WRITE, FREQ=1

\*\*

\*\*

\*FILE FORMAT, ZERO INCREMENT

\*\*

\*\*\*\*\*

\*\*

**MESH GENERATION**

\*\*\*\*\*

\*\*

**NODE DEFINITION**

\*\*\*\*\*

\*\* DIMENSIONS are in N, mm

\*\*\*\*\*

\*NODE

101, 0.0, 0.0  
119, 750.0, 0.0  
1919, 0.0, 750.0  
123, 900.0, 0.0  
127, 1200.0, 0.0  
147, 4200.0, -1200.0  
148, 4200.0, 1550.0  
152, 4200.0, 2250.0  
1023, 900.0, 900.0  
1027, 1200.0, 1350.0  
1047, 4200.0, 1350.0  
1923, 0.0, 900.0  
1927, 0.0, 1350.0  
2148, 1200.0, 1550.0  
2152, 1200.0, 2250.0  
2823, -900.0, 900.0  
2827, -1200.0, 1350.0  
2847, -4200.0, 1350.0  
3719, -750.0, 0.0  
3723, -900.0, 0.0  
3727, -1200.0, 0.0  
3948, -1200.0, 1550.0  
3952, -1200.0, 2250.0  
4623, -900.0, -900.0  
4627, -1200.0, -1200.0  
4647, -4200.0, -4200.0  
5523, 0.0, -900.0  
5527, 0.0, -1200.0  
5519, 0.0, -750.0

5948, -4200.0, 1550.0  
5952, -4200.0, 2250.0  
6423, 900.0, -900.0  
6427, 1200.0, -1200.0  
6447, 4200.0, -4200.0  
7219, 747.146, -65.3668  
7223, 900.0, -78.74  
7227, 1200.0, -104.9864  
7247, 4200.0, -1500.0

\*\*\*\*\*

\*\* NODE GENERATION

\*\*\*\*\*

\*NGEN, LINE=C, NSET=HOLE1  
119, 1919, 100, 101  
\*NGEN, LINE=C, NSET=HOLE2  
1919, 3719, 100, 101  
\*NGEN, LINE=C, NSET=HOLE3  
3719, 5519, 100, 101  
\*NGEN, LINE=C, NSET=HOLE4  
5519, 7219, 100, 101  
\*\*NGEN, LINE=C, NSET=HOLE5  
\*\*119, 7219, 7100, 101  
\*\*

\*NGEN, NSET=OUTER1  
123, 1023, 100  
\*NGEN, NSET=OUTER1  
1023, 1923, 100  
\*NGEN, NSET=OUTER2  
1923, 2823, 100  
\*NGEN, NSET=OUTER2  
2823, 3723, 100  
\*NGEN, NSET=OUTER3  
3723, 4623, 100  
\*NGEN, NSET=OUTER3  
4623, 5523, 100  
\*NGEN, NSET=OUTER4  
5523, 6423, 100  
\*NGEN, NSET=OUTER4  
6423, 7223, 100  
\*NGEN, NSET=OUTER5  
123, 7223, 7100

\*\*\*\*\*

\*\* NODE FILL

\*\*\*\*\*

\*NFILL, NSET=PLATE1, BIAS=1  
HOLE1, OUTER1, 4, 1  
\*NFILL, NSET=PLATE2, BIAS=1  
HOLE2, OUTER2, 4, 1  
\*NFILL, NSET=PLATE3, BIAS=1  
HOLE3, OUTER3, 4, 1  
\*NFILL, NSET=PLATE4, BIAS=1  
HOLE4, OUTER4, 4, 1

```

*****
**      ELEMENT CONNECTIVITY DEFINITION
*****
*ELEMENT, TYPE=CPE4
19, 119, 120, 220, 219
*ELEMENT, TYPE=CPE4
1819, 1919, 1920, 2020, 2019
*ELEMENT, TYPE=CPE4
3619, 3719, 3720, 3820, 3819
*ELEMENT, TYPE=CPE4
5419, 5519, 5520, 5620, 5619
*ELEMENT, TYPE=CPE4
7119, 7219, 7220, 120, 119
*****
**ELEMENT GENERATE
*****
*ELGEN, ELSET=HAUNCH
19, 4, 1, 1, 18, 100, 100
*ELGEN, ELSET=HAUNCH
1819, 4, 1, 1, 18, 100, 100
*ELGEN, ELSET=HAUNCH
3619, 4, 1, 1, 18, 100, 100
*ELGEN, ELSET=HAUNCH
5419, 4, 1, 1, 17, 100, 100
*ELGEN, ELSET=HAUNCH
7119, 4, 1, 1, 1, 7100, 100
*****
** BEAM ELEMENT
*****
*ELEMENT, TYPE=B21, ELSET=PIPE
10001, 119, 219
*ELGEN, ELSET=PIPE
10001, 71, 100, 1, 1
*ELEMENT, TYPE=B21, ELSET=PIPE
10072, 7219, 119
*****
** MIDDLE ZONE
*****
*NGEN, NSET=OUTER
127, 1027, 100
*NGEN, NSET=OUTER
1027, 1927, 100
*NGEN, NSET=OUTER
1927, 2827, 100
*NGEN, NSET=OUTER
2827, 3727, 100
*NGEN, NSET=OUTER
3727, 4627, 100
*NGEN, NSET=OUTER
4627, 5527, 100
*NGEN, NSET=OUTER
5527, 6427, 100
*NGEN, NSET=OUTER

```



```

6427, 7227, 100
**
*NSET, NSET=INNER, GENERATE
123, 7223, 100
*NFILL, NSET=SOILB, BIAS=1
INNER, OUTER, 4, 1
*****
**      ELEMENT CONNECTIVITY MIDDLE
*****
*ELEMENT, TYPE=CPE4
23, 123, 124, 224, 223
*ELGEN, ELSET=BACKS
23, 4, 1, 1, 71, 100, 100
*ELEMENT, TYPE=CPE4
7123, 7223, 7224, 124, 123
*ELGEN, ELSET=BACKS
7123, 4, 1, 1, 1, 7100, 100
*****
** OUTER NODE
*****
*NGEN, NSET=OUTER11
147, 1047, 100
*NGEN, NSET=OUTEROUT
2847, 4647, 100
*NGEN, NSET=OUTEROUT
4647, 6447, 100
*NGEN, NSET=OUTEROUT
6447, 7247, 100
**
*NSET, NSET=MIDDLE, GENERATE
2827, 7227, 100
*NFILL, NSET=SOILN, BIAS=1
MIDDLE, OUTEROUT, 20, 1
*NSET, NSET=MIDDLE11, GENERATE
127, 1027, 100
*NFILL, NSET=SOILN, BIAS=1
MIDDLE11, OUTER11, 20, 1
*****
**      ELEMENT CONNECTIVITY OUTER
*****
*ELEMENT, TYPE=CPE4
2727, 2827, 2828, 2928, 2927
*ELGEN, ELSET=NATIVS
2727, 20, 1, 1, 44, 100, 100
*ELEMENT, TYPE=CPE4
7127, 7227, 7228, 128, 127
*ELGEN, ELSET=NATIVS
7127, 20, 1, 1, 1, 7100, 100
*ELEMENT, TYPE=CPE4
27, 127, 128, 228, 227
*ELGEN, ELSET=NATIVS
27, 20, 1, 1, 9, 100, 100

```

```

*****
**      OUTER OUTER
*****
*NSET, NSET=OUTERROUTER2, GENERATE
1027, 1047, 1
*NSET, NSET=OUTERROUTER5, GENERATE
1027, 2827, 100
*NSET, NSET=OUTERROUTER8, GENERATE
2827, 2847, 1
*NGEN, NSET=OUTERROUTER3
148, 2148, 100
*NGEN, NSET=OUTERROUTER6
2148, 3948, 100
*NGEN, NSET=OUTERROUTER9
3948, 5948, 100
*NGEN, NSET=OUTERROUTER4
152, 2152, 100
*NGEN, NSET=OUTERROUTER7
2152, 3952, 100
*NGEN, NSET=OUTERROUTER10
3952, 5952, 100
*****
**NODE FILL
*****
*NFILL, NSET=SOILN, BIAS=1
OUTERROUTER3, OUTERROUTER4, 4, 1
*NFILL, NSET=SOILB, BIAS=1
OUTERROUTER6, OUTERROUTER7, 4, 1
*NFILL, NSET=SOILN, BIAS=1
OUTERROUTER9, OUTERROUTER10, 4, 1
*****
**      ELEMENT CONNECTIVITY OUTERROUTER
*****
*ELEMENT, TYPE=CPE4
200000,148, 149, 249, 248
*ELGEN, ELSET=NATIVS
200000, 4, 1, 1, 20, 100, 100
*ELEMENT, TYPE=CPE4
220000, 2148, 2149, 2249, 2248
*ELGEN, ELSET=BACKS
220000, 4, 1, 1, 18, 100, 100
*ELEMENT, TYPE=CPE4
230000, 3948, 3949, 4049, 4048
*ELGEN, ELSET=NATIVS
230000, 4, 1, 1, 20, 100, 100
*ELEMENT, TYPE=CPE4
2000000, 2148, 2248, 1127, 1027
*ELGEN, ELSET=BACKS
2000000, 1, 1, 1121, 18, 100, 100
**
**
*ELEMENT, TYPE=CPE4, ELSET=NATIVS
2100000,148, 248, 1046, 1047
*ELEMENT, TYPE=CPE4, ELSET=NATIVS

```

2100001,248, 348, 1045, 1046  
\*ELEMENT, TYPE=CPE4, ELSET=NATIVS  
2100002,348, 448, 1044, 1045  
\*ELEMENT, TYPE=CPE4, ELSET=NATIVS  
2100003,448, 548, 1043, 1044  
\*ELEMENT, TYPE=CPE4, ELSET=NATIVS  
2100004,548, 648, 1042, 1043  
\*ELEMENT, TYPE=CPE4, ELSET=NATIVS  
2100005,648, 748, 1041, 1042  
\*ELEMENT, TYPE=CPE4, ELSET=NATIVS  
2100006,748, 848, 1040, 1041  
\*ELEMENT, TYPE=CPE4, ELSET=NATIVS  
2100007,848, 948, 1039, 1040  
\*ELEMENT, TYPE=CPE4, ELSET=NATIVS  
2100008,948, 1048, 1038, 1039  
\*ELEMENT, TYPE=CPE4, ELSET=NATIVS  
2100009, 1048, 1148, 1037, 1038  
\*ELEMENT, TYPE=CPE4, ELSET=NATIVS  
2100010, 1148, 1248, 1036, 1037  
\*ELEMENT, TYPE=CPE4, ELSET=NATIVS  
2100011, 1248, 1348, 1035, 1036  
\*ELEMENT, TYPE=CPE4, ELSET=NATIVS  
2100012, 1348, 1448, 1034, 1035  
\*ELEMENT, TYPE=CPE4, ELSET=NATIVS  
2100013, 1448, 1548, 1033, 1034  
\*ELEMENT, TYPE=CPE4, ELSET=NATIVS  
2100014, 1548, 1648, 1032, 1033  
\*ELEMENT, TYPE=CPE4, ELSET=NATIVS  
2100015, 1648, 1748, 1031, 1032  
\*ELEMENT, TYPE=CPE4, ELSET=NATIVS  
2100016, 1748, 1848, 1030, 1031  
\*ELEMENT, TYPE=CPE4, ELSET=NATIVS  
2100017, 1848, 1948, 1029, 1030  
\*ELEMENT, TYPE=CPE4, ELSET=NATIVS  
2100018, 1948, 2048, 1028, 1029  
\*ELEMENT, TYPE=CPE4, ELSET=NATIVS  
2100019, 2048, 2148, 1027, 1028  
\*\*  
\*\*  
\*ELEMENT, TYPE=CPE4, ELSET=NATIVS  
2100040, 3948, 4048, 2828, 2827  
\*ELEMENT, TYPE=CPE4, ELSET=NATIVS  
2100021, 4048, 4148, 2829, 2828  
\*ELEMENT, TYPE=CPE4, ELSET=NATIVS  
2100022, 4148, 4248, 2830, 2829  
\*ELEMENT, TYPE=CPE4, ELSET=NATIVS  
2100023, 4248, 4348, 2831, 2830  
\*ELEMENT, TYPE=CPE4, ELSET=NATIVS  
2100024, 4348, 4448, 2832, 2831  
\*ELEMENT, TYPE=CPE4, ELSET=NATIVS  
2100025, 4448, 4548, 2833, 2832  
\*ELEMENT, TYPE=CPE4, ELSET=NATIVS  
2100026, 4548, 4648, 2834, 2833  
\*ELEMENT, TYPE=CPE4, ELSET=NATIVS  
2100027, 4648, 4748, 2835, 2834  
\*ELEMENT, TYPE=CPE4, ELSET=NATIVS

21000028, 4748, 4848, 2836, 2835  
\*ELEMENT, TYPE=CPE4, ELSET=NATIVS  
21000029, 4848, 4948, 2837, 2836  
\*ELEMENT, TYPE=CPE4, ELSET=NATIVS  
21000030, 4948, 5048, 2838, 2837  
\*ELEMENT, TYPE=CPE4, ELSET=NATIVS  
21000031, 5048, 5148, 2839, 2838  
\*ELEMENT, TYPE=CPE4, ELSET=NATIVS  
21000032, 5148, 5248, 2840, 2839  
\*ELEMENT, TYPE=CPE4, ELSET=NATIVS  
21000033, 5248, 5348, 2841, 2840  
\*ELEMENT, TYPE=CPE4, ELSET=NATIVS  
21000034, 5348, 5448, 2842, 2841  
\*ELEMENT, TYPE=CPE4, ELSET=NATIVS  
21000035, 5448, 5548, 2843, 2842  
\*ELEMENT, TYPE=CPE4, ELSET=NATIVS  
21000036, 5548, 5648, 2844, 2843  
\*ELEMENT, TYPE=CPE4, ELSET=NATIVS  
21000037, 5648, 5748, 2845, 2844  
\*ELEMENT, TYPE=CPE4, ELSET=NATIVS  
21000038, 5748, 5848, 2846, 2845  
\*ELEMENT, TYPE=CPE4, ELSET=NATIVS  
21000039, 5848, 5948, 2847, 2846  
\*\*\*\*\*

\*\* BEAM PROPERTIES

\*\*\*\*\*  
\*BEAM GENERAL SECTION, ELSET=PIPE, SECTION=GENERAL  
20, 15700, 10000, 15700, 10000

760.300  
\*SOLID SECTION, MATERIAL=SOILB, ELSET=HAUNCH  
\*SOLID SECTION, MATERIAL=SOILB, ELSET=BACKS  
\*SOLID SECTION, MATERIAL=SOILN, ELSET=NATIVS  
\*\*\*\*\*

\*\* MATERIAL PROPERTY DEFINITION

\*\*\*\*\*  
\*MATERIAL, NAME=SOILB  
\*ELASTIC  
10, 0.25  
\*MATERIAL, NAME=SOILN  
\*ELASTIC  
10, 0.25  
\*\*\*\*\*

\*\* TIME INDEPENDENT BOUNDARY CONDITIONS

\*\*\*\*\*  
\*NSET, NSET=BOTTOM, GENERATE  
4647, 6447, 100  
\*NSET, NSET=LEFT, GENERATE  
2847, 4647, 100  
\*NSET, NSET=RIGHT, GENERATE  
147, 1047, 100  
\*NSET, NSET=RIGHT, GENERATE  
6447, 7247, 100

```

*****
**BOUNDARY CONDITION
*****
*BOUNDARY
RIGHT, YSYMM
LEFT, YSYMM
BOTTOM, PINNED
*****
** SPECIFIC OUTPUT REQUESTS
*****
*NSET, NSET=PIPNO, GENERATE
119, 7219, 100
*NSET, NSET=HOR1012.5, GENERATE
1024, 2824, 100
*NSET, NSET=VERT, GENERATE
3048, 3052, 1
*NSET, NSET=HOR900, GENERATE
1023, 2823, 100
*NSET, NSET=HOR866, GENERATE
1022, 2822, 100
*NSET, NSET=HOR825, GENERATE
1021, 2821, 100
*ELSET, ELSET=VERT, GENERATE
1819, 1827, 1
*ELSET, ELSET=VERT, GENERATE
1719, 1727, 1
*ELSET, ELSET=VERT, GENERATE
220800, 220803, 1
*ELSET, ELSET=VERT, GENERATE
220900, 220903, 1
*ELSET, ELSET=VERT, GENERATE
2000800, 2000900, 100
*ELSET, ELSET=HOR900, GENERATE
923, 2623, 100
*ELSET, ELSET=HOR825, GENERATE
921, 2621, 100
*****
** SURFACE LOADS
*****
*STEP
*STATIC
*CLOAD
3052, 2, -8.3
*****
** OUTPUT COMMANDS
*****
*NODE PRINT, NSET=PIPNO
COORD, U
*NODE PRINT, NSET=VERT
COORD
*NODE PRINT, NSET=HOR825
COORD
*NODE PRINT, NSET=HOR866

```

```
COORD
*NODE PRINT, NSET=HOR900
COORD
*NODE PRINT, NSET=HOR1012.5
COORD
*EL PRINT, POSITION=AVERAGED AT NODES, ELSET=PIPE
SF
*EL PRINT, POSITION=AVERAGED AT NODES, ELSET=VERT
S, E
*EL PRINT, POSITION=AVERAGED AT NODES, ELSET=HOR825
S, E
*EL PRINT, POSITION=AVERAGED AT NODES, ELSET=HOR900
S, E
*END STEP
```

\*\*\*\*\*

FOR BURIAL DEPTH = 3000 mm

\*\*\*\*\*

\*HEADING  
STRESS ANALYSIS FOR A BURIED PIPE

\*\*  
\*\*

\*PREPRINT, ECHO=YES, HISTORY=YES, MODEL=YES

\*\*  
\*\*

\*RESTART, WRITE, FREQ=1

\*\*  
\*\*

\*FILE FORMAT, ZERO INCREMENT

\*\*  
\*\*

\*\*\*\*\*

\*\* MESH GENERATION

\*\*\*\*\*

\*\* NODE DEFINITION

\*\*\*\*\*

\*\* DIMENSIONS are in N,mm

\*\*\*\*\*

\*NODE

- 101, 0.0, 0.0
- 119, 750.0, 0.0
- 1919, 0.0, 750.0
- 123, 900.0, 0.0
- 127, 1200.0, 0.0
- 147, 4200.0, -1200.0
- 148, 4200.0, 1550.0
- 157, 4200.0, 3750.0
- 1023, 900.0, 900.0
- 1027, 1200.0, 1350.0
- 1047, 4200.0, 1350.0
- 1923, 0.0, 900.0
- 1927, 0.0, 1350.0
- 2148, 1200.0, 1550.0
- 2157, 1200.0, 3750.0
- 2823, -900.0, 900.0
- 2827, -1200.0, 1350.0
- 2847, -4200.0, 1350.0
- 3719, -750.0, 0.0
- 3723, -900.0, 0.0
- 3727, -1200.0, 0.0
- 3948, -1200.0, 1550.0
- 3957, -1200.0, 3750.0
- 4623, -900.0, -900.0
- 4627, -1200.0, -1200.0
- 4647, -4200.0, -4200.0
- 5523, 0.0, -900.0
- 5527, 0.0, -1200.0
- 5519, 0.0, -750.0

5948, -4200.0, 1550.0  
5957, -4200.0, 3750.0  
6423, 900.0, -900.0  
6427, 1200.0, -1200.0  
6447, 4200.0, -4200.0  
7219, 747.146, -65.3668  
7223, 900.0, -78.74  
7227, 1200.0, -104.9864  
7247, 4200.0, -1500.0

\*\*\*\*\*

\*\*NODE GENERATE

\*\*\*\*\*

\*NGEN, LINE=C, NSET=HOLE1  
119, 1919, 100, 101  
\*NGEN, LINE=C, NSET=HOLE2  
1919, 3719, 100, 101  
\*NGEN, LINE=C, NSET=HOLE3  
3719, 5519, 100, 101  
\*NGEN, LINE=C, NSET=HOLE4  
5519, 7219, 100, 101  
\*\*NGEN, LINE=C, NSET=HOLES  
\*\*119, 7219, 7100, 101  
\*\*

\*\*  
\*NGEN, NSET=OUTER1  
123, 1023, 100  
\*NGEN, NSET=OUTER1  
1023, 1923, 100  
\*NGEN, NSET=OUTER2  
1923, 2823, 100  
\*NGEN, NSET=OUTER2  
2823, 3723, 100  
\*NGEN, NSET=OUTER3  
3723, 4623, 100  
\*NGEN, NSET=OUTER3  
4623, 5523, 100  
\*NGEN, NSET=OUTER4  
5523, 6423, 100  
\*NGEN, NSET=OUTER4  
6423, 7223, 100  
\*NGEN, NSET=OUTER5  
123, 7223, 7100

\*\*\*\*\*

\*\*NODE FILL

\*\*\*\*\*

\*NFILL, NSET=PLATE1, BIAS=1  
HOLE1, OUTER1, 4, 1  
\*NFILL, NSET=PLATE2, BIAS=1  
HOLE2, OUTER2, 4, 1  
\*NFILL, NSET=PLATE3, BIAS=1  
HOLE3, OUTER3, 4, 1  
\*NFILL, NSET=PLATE4, BIAS=1  
HOLE4, OUTER4, 4, 1



\*\*\*\*\*

\*\* ELEMENT CONNECTIVITY DEFINITION

\*\*\*\*\*

\*ELEMENT, TYPE=CPE4

19, 119, 120, 220, 219

\*ELEMENT, TYPE=CPE4

1819, 1919, 1920, 2020, 2019

\*ELEMENT, TYPE=CPE4

3619, 3719, 3720, 3820, 3819

\*ELEMENT, TYPE=CPE4

5419, 5519, 5520, 5620, 5619

\*ELEMENT, TYPE=CPE4

7119, 7219, 7220, 120, 119

\*\*

\*\*

\*ELGEN, ELSET=HAUNCH

19, 4, 1, 1, 18, 100, 100

\*ELGEN, ELSET=HAUNCH

1819, 4, 1, 1, 18, 100, 100

\*ELGEN, ELSET=HAUNCH

3619, 4, 1, 1, 18, 100, 100

\*ELGEN, ELSET=HAUNCH

5419, 4, 1, 1, 17, 100, 100

\*ELGEN, ELSET=HAUNCH

7119, 4, 1, 1, 1, 7100, 100

\*\*

\*\*

\*ELEMENT, TYPE=B21, ELSET=PIPE

10001, 119, 219

\*ELGEN, ELSET=PIPE

10001, 71, 100, 1, 1

\*ELEMENT, TYPE=B21, ELSET=PIPE

10072, 7219, 119

\*\*\*\*\*

\*\* MIDDLE ZONE

\*\*\*\*\*

\*NGEN, NSET=OUTER

127, 1027, 100

\*NGEN, NSET=OUTER

1027, 1927, 100

\*NGEN, NSET=OUTER

1927, 2827, 100

\*NGEN, NSET=OUTER

2827, 3727, 100

\*NGEN, NSET=OUTER

3727, 4627, 100

\*NGEN, NSET=OUTER

4627, 5527, 100

\*NGEN, NSET=OUTER

5527, 6427, 100

\*NGEN, NSET=OUTER

6427, 7227, 100

\*\*

\*NSET, NSET=INNER, GENERATE

123, 7223, 100

0

11

```

*NFILL, NSET=SOILB, BIAS=1
INNER, OUTER, 4, 1
*****
**   ELEMENT CONNECTIVITY MIDDLE
*****
*ELEMENT, TYPE=CPE4
23, 123, 124, 224, 223
*ELGEN, ELSET=BACKS
23, 4, 1, 1, 71, 100, 100
*ELEMENT, TYPE=CPE4
7123, 7223, 7224, 124, 123
*ELGEN, ELSET=BACKS
7123, 4, 1, 1, 1, 7100, 100
*****
**   OUTER NODE
*****
*NGEN, NSET=OUTER11
147, 1047, 100
*NGEN, NSET=OUTEROUT
2847, 4647, 100
*NGEN, NSET=OUTEROUT
4647, 6447, 100
*NGEN, NSET=OUTEROUT
6447, 7247, 100
**
*NSET, NSET=MIDDLE, GENERATE
2827, 7227, 100
*NFILL, NSET=SOILN, BIAS=1
MIDDLE, OUTEROUT, 20, 1
*NSET, NSET=MIDDLE11, GENERATE
127, 1027, 100
*NFILL, NSET=SOILN, BIAS=1
MIDDLE11, OUTER11, 20, 1
*****
**   ELEMENT CONNECTIVITY OUTER
*****
*ELEMENT, TYPE=CPE4
2727, 2827, 2828, 2928, 2927
*ELGEN, ELSET=NATVS
2727, 20, 1, 1, 44, 100, 100
*ELEMENT, TYPE=CPE4
7127, 7227, 7228, 128, 127
*ELGEN, ELSET=NATVS
7127, 20, 1, 1, 1, 7100, 100
*ELEMENT, TYPE=CPE4
27, 127, 128, 228, 227
*ELGEN, ELSET=NATVS
27, 20, 1, 1, 9, 100, 100
*****
**   OUTER OUTER
*****
*NSET, NSET=OUTEROUTER2, GENERATE
1027, 1047, 1

```

```

*NSET, NSET=OUTERROUTER5, GENERATE
1027, 2827, 100
*NSET, NSET=OUTERROUTER8, GENERATE
2827, 2847, 1
*NGEN, NSET=OUTERROUTER3
148, 2148, 100
*NGEN, NSET=OUTERROUTER6
2148, 3948, 100
*NGEN, NSET=OUTERROUTER9
3948, 5948, 100
*NGEN, NSET=OUTERROUTER4
157, 2157, 100
*NGEN, NSET=OUTERROUTER7
2157, 3957, 100
*NGEN, NSET=OUTERROUTER10
3957, 5957, 100
**
**
*NFILL, NSET=SOILN, BIAS=1
OUTERROUTER3, OUTERROUTER4, 9, 1
*NFILL, NSET=SOILB, BIAS=1
OUTERROUTER6, OUTERROUTER7, 9, 1
*NFILL, NSET=SOILN, BIAS=1
OUTERROUTER9, OUTERROUTER10, 9, 1
*****
**      ELEMENT CONNECTIVITY OUTERROUTER
*****
*ELEMENT, TYPE=CPE4
200000, 148, 149, 249, 248
*ELGEN, ELSET=NATV5
200000, 9, 1, 1, 20, 100, 100
*ELEMENT, TYPE=CPE4
220000, 2148, 2149, 2249, 2248
*ELGEN, ELSET=BACKS
220000, 9, 1, 1, 18, 100, 100
*ELEMENT, TYPE=CPE4
230000, 3948, 3949, 4049, 4048
*ELGEN, ELSET=NATV5
230000, 9, 1, 1, 20, 100, 100
*ELEMENT, TYPE=CPE4
2000000, 2148, 2248, 1127, 1027
*ELGEN, ELSET=BACKS
2000000, 1, 1, 1121, 18, 100, 100
**
**
*ELEMENT, TYPE=CPE4, ELSET=NATV5
2100000, 148, 248, 1046, 1047
*ELEMENT, TYPE=CPE4, ELSET=NATV5
2100001, 248, 348, 1045, 1046
*ELEMENT, TYPE=CPE4, ELSET=NATV5
2100002, 348, 448, 1044, 1045
*ELEMENT, TYPE=CPE4, ELSET=NATV5
2100003, 448, 548, 1043, 1044
*ELEMENT, TYPE=CPE4, ELSET=NATV5
2100004, 548, 648, 1042, 1043

```

\*ELEMENT, TYPE=CPE4, ELSET=NATVS  
 2100005,648, 748, 1041, 1042  
 \*ELEMENT, TYPE=CPE4, ELSET=NATVS  
 2100006,748, 848, 1040, 1041  
 \*ELEMENT, TYPE=CPE4, ELSET=NATVS  
 2100007,848, 948, 1039, 1040  
 \*ELEMENT, TYPE=CPE4, ELSET=NATVS  
 2100008,948, 1048, 1038, 1039  
 \*ELEMENT, TYPE=CPE4, ELSET=NATVS  
 2100009, 1048, 1148, 1037, 1038  
 \*ELEMENT, TYPE=CPE4, ELSET=NATVS  
 2100010, 1148, 1248, 1036, 1037  
 \*ELEMENT, TYPE=CPE4, ELSET=NATVS  
 2100011, 1248, 1348, 1035, 1036  
 \*ELEMENT, TYPE=CPE4, ELSET=NATVS  
 2100012, 1348, 1448, 1034, 1035  
 \*ELEMENT, TYPE=CPE4, ELSET=NATVS  
 2100013, 1448, 1548, 1033, 1034  
 \*ELEMENT, TYPE=CPE4, ELSET=NATVS  
 2100014, 1548, 1648, 1032, 1033  
 \*ELEMENT, TYPE=CPE4, ELSET=NATVS  
 2100015, 1648, 1748, 1031, 1032  
 \*ELEMENT, TYPE=CPE4, ELSET=NATVS  
 2100016, 1748, 1848, 1030, 1031  
 \*ELEMENT, TYPE=CPE4, ELSET=NATVS  
 2100017, 1848, 1948, 1029, 1030  
 \*ELEMENT, TYPE=CPE4, ELSET=NATVS  
 2100018, 1948, 2048, 1028, 1029  
 \*ELEMENT, TYPE=CPE4, ELSET=NATVS  
 2100019, 2048, 2148, 1027, 1028  
 \*\*  
 \*\*  
 \*ELEMENT, TYPE=CPE4, ELSET=NATVS  
 2100040, 3948, 4048, 2828, 2827  
 \*ELEMENT, TYPE=CPE4, ELSET=NATVS  
 2100021, 4048, 4148, 2829, 2828  
 \*ELEMENT, TYPE=CPE4, ELSET=NATVS  
 2100022, 4148, 4248, 2830, 2829  
 \*ELEMENT, TYPE=CPE4, ELSET=NATVS  
 2100023, 4248, 4348, 2831, 2830  
 \*ELEMENT, TYPE=CPE4, ELSET=NATVS  
 2100024, 4348, 4448, 2832, 2831  
 \*ELEMENT, TYPE=CPE4, ELSET=NATVS  
 2100025, 4448, 4548, 2833, 2832  
 \*ELEMENT, TYPE=CPE4, ELSET=NATVS  
 2100026, 4548, 4648, 2834, 2833  
 \*ELEMENT, TYPE=CPE4, ELSET=NATVS  
 2100027, 4648, 4748, 2835, 2834  
 \*ELEMENT, TYPE=CPE4, ELSET=NATVS  
 2100028, 4748, 4848, 2836, 2835  
 \*ELEMENT, TYPE=CPE4, ELSET=NATVS  
 2100029, 4848, 4948, 2837, 2836  
 \*ELEMENT, TYPE=CPE4, ELSET=NATVS  
 2100030, 4948, 5048, 2838, 2837  
 \*ELEMENT, TYPE=CPE4, ELSET=NATVS  
 2100031, 5048, 5148, 2839, 2838

```

*ELEMENT, TYPE=CPE4, ELSET=NATIVS
21000032, 5148, 5248, 2840, 2839
*ELEMENT, TYPE=CPE4, ELSET=NATIVS
21000033, 5248, 5348, 2841, 2840
*ELEMENT, TYPE=CPE4, ELSET=NATIVS
21000034, 5348, 5448, 2842, 2841
*ELEMENT, TYPE=CPE4, ELSET=NATIVS
21000035, 5448, 5548, 2843, 2842
*ELEMENT, TYPE=CPE4, ELSET=NATIVS
21000036, 5548, 5648, 2844, 2843
*ELEMENT, TYPE=CPE4, ELSET=NATIVS
21000037, 5648, 5748, 2845, 2844
*ELEMENT, TYPE=CPE4, ELSET=NATIVS
21000038, 5748, 5848, 2846, 2845
*ELEMENT, TYPE=CPE4, ELSET=NATIVS
21000039, 5848, 5948, 2847, 2846
*****

```

**\*\* BEAM PROPERTIES**

```

*****
*BEAM GENERAL SECTION, ELSET=PIPE, SECTION=GENERAL
20, 15700,10000,15700,10000

```

760,300

```

*SOLID SECTION, MATERIAL=SOILB, ELSET=HAUNCH
*SOLID SECTION, MATERIAL=SOILB, ELSET=BACKS
*SOLID SECTION, MATERIAL=SOILN, ELSET=NATIVS
*****

```

**\*\* MATERIAL PROPERTY DEFINITION**

```

*****
*MATERIAL, NAME=SOILB
*ELASTIC
10, 0.25
*MATERIAL, NAME=SOILN
*ELASTIC
10, 0.25
*****

```

**\*\* TIME INDEPENDENT BOUNDARY CONDITIONS**

```

*****
*NSET, NSET=BOTTOM, GENERATE
4647, 6447, 100
*NSET, NSET=LEFT, GENERATE
2847, 4647, 100
*NSET, NSET=RIGHT, GENERATE
147, 1047, 100
*NSET, NSET=RIGHT, GENERATE
6447, 7247, 100
*****

```

**\*\*BOUNDARY CONDITION**

```

*****
*BOUNDARY
RIGHT, YSYMM
LEFT, YSYMM
BOTTOM, PINNED

```

\*\*\*\*\*

**\*\* SPECIFIC OUTPUT REQUESTS**

\*\*\*\*\*

\*NSET, NSET=PIPNOD, GENERATE  
119, 7219, 100  
\*NSET, NSET=HOR1012.5, GENERATE  
1024, 2824, 100  
\*NSET, NSET=VERT, GENERATE  
3048, 3057, 1  
\*NSET, NSET=HOR900, GENERATE  
1023, 2823, 100  
\*NSET, NSET=HOR866, GENERATE  
1022, 2822, 100  
\*NSET, NSET=HOR825, GENERATE  
1021, 2821, 100  
\*ELSET, ELSET=VERT, GENERATE  
1819, 1827, 1  
\*ELSET, ELSET=VERT, GENERATE  
1719, 1727, 1  
\*ELSET, ELSET=VERT, GENERATE  
220800, 220808, 1  
\*ELSET, ELSET=VERT, GENERATE  
220900, 220908, 1  
\*ELSET, ELSET=VERT, GENERATE  
2000800, 2000900, 100  
\*ELSET, ELSET=HOR900, GENERATE  
923, 2623, 100  
\*ELSET, ELSET=HOR825, GENERATE  
921, 2621, 100

\*\*\*\*\*

**\*\* SURFACE LOADS**

\*\*\*\*\*

\*STEP  
\*STATIC  
\*CLOAD  
3057, 2, -8.3

\*\*\*\*\*

**\*\* OUTPUT COMMANDS**

\*\*\*\*\*

\*NODE PRINT, NSET=PIPNOD  
COORD, U  
\*NODE PRINT, NSET=VERT  
COORD  
\*NODE PRINT, NSET=HOR825  
COORD  
\*NODE PRINT, NSET=HOR866  
COORD  
\*NODE PRINT, NSET=HOR900  
COORD  
\*NODE PRINT, NSET=HOR1012.5  
COORD  
\*EL PRINT, POSITION=AVERAGED AT NODES, ELSET=PIPE  
SF  
\*EL PRINT, POSITION=AVERAGED AT NODES, ELSET=VERT

S, E

\*EL PRINT, POSITION=AVERAGED AT NODES, ELSET=HOR825

S, E

\*EL PRINT, POSITION=AVERAGED AT NODES, ELSET=HOR900

S, E

\*END STEP

